

**An electrochemical study of the oxidation of platinum employing ozone as oxidant and
chloride as complexing agent**

by

B.M.S. Mogwase

**Dissertation submitted in fulfilment of the requirements for the degree of Master of
Science in Chemistry at the Potchefstroom Campus of the North-West University**

Supervisor: Dr. R.J. Kriek

November 2012

Declaration

I declare that this dissertation is my own account of research, unless otherwise stated. It contains as its main content, work which has not previously been submitted for a degree at any tertiary institution.

Signature:

Date:

Acknowledgements

I would like to thank the following for their help and support during this project:

- Firstly, I would like to thank God Almighty for being my creator – may Your greatness and glory be displayed through my work.
- I am also deeply indebted to my supervisor Dr. R.J. Kriek for his encouragement, support and supervision throughout this project.
- My sincere gratitude to Professor Schalk Vorster for his valuable input and support in the project and text editing.
- I would also like to warmly thank Mr Fouché, Mrs Van der Walt and Dr Williams for their administrative arrangements concerning laboratory chemicals, glassware, etc. Frans Marx for the gas cylinders, Neels Le Roux for administrative IT works and the PGM group at large for the productive discussions we shared.
- I would furthermore like to acknowledge the support of my family and friends, for reasons too numerous to list, extend to them my deepest thanks for “living” this journey with me.
- Finally, I would like to acknowledge HySA and NRF for funding my studies, and many thanks to the Chemical Resource Beneficiation research focus area of the North-West University (Potchefstroom Campus) for funding of laboratory chemicals and equipment.

Opsomming

Motor-uitlaatkatalisators is een van die belangrikste gebruikers van platinum en baie aandag word bestee aan die herwinning van afval-platinum uit gebruikte uitlaatstelsels. Die oplos van platinum uit sodanige afval was vroeër slegs moontlik deur pirometallurgiese prosesse of die gebruik van aggressiewe chemikalieë, soos aqua regia en sianied, wat eger besoedelingsprobleme meebring. Onlangs is die potensiaal vir die ontwikkeling van hidrometallurgiese prosesse geïdentifiseer. Sulke prosesse is meer effektief en ook omgewingsvriendeliker as die tradisionele prosesse.

Dit was die doel van hierdie studie om die oksidasie van platinum met osoon as oksideermiddel te ondersoek in die teenwoordigheid van chloried as komplekseermiddel. Die invloed van verskeie faktore, soos chloriedioon-konsentrasie, pH en temperatuur is termodinamies en elektrochemies bestudeer ten einde gunstige loging te bewerkstellig.

Die termodinamiese ondersoek met die oog op die konstruksie van Pourbaix-diagramme van platinum in die teenwoordigheid van chloried het die vorming van stabiele waterige komplekse bevestig, sowel as platinumoksiedes.

Van die elektrochemiese resultate kan afgelei word dat osoon nuttig as 'n oksideermiddel gebruik kan word, maar volgens die bevindings wat met loging verkry is, hou osoon weinig voordele in vir logingsprosesse. Die relatief lae platinum-opbrengs wat met loging verkry is, kan moontlik aan die snelle ontbinding van osoon toegeskryf word. Die ontbinding van osoon word deur verskeie faktore beïnvloed, soos byvoorbeeld temperatuur, pH, die aanvanklike konsentrasie van osoon, ioniese sterkte en die roersnelheid. Optimalisering van hierdie faktore kan osoon moontlik bewys as 'n goeie oksideermiddel vir die herwinning van platinum.

Sleutelwoorde: uitlaatkatalisators, katalitiese omsetters, platinum, Pourbaix-diagramme, elektrochemie, komplekseermiddels, oksideermiddels

Abstract

Motor car exhaust catalysts are some of the most important users of platinum, and much attention is given to the recycling of scrap platinum from spent exhaust systems. The dissolution of platinum from waste exhausts was previously only possible by pyrometallurgical processes or by the use of aggressive chemicals, such as aqua regia and cyanide, all of which, however, cause pollution problems. Recently the potential for the development of hydrometallurgical processes was identified. These processes are more efficient and more environmentally friendly than traditional processes.

It was the aim of this study to investigate the oxidation of platinum with ozone as oxidizing agent in the presence of chloride as complexing agent. The influence of various factors, such as chloride ion concentration, pH and temperature were studied thermodynamically and electrochemically in order to achieve efficient leaching.

The thermodynamic investigation, leading to the construction of Pourbaix diagrams of platinum in the presence of chloride, confirmed the possibility of the formation of stable aqueous complexes, as well as platinum oxides.

From the electrochemical results obtained it can be concluded that ozone may be useful as an oxidizing agent, but according to the leaching results obtained, ozone holds few benefits compared to aqua regia and cyanide, although they still present some environmental challenges. The relatively low percentages of recovery obtained with leaching may be attributed to the rapid decomposition of ozone, which is affected by several factors, such as temperature, pH, initial concentration of ozone, ionic strength and stirring rate. Further optimisation of these factors can possibly prove ozone to be a useful oxidizing agent for the recovery of platinum.

Keywords: exhaust catalysts, catalytic converters, platinum, Pourbaix diagrams, electrochemistry, complexing agents, oxidants

Contents

Declaration	i
Acknowledgements	ii
Opsomming	iii
Abstract	iv
List of Figures	viii
List of Tables	x
List of Acronyms	x
Chapter 1: Introduction	1
1.1 Introduction	1
1.1.1 Air pollution	1
1.2 PGM Review	2
1.2.1 PGM supply	2
1.2.2 PGM demand per application	3
1.3 Use of PGMs in automotive catalytic converters	5
1.3.1 Three-way catalysts	5
1.3.2 Structure and components of a three-way catalyst	6
1.3.3 Loading of PGMs in automotive catalytic converters	6
1.3.4 Recovery of PGMs from autocatalysts	7
1.4 Summary	8
1.5 Aims and objectives	9
1.6 Scope of the project	9
1.7 Dissertation outline	9
Chapter 2: Literature review	11
2.1 Ozone	11
2.1.1 General properties of ozone	11
2.1.2 Ozone solubility in water	12
2.1.3 Decomposition of ozone	13
2.1.4 Summary	16
2.2 Current trends in recovering PGMs	16
2.2.1 Pressure cyanidation	17
2.2.2 Fluoride solutions	17
2.2.3 Aqua regia	17
2.2.4 Aqueous ozone and dilute chloride media	18
2.2.5 Iodine/iodide solutions	18

2.2.6	Summary	19
2.3	Thermodynamics	19
2.3.1	Thermodynamics of platinum and chloride ions	20
2.4	Fundamentals of electrochemistry	20
2.4.1	Introduction	20
2.4.2	The Nernst equation	21
2.4.3	Butler-Volmer equation	21
2.4.4	Passivation	23
2.4.5	Arrhenius equation	24
2.5	Electrochemistry of platinum	24
2.5.1	Standard reduction potentials	25
2.5.2	Chemistry of platinum with chloride	26
2.5.3	Summary	27
2.6	Conclusions	27
Chapter 3: Experimental		28
3.1	Thermodynamics	28
3.1.1	Experimental	28
3.2	Electrochemistry	29
3.2.1	Materials	29
3.2.1.1	Hydrochloric acid	29
3.2.1.2	Sodium chloride	29
3.2.1.3	Ozone	29
3.2.1.4	Platinum working electrode	32
3.2.2	Experimental apparatus	32
3.2.2.1	Experimental methods	33
3.2.2.2	The electrochemical set-up	33
3.2.2.3	Electrochemical investigation	35
3.3	Leaching	36
3.3.1	Automotive catalytic converters	36
3.3.2	Leaching apparatus	36
3.3.3	Physical leaching runs	37
3.3.3.1	Treatment of leach solution	37
3.3.3.2	Solution analysis	38

Chapter 4: Results and discussion	39
4.1 Introduction	39
4.2 Pourbaix diagrams	39
4.3 Potentiodynamic polarisation studies	40
4.3.1 Potentiostatic polarisation curves (Evans diagrams)	41
4.3.2 Influence of temperature	41
4.3.3 Influence of chloride concentration	42
4.3.4 Influence of pH	43
4.3.5 Determination of exchange current density	43
4.3.6 Activation energy of the Tafel region	45
4.3.7 Discussion of potentiodynamic results	48
4.3.7.1 In the absence of ozone	48
4.3.7.2 In the presence of nitrogen	50
4.3.7.3 In the presence of ozone	51
4.4 Leaching	53
4.4.1 Recovery of platinum in chloride/ozone media	53
4.4.2 Summary	55
Chapter 5: Conclusions and recommendations	57
5.1 Conclusions	57
5.2 Recommendations	57
References	59
Appendix A: Calculated standard Gibb's free energy of formation	64
Appendix B: Solution numbering	65
Appendix C: Pourbaix diagrams of Pt with chloride	66
Appendix D: Polarisation curves of platinum	70
Appendix E: Influence of temperature, chloride ion concentration and pH	76
Appendix F: Arrhenius plots for determining the activation energy of Tafel processes	81
Appendix E: Percentage recovery of platinum	85

List of figures

Figure 1.1	Platinum demand by application from 1999 to 2011	3
Figure 1.2	Palladium demand by application from 1999 to 2011	4
Figure 1.3	Rhodium demand by application from 1999 to 2011	4
Figure 1.4	Prices of PGMs from 1999 to 2011	5
Figure 1.5	Automotive catalyst structural design including honeycomb support	6
Figure 1.5	Percentage recovery of PGMs from autocatalysts from 1999 to 2011	8
Figure 2.1	Resonance structure of ozone	11
Figure 2.2	Solubility of ozone in water	13
Figure 2.3	The rate of the spontaneous decomposition of ozone as a function of the concentration of dissolved ozone for the first reaction step	14
Figure 2.4	pH-dependency of the reaction rate constants (in Fig. 2.3) for the spontaneous decomposition of ozone	14
Figure 2.5	Dependency of the reaction rate constants (in Fig. 2.3) with temperature for the spontaneous decomposition of ozone	15
Figure 2.6	Current-potential for a metal dissolution and deposition	22
Figure 2.7	(a) Current-potential relationships for the metal/deposition and the accompanied redox reactions	23
Figure 2.7	(b) Evans diagram	23
Figure 3.1	Ozone generator manifold	30
Figure 3.2	Plot of absorbance of ozone for different pH levels at 1 M Cl ⁻ and 15 °C	31
Figure 3.3	Plot of absorbance of ozone for different temperatures at 1 M Cl ⁻ and pH 0.5	31
Figure 3.4	Plot of absorbance of ozone for different [Cl ⁻] at 15 °C and pH 0.5	32
Figure 3.5	Electrochemical cell set-up	34
Figure 3.6	Electrochemical investigation set-up	35
Figure 3.7	Leaching set-up	37
Figure 3.8	Büchner funnel	38
Figure 3.9	ICP – OES machine	38
Figure 4.1	E _n -pH diagram of Pt-Cl-H ₂ O, 10 ⁻³ M Pt ⁺ , 1M Cl ⁻ at 25 °C	39
Figure 4.2	E _n -pH diagram of Pt-Cl-H ₂ O, 10 ⁻³ M Pt ⁺ , 4M Cl ⁻ at 25 °C	40
Figure 4.3	(a) Polarisation curve of Pt at different temperatures in 1 M [Cl ⁻] at pH 0.5 with ozone	41
Figure 4.3	(b) Polarisation curve of Pt at different temperatures in 2 M [Cl ⁻] at pH 0.5 with ozone	41
Figure 4.4	(a) Polarisation curve of Pt at different [Cl ⁻] at pH 0.5 with ozone at 15 °C	42
Figure 4.4	(b) Polarisation curve of Pt at different [Cl ⁻] at pH 0.5 with ozone at 25 °C	42

Figure 4.5	(a) Polarisation curve of Pt at different pH levels and different temperatures in 1 M [Cl ⁻] with ozone	43
Figure 4.5	(b) Polarisation curve of Pt at different pH levels and different temperatures in 2 M [Cl ⁻] with ozone	43
Figure 4.6	Polarisation curve of Pt in 1 M [Cl ⁻] at 15 °C pH level of 0.5 in the absence of ozone	44
Figure 4.7	Arrhenius plots for determining the activation energy of Tafel processes in 1 M [Cl ⁻] of pH 0.5 in the presence of ozone	46
Figure 4.8	Polarisation curve of Pt in 1 M [Cl ⁻], pH of 0.5 at 15 °C without ozone	49
Figure 4.9:	Polarisation curve of Pt in 1 M [Cl ⁻], pH of 0.5 at 15 °C with N ₂	51
Figure 4.10:	Polarisation curve of Pt in 1 M [Cl ⁻], pH of 0.5 at 15 °C in the presence of ozone	52
Figure 4.11:	Polarisation curves of Pt in 1 M [Cl ⁻], pH of 0.5 at 15 °C without ozone, with nitrogen and in the presence of ozone	53
Figure 4.12:	Percentage recovery of Pt in 1 M [Cl ⁻] at 15 °C at different pH levels	54
Figure 4.13:	Percentage recovery of Pt in 2 M [Cl ⁻] of pH 2 at different temperatures	54
Figure 4.14:	Percentage recovery of Pt in different Cl ⁻ concentrations of pH 0.5 at 25 °C	55

List of tables

Table 1.1	Vehicle polluting emission	2
Table 1.2	PGM content of automotive catalysts	7
Table 2.1	Relative oxidation potentials	12
Table 2.2	Reaction mechanism for the decomposition of ozone	16
Table 2.3	Stability constants of Pt with Cl ⁻ ligand	20
Table 3.1	Thermodynamic data for the individual cations and anions	29
Table 3.2	Chloride solutions	33
Table 4.1	Tafel parameters determined from experimental polarization curves	45
Table 4.2	Activation energies of Tafel regions in the presence of ozone	47
Table 4.3	Activation energies of Tafel regions in the absence of ozone	48
Table 4.4	Total percentage extraction of Pt after 8 hours	55

List of acronyms and Units

PGMs	platinum group metals
Oz	ounce
ppm	parts per million
M	molarity
ml	millilitre
g	gram
mg ℓ^{-1} .	milligram per meter
$^{\circ}\text{C}$	degrees celcius
wt %	weight percentage
μm	micrometer
rpm	rotation per minute
kPa	kilopascal
kWh.kg $^{-1}$	kilowatt per kilogram
h	hour
s	second
V	voltage
E°	standard redox potential
A/cm 2	ampere per centimeter square
SHE	standard hydrogen electrode
STP	standard temperature and pressure
kJ mol $^{-1}$	kilojoule per mole
kJ. mol $^{-1}$.K $^{-1}$	kilojoule per mole per Kelvin
ΔG	change in gibbs free energy
ΔH	change in enthalpy
ΔS	change in entropy
T	temperature
R	universal gas constant
β	overall formation constant

CHAPTER 1

INTRODUCTION

1.1 Introduction

There is great concern for the environment, largely brought about by transportation as a major source of air pollution. It is responsible for the carbon monoxide, hydrocarbons and nitrogen oxides in the atmosphere, contained in the exhaust gases that cars release through the tailpipes, unless proper and effective methods are put into practice to reduce them to less harmful pollutants. It is believed that these harmful pollutants are causing what is known as global warming because they are part of the so-called “greenhouse” gases. Hence, this study is undertaken against the background of increasing concerns about the state of the environment, specifically the atmosphere. In this chapter the background to the research problem is provided.

1.1.1 Air pollution

There are at present many factors that cause air pollution, mainly due to human industrial activities concerned with energy production and transportation. These factors can be problematic to human health and the environment as they are mainly based on the combustion of carbon-containing materials releasing harmful chemicals into the air. Hence, motor vehicles contribute tremendously to atmospheric pollution. Table 1.1 below will summarise the best known vehicle pollution emissions and their impacts (USEPA, 2002) (cited by Victoria Transport Policy Institute, 2012).

Table 1.1 Vehicle Polluting Emission (USEPA, 2002) (cited by Victoria Transport Policy Institute, 2012)

Emission	Description	Sources	Harmful Effects	Scale
Carbon monoxide(CO)	A toxic gas caused by incomplete combustion	Tailpipes	Human health, Climate change	Very local
Nitrogen oxide(NO _x) and nitrous oxide (N ₂ O)	Various Compounds, some are toxic, all contribute to ozone	Tailpipes	Human health, ozone	Local and Regional
VOC (volatile organic hydrocarbons)	Various hydrocarbons (HC) gases	Fuel production and, storage & tailpipes	Human health, ozone precursor	Local and Regional

1.2 PGM review

Platinum (Pt), palladium (Pd), rhodium (Rh), iridium (Ir), osmium (Os), and ruthenium (Ru) constitute the platinum group of metals (PGMs). PGMs form the family of precious metals (Cotton, 1980). The platinum group metals are also referred to as “noble metals” due to their resistance to oxidation.

1.2.1 PGM supply

PGMs occur naturally only at very low concentrations in the earth’s crust. Their abundance is estimated to be: 0.005 ppm for platinum, 0.001 ppm for palladium and 0.0004 ppm for rhodium and for osmium, iridium and ruthenium 0.0004 ppm (Goldschmidt, 1954; Robson, 1985). Major PGM reserves and producers are in South Africa, with Russia taking the second place, Canada the third with other countries such as Zimbabwe, China, Columbia, Western Australia playing minor but important roles (Platinum Interim Review, 2011). According to Platinum Interim Review (2011), South Africa supplied 4 855 million ounces, Russia 835, North America 350, Zimbaqwe 340, and other countries supplied 100 million ounces. South Africa is the only country amongst the major producers that produces the metals from PGM-bearing ores whilst in Russia and Canada, the PGMs are derived mainly as a by-product of the processing of high grade copper/nickel ores (Ryder, 1990).

1.2.2 PGM demand per application

The use of PGMs includes various industrial processes, catalysts in petroleum refining and chemical processing, electrical conductors, etc. Previously, platinum found most of its demand in the jewellery industry, but as technologies changed with time, it found a great demand in the autocatalyst industry. In 2002, when platinum demand for jewellery weakened, autocatalyst made a mark in the history of platinum application showing a great increase for autocatalyst as seen in Figure 1.1. In 2009 (Figure 1.1), there was a decline of demand for platinum as autocatalysts. Platinum Interim Review (2011) ascribed it to the global economic concerns. Other industrial uses of platinum include chemical, electrical, glass and petroleum applications.

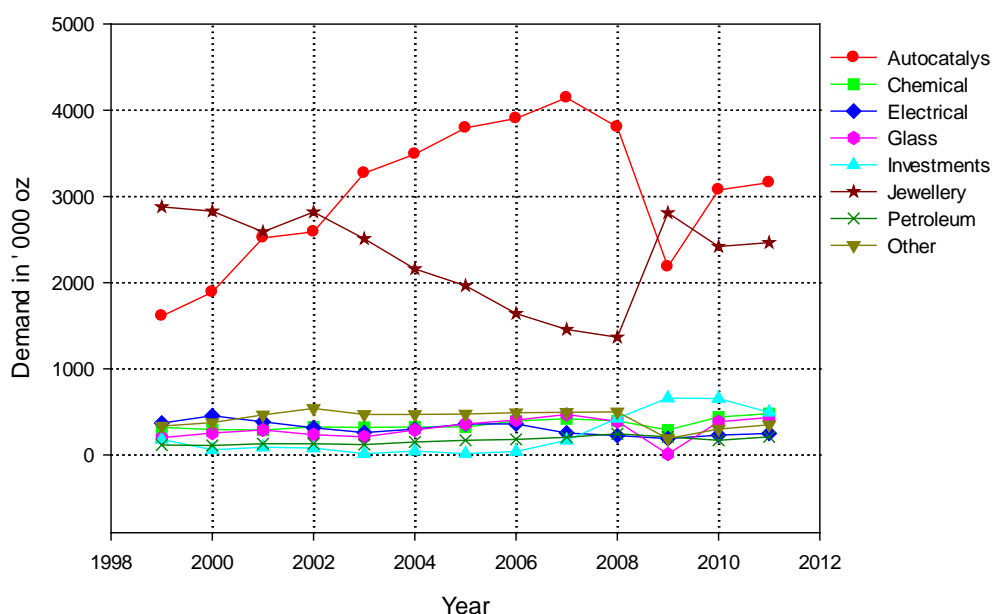


Figure 1.1: Platinum demand by application from 1999 to 2011 (Platinum 2011)

Palladium, on the other hand, has played a dominant role in autocatalysts as seen in Figure 1.2, and there has been a greater demand for palladium in industries such as the chemical, dental, electronics and jewellery industries. Following platinum, in 2009 (Figure 1.2), the demand for palladium in autocatalysts declined for the same reason given by Platinum Interim Review (2011), namely that it might be due to economic changes.

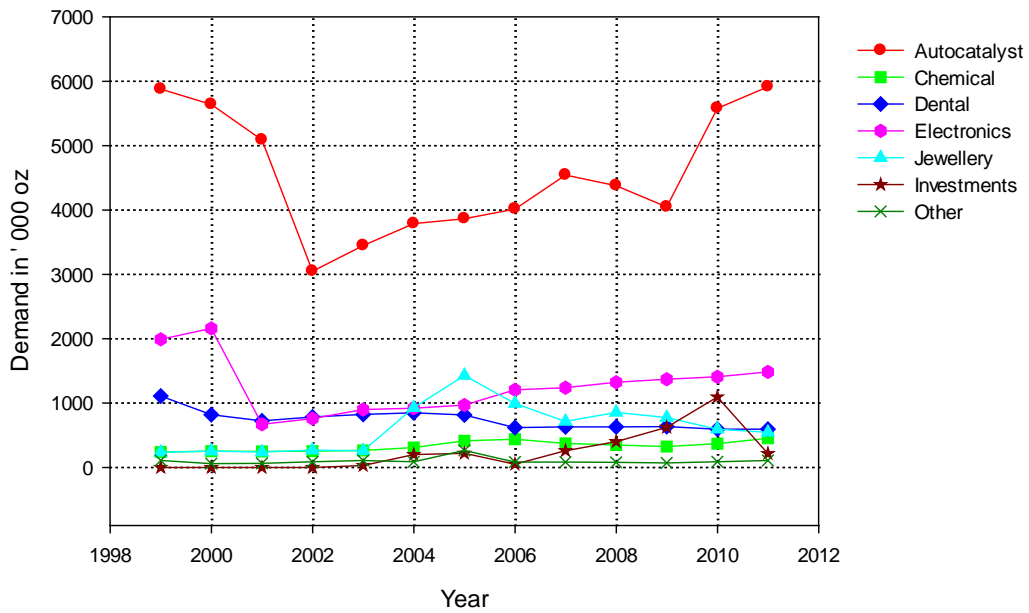


Figure 1.2: Palladium demand by application from 1999 to 2011 (Platinum 2011)

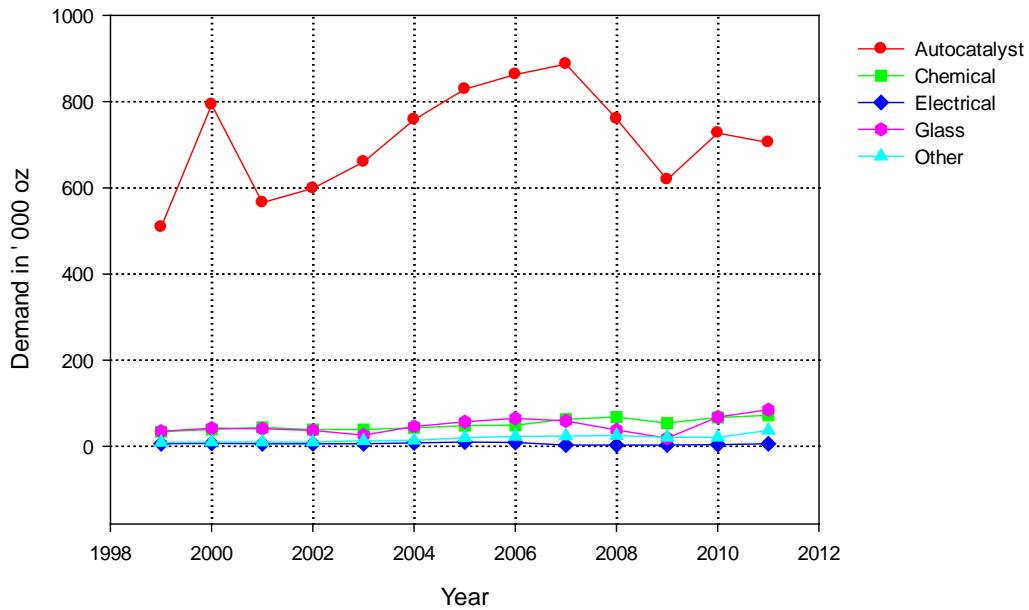


Figure 1.3: Rhodium demand by application from 1999 to 2011(Platinum 2011)

From Figure 1.3, it can be seen that Rh is predominantly used in autocatalysts, which seems to be increasing. However, it has not found as many uses as Pt and Pd metals, and there has not been as big a demand for the metal as yet. As of 2008 and 2009 (Figure 1.3) Rh has shown a decline in autocatalyst usage due to economic changes (Platinum Interim Review, 2011). As of 2010 the demand has increased again, due to retailers and manufacturers rebuilding their stocks.

PGMs are very expensive and their prices change significantly with time. Figure 1.4 depicts the prices of PGMs, whereby the rhodium price was exceptionally volatile during 2008. Platinum Interim Review (2011) states that Rh hit an all-time record of \$10, 100 per ounce in June 2008, followed by platinum being the most expensive, followed by palladium. As of 2009 the prices of platinum, palladium and rhodium have dropped due to concerns over the global economy and the weakening of the US Dollar according to Platinum Interim Review (2011).

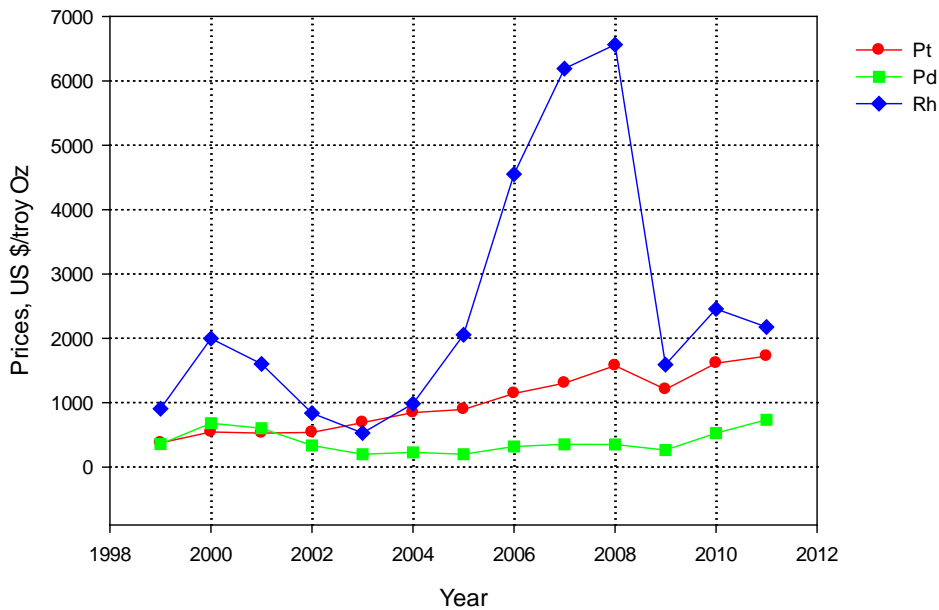


Figure 1.4: Prices of PGMs from 1999 to 2011 (Platinum 2011)

1.3 Use of PGMs in automotive catalytic converters

Motor vehicles produce various pollutants as shown in Table 1.1. Hence, in the U.S.A. during the mid-1970s, automotive catalytic converters were first used to meet emission legislation (Hennion *et al.*, 1983). Since that time emission limits have been markedly reduced. These converters make use of two or more PGMs. There are different types of designs available for autocatalysts, but only one typical “three-way” automotive catalyst will be discussed.

1.3.1 Three-way catalysts

Heck and Farrauto (2001), describe a typical three-way catalyst as facilitating the simultaneous reaction of CO, HC and NO_x with atmospheric oxygen. Usually autocatalysts contain platinum, palladium and rhodium. According to Fornalczyk and Saternus (2009), platinum is a good metal for the transformation of CO and HC to water and carbon dioxide,

whereas rhodium is an excellent metal for the reduction of NO_x to nitrogen, but palladium can handle all three pollutants.

1.3.2 Structure and components of a three-way catalyst

Figure 1.5 shows a typical autocatalyst design (Heck and Farrauto, 2001) which includes a honeycomb support. The honeycomb structure is made of magnesium cordierite, $2\text{MgO} \cdot 2\text{Al}_2\text{O}_3 \cdot 5\text{SiO}_2$ and a washcoat of 10-30 wt % cordierite, a mixture of predominantly gamma-alumina which provides an area for the PGMs to be dispersed onto (Woo, 2000).

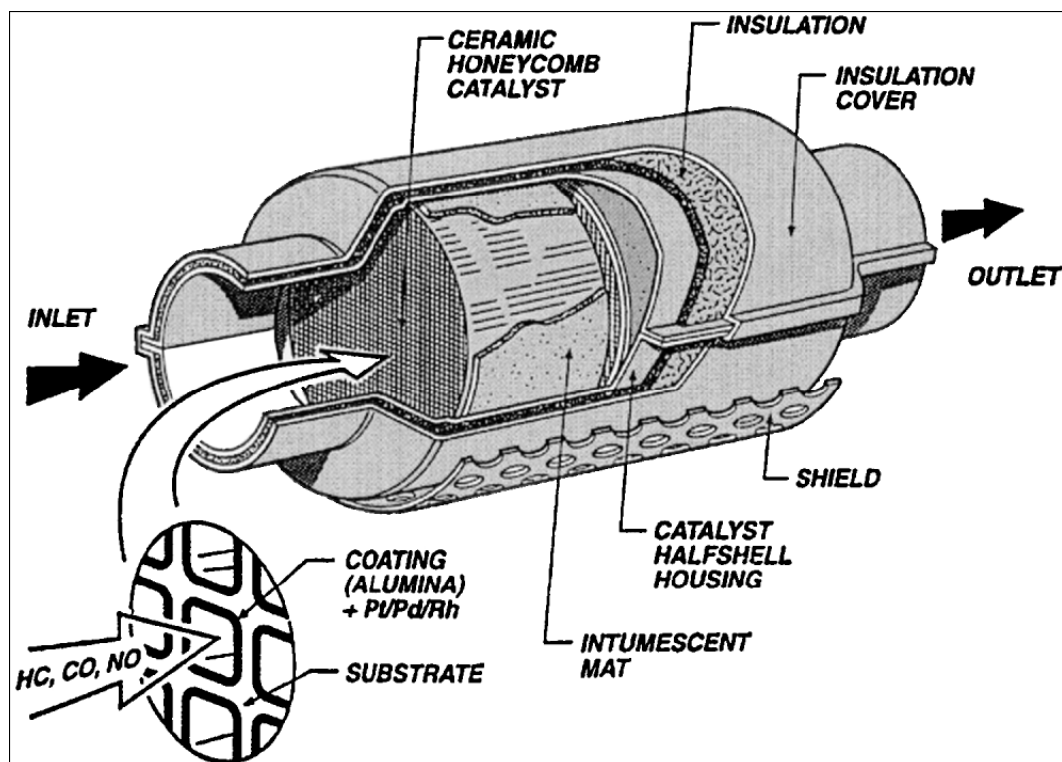


Figure 1.5: Automotive catalyst structural design including honeycomb support (Heck and Farrauto, 2001)

1.3.3 Loading of PGMs in automotive catalytic converters

The PGM content of these autocatalysts varies greatly according to the type and manufacturer (Barefoot, 1997). Table 1.2 below lists some reported PGM contents (Wu, 1993). It is confirmed by these contents that they have increased over the years. The average content of platinum group metals per catalytic converter has been 0.05 million ounces of platinum, 0.02 million ounces of palladium and 0.005 million ounces of rhodium (Zysk, 1986).

Table 1.2: PGM content of Automotive Catalysts (Wu, 1993)

Catalyst type	Pt(ppm)	Pd(ppm)	Rh(ppm)	Reference
Unspecified	500	100		Musco, 1978
Pellet	270-350	80-150		Chemical week, 1983
Monolith	500-1200	0-300		Malhotra, 1983
Pellet	350	150		Cichy, 1983
Monolith	0.085%			
Alumina Pellet	330-500	100-200		Letowski & Distin, 1985
Silica monolith	800-1500	100-300		
Pellet	345	145		Mishra & Reddy, 1986
Honeycomb	1220	170		
Pellet	500-1200	0-300	139	Tyson & Bautista, 1987
Honeycomb	330-500	80-150		
Pellet	800-1500	100-200		Letowski & Distin, 1987
Silica monolith	0.8-1.5	100-350		
Two-way	0.04%	0.015%		Hoffman, 1988a
Three-way	0.08%	0.04%		
Pellet(two-way)	350	150	60	Mishra, 1989
Pellet(three way)	850	300		
Honeycomb(two-way)	900	300		
Honeycomb(three-way)	1100	300	100	
Pellet	400	150		Letowski & Distin, 1989
Honeycomb	800-1500	100-400		

1.3.4 Recovery of Pt metals from autocatalysts

The PGM concentration in these catalytic converters is said to be generally higher than those of the richest ore bodies (Hoffman, 1988). As can be seen in Figure 1.6 the recovery of PGMs from autocatalysts has increased tremendously over the past years. The growth is driven partly by an increase in average loadings of the catalysts (Platinum Interim Review, 2011). These tremendous increases indicate that reliable technologies for recovering PGMs become important.

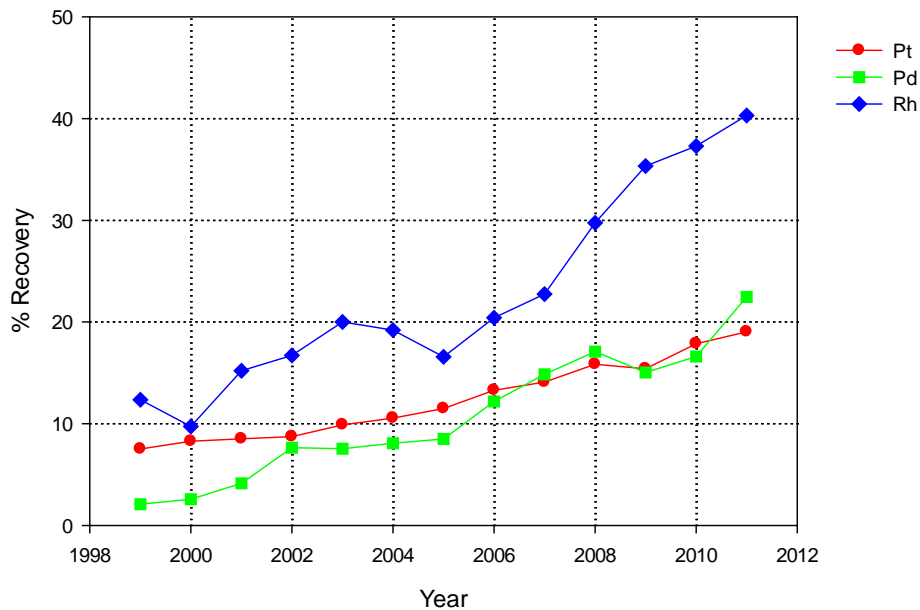


Figure 1.6: Percentage recoveries of PGMs from autocatalysts from 1999 to 2011 (Platinum 2011)

The most common methods of extracting PGMs from their ores or secondary sources are cyanide and aqua regia solutions (Duyvesteyn *et al.*, 1994). They further explain that there are many advantages of the two methods over other extractive methods because extraction is effective and fast. However, the economics of the processes is not only challenging, but present environmental impact challenges. According to De Sá Pinheiro *et al.* (2004) pyrometallurgy and hydrometallurgy were used to recover PGMs from autocatalysts but these methods require high energy, hence it is necessary to search for an adequate recycling process to optimise metals recovery and reduce energy consumption. Perhaps the most promising alternative is hydrometallurgy employing chloride in the presence of an oxidant, for example ozone.

1.4 Summary

- Autocatalysts generally comprise a refractory oxide carrier on which two or more PGMs are dispersed in very low concentrations.
- The PGM concentration in these catalytic converters is generally higher than those of the richest ore bodies.
- Hence, it is important to recycle PGMs from their secondary sources with less aggressive methods to instrumentation and the environment.

1.5 Aims and objectives of the study

The aim of this research project is to investigate the oxidation of platinum with ozone (O_3) as an oxidising agent in the presence of chloride, which is referred to as a complexing agent. The objective of this study is to find the optimum conditions for the maximum recovery of platinum from virgin automotive catalytic converter material.

1.6 Scope of the project

A thorough literature study regarding the following topics was conducted:

- Current trends of recovering platinum from catalytic converter material.
- Electrochemistry of platinum.
- Ozone (O_3).
- Chloride.

This project entails:

- a. A thermodynamic study of the stability areas of the aqueous complex ions of platinum with Cl^- .
- b. An electrochemical investigation of the interaction of platinum within various chloride solutions in the presence of ozone, together with a change in temperature and pH.
- c. Physical leaching tests under different conditions as determined by a. and b. with ozone as an oxidising agent and chloride as complexing agent.

1.7 Dissertation outline

Chapter 2: Literature studies

This chapter will focus on the literature concerning the following:

- Current trends of recovering platinum from catalytic converter material.
- Electrochemistry of platinum.
- Polarisation curves and Evans diagrams.
- Ozone (O_3).
- Chloride.

Chapter 3: Experimental

This chapter will contain the details regarding the investigation of the efficiency of ozone as an oxidising agent in the leaching of PGMs. Electrochemical tests will be conducted in order to optimise the conditions for leaching process, where physical leaching tests will reveal the recovery of PGMs. The experimental apparatus, as well as procedures, will be thoroughly discussed in this chapter.

Chapter 4: Results and discussion

Results regarding the thermodynamic study, electrochemical investigation and physical leaching tests will be thoroughly discussed in this chapter.

Chapter 5: Conclusions

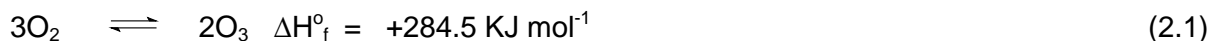
Conclusions regarding this study will be made in this chapter, whether the optimum conditions for recovering PGMs from automotive catalytic converters were met or not, and recommendations for future work, followed by references.

CHAPTER 2

LITERATURE REVIEW

2.1 Ozone (O₃)

Today, ozone is known to be a powerful oxidant for water treatment. It is an allotrope of oxygen. According to reaction 2.1, the formation of ozone is endothermic (Rakovsky *et al.*, 2009).



Ozone is unstable, hence it spontaneously reverts back to oxygen as seen in reaction 2.1 (Rakovsky *et al.*, 2009). Ozone is a powerful oxidant and hence important industrial applications include its application as chemical reagent, as disinfectant for sewage treatment and as a bleaching agent. According to Rice (1989) (cited by Wu, 1996) there exist more than 3 000 water treatment plants throughout the world that use ozone for disinfection.

2.1.1 General properties of ozone

At ordinary temperatures pure ozone is said to be a pale blue gas with a sharp, cold, irritating odour that condenses to an indigo blue liquid and freezes to a deep blue-violet solid (Rakovsky *et al.*, 2009). In the earth's stratosphere, ozone forms a protective absorbing layer on the altitude of 20-30 km. It occurs naturally, with a concentration of about 50 ppm, protecting the planet and its inhabitants by absorbing ultraviolet radiation of wavelength 290-320 nm (Rakovsky *et al.*, 2009). Figure 2.1 depicts the resonance structure of ozone. It is characterised by end oxygen atoms with only six electrons.

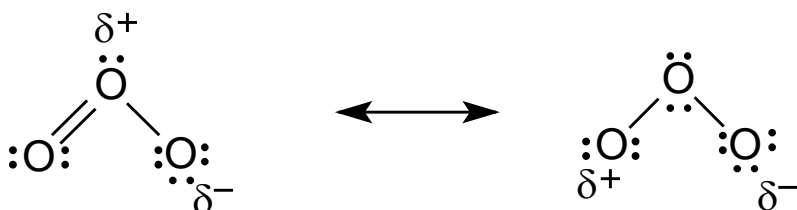


Figure 2.1: Resonance structure of ozone (Langlais *et al.*, 1991) (cited by Nawrocki *et al.*, 2003)

This fact defines the electrophilic nature that ozone shows in most of its chemical reactions. The standard half-cell reaction of ozone is given by CRC handbook of Chemistry and Physics, (2001-2002) as:



Ozone reacts readily with organic and inorganic compounds due to its high reduction potential and reactivity. It is highly unstable and has to be generated *in situ*. The well-known method is the corona discharge technique whereby oxygen flows through an electric field (Rakovsky *et al.*, 2009). It is important to remember that oxygen always will be present when performing subsequent experiments involving ozone. Ozone can also be produced by exposing oxygen gas to ultraviolet light, however, these methods are normally less efficient and produce lower concentrations of ozone (Dohan and Masschelein, 1987) (cited by Summerfelt, 1997).

Ozone is the fourth most powerful oxidising agent known (as shown in Table 2.1), and it is the most powerful oxidising agent available for water treatment. The oxidation potential of ozone is considerably higher than other disinfecting agents, but is surpassed in oxidant power by fluorine, hydroxyl radicals and atomic oxygen. The oxidation potentials of some disinfectant agents are shown in Table 2.1 below.

Table 2.1: Relative oxidation potentials (Iglesias, 2002)

Species	Oxidation potentials, eV
Fluorine	3.03
Hydroxyl radicals	2.80
Atomic oxygen	2.42
Ozone	2.07
Hydrogen peroxide	1.77
Permanganate	1.67
Hypobromous acid	1.59
Chlorine dioxide	1.50
Hypochlorous acid	1.49
Hypoiodous acid	1.45
Chlorine	1.36
Bromide	1.09
Iodine	0.54

2.1.2 Ozone solubility in water

According to Wu (1996) several researchers studied the solubility of ozone in water and acidic medium, and observed in their diverse research that ozone solubility decreases as the normality of the acid is increased. Figure 2.2 shows that when the temperature is increased, the ozone solubility decreases, and solubility decreases when the pH is increased. Henry's law constants also decrease as the temperature is increased.

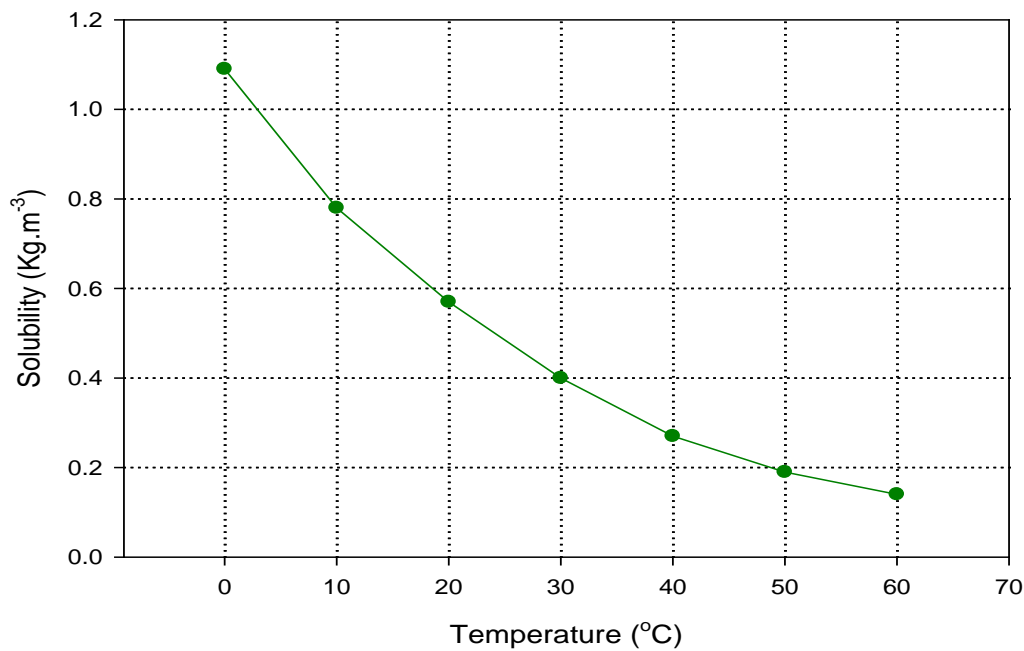


Figure 2.2: Solubility of ozone in water (Ullmann's, 1991) (cited by Iglesias, 2000)

2.1.3 Decomposition of ozone

The decomposition of ozone in aqueous solutions is complex, and is affected by many properties, such as pH, temperature and substances present in the water. Optimising these factors could prove ozone to be a good oxidising agent.

Previous investigations conducted at the former Potchefstroom University have determined the dependency of its decay upon factors such as (a) pH, (b) the initial concentration of the ozone, as well as (c) temperature.

(a) Influence of pH level

Solutions with identical concentrations were tested at different pH levels by Hahn (1997). The rate constants regarding the decay of ozone increased with one order of magnitude as the pH level was increased from 1.9 to 6. This implies that half of the initial ozone concentration will be reached within 10 minutes at pH = 6 opposed to the 240 minutes at a level of 1.9. It was observed that the pH level slightly influences the rate constant in the lower pH region. Thus the lower the pH level of a solution the longer ozone will remain relatively stable as seen in Figure 2.3.

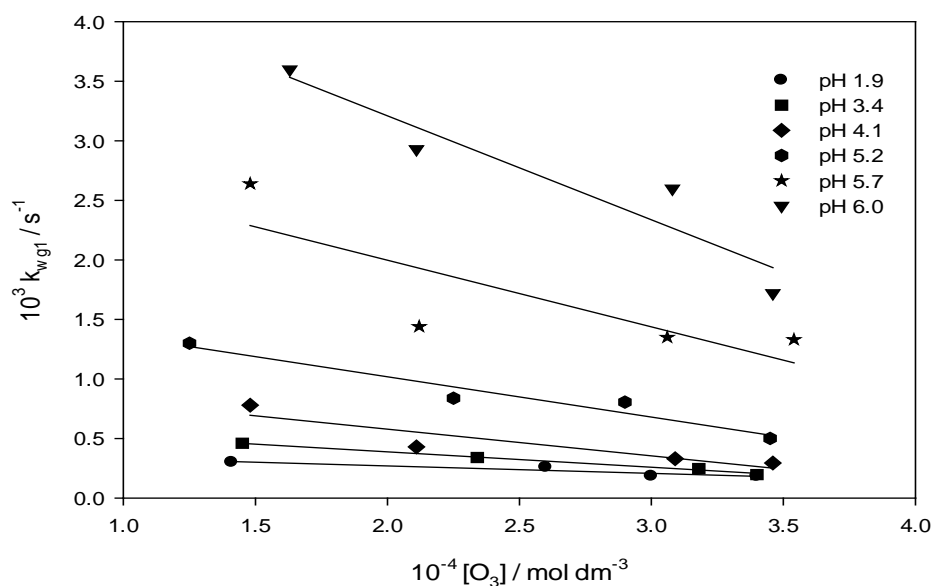


Figure 2.3: The rate of the spontaneous decomposition of ozone as a function of the concentration of dissolved ozone for the first reaction step (Hahn, 1997)

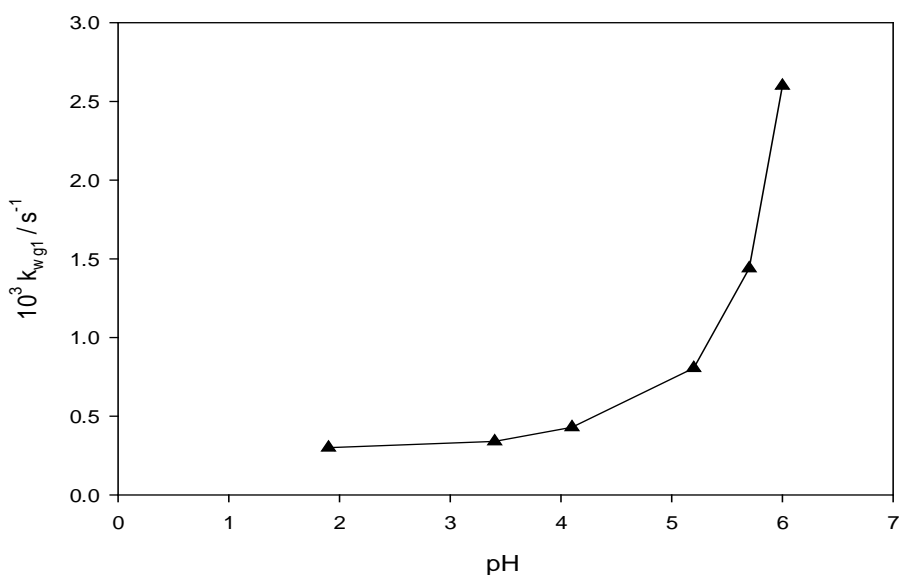


Figure 2.4: pH-dependency of the reaction rate constants (in Fig. 2.3) for the spontaneous decomposition of ozone (Hahn, 1997)

(b) Influence of initial ozone concentration

The influence of initial ozone concentration was investigated by Hahn (1997). Four different initial ozone concentrations were tested at six respective pH levels in the pH range of one to seven. A decrease was observed in the rate constants as the initial ozone concentrations

were increased. Lower concentrations of aqueous ozone would thus remain relatively stable over a longer time period as seen in Figure 2.4.

(c) Influence of temperature

Hahn (1997) also investigated the influence of temperature on the decay of ozone. In the temperature range of 10°C – 30°C the pH level and the ionic strength were constant. It was observed that the rate constants of both reactions responsible for the decomposition of ozone increased with increasing temperature, and concluded that lower temperatures provide an environment for aqueous ozone to remain stable for longer, as seen in Figure 2.5.

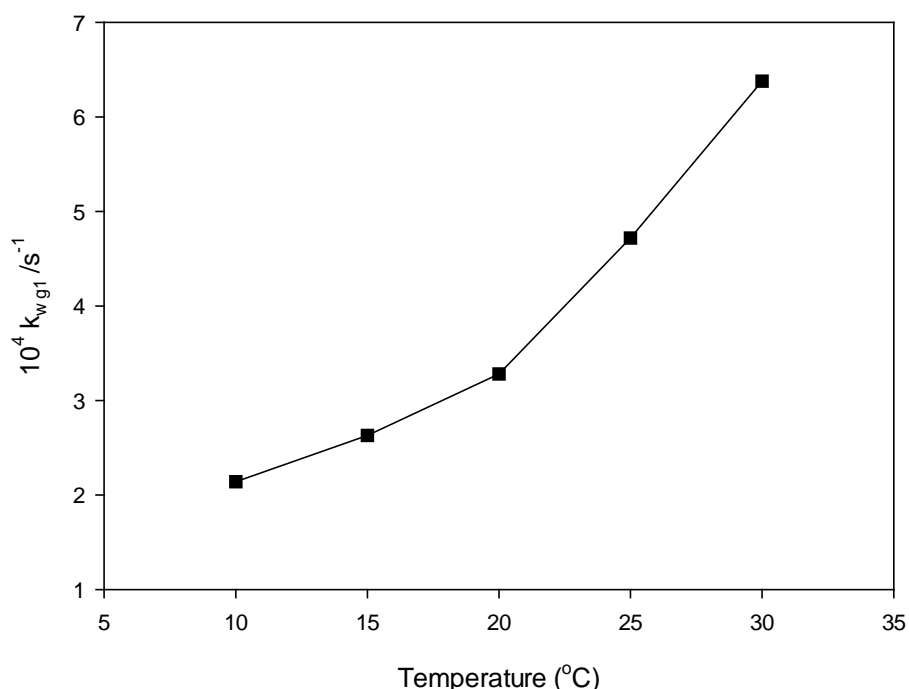


Figure 2.5: Dependency of the reaction rate constants (in Fig. 2.3) with temperature for the spontaneous decomposition of ozone (Hahn, 1997)

According to (Sotelo *et al.*, 1987) faster decomposition of ozone can be ascribed also to higher stirring speed in the solution, which can be explained by desorption. Also, higher ionic strength accelerates the depletion (Hahn *et al.*, 2000). The decomposition of ozone follows a pseudo first-order kinetic law, where k' is a pseudo first-order rate constant at a given pH value (Langlais *et al.*, 1991) (cited by Nawrocki *et al.*, 2003) as seen in equation 2.1 below:

$$- (d[O_3]/dt)_{pH} = k' [O_3] \tag{2.1}$$

Ozone can decompose leading to a five-step chain reaction as shown in Table 2.2 (Masschelein, 1992) (cited by Nawrocki *et al.*, 2003):

Table 2.2: Reaction mechanism for the decomposition of ozone (Masschelein, 1992) (cited by Nawrocki *et al.*, 2003)

Reactions		Rate constants
$O_3 + H_2O \rightarrow 2HO^\bullet + O_2$	(2.3)	$k_2 = 1.1 \times 10^{-4} M^{-1} s^{-1}$
$O_3 + OH^- \rightarrow O_2^{\bullet-} + HO_2^\bullet$	(2.4)	
$O_3 + HO^\bullet \rightarrow O_2 + HO_2^\bullet \rightleftharpoons O_2^{\bullet-} + H^+$	(2.5)	$k_2 = 70 M^{-1} s^{-1}$
$O_3 + HO_2^\bullet \rightleftharpoons 2O_2 + HO^\bullet$	(2.6)	
$2HO_2^\bullet \rightarrow O_2 + H_2O_2$	(2.7)	$k_2 = 1.6 \times 10^9 M^{-1} s^{-1}$

Ozone has good oxidising abilities and the stability can be influenced by various factors, so a compromise between the various stable conditions could prove ozone to be an efficient oxidising agent in the recovery of PGMs.

2.1.4 Summary

- Ozone solubility in water and acidic medium decreases as the normality of the acid is increased.
- When the temperature is increased, the ozone solubility decreases, and solubility decreases when the pH is increased.
- Ozone cannot be shipped, therefore it must be generated and applied on site.
- The decomposition in aqueous solutions is complex, and is affected by many properties such as pH, temperature and substances present in the water.
- Optimizing these factors could prove ozone to be a good oxidising agent.

2.2 Current trends in recovering PGMs

PGMs are either obtained from mined ores associated with Cu-Ni deposits, or from secondary sources such as used catalysts (Giandomenico, 2000). The PGMs are typically dissolved in acidic-oxidising solutions, after the initial processing to form concentrates (Hartley, 1991) cited by (Giandomenico, 2000). The efficiency and methods of final refining processes used to produce pure metals from solutions have evolved considerably in the past few decades (Giandomenico, 2000). Davies *et al.*, 1993 states that there exist different combinations of oxidants (such as hypochlorite, hydrogen peroxide, bromine and iodine)

which can be used in conjunction with the complexant (chloride for example) to provide the optimum leaching conditions. He further explains that each combination has its own characteristics regarding dissolution, yielding optimum pHs and oxidant/complexant molar ratio. The following are the current trends in recovering PGMs, more specifically platinum, with their advantages and disadvantages.

2.2.1 Pressure cyanidation

The reaction of sodium cyanide and PGMs has been studied extensively over high temperatures of 120 to 180 °C and pressures of at least 3.0 MPa, whereby the kinetics of the reaction is very low (Chen and Huang, 2006). They reported a pre-treatment procedure, whereby the spent catalysts were pre-treated by pressure alkaline leach, followed by two steps of pressure cyanide leaching. The achieved percentage recovery for Pt was 95-96%, also reported for Pd and Rh to be 97-98% and 90-92%, respectively. The order of cyanide leaching was found to be Pd > Pt > Rh. Though the percentage recovery is high, the method itself is challenging due to high-energy consumption and cyanide itself is toxic.

2.2.2 Fluoride solutions

De Sá Pinheiro *et al.* (2004) studied the dissolution of spent catalysts in aqueous solutions containing fluoride, a strong complexing agent, and other species. In the presence of fluoride only, Pt recovery was insignificant and (<1 wt% soluble) for aluminium, even when excess fluoride salts, lower catalyst masses or higher temperatures (above 90°C) were employed. In 20M HF very little Pt (5wt%) was recovered, together with only a little alumina dissolution (9 wt%). Combining 20M HF with 12M HCl resulted in only a slight increase with regard to Pt recovery, i.e. 7 wt%, but all of the alumina substrate was dissolved (>99 wt%). Substituting HCl with 36 wt% H₂O₂, in the presence of 20M HF, resulted in an increased Pt recovery of 10 wt% with alumina dissolution still greater than 99 wt%, and a combination of all three, namely 20M HF, 36 wt% H₂O₂, 12M HCl, increased Pt recovery to only 15 wt%, with alumina dissolution still greater than 99 wt%. This technique, therefore, seemed to be effective for alumina substrate dissolution, but not for PGM dissolution.

2.2.3 Aqua regia

Aqua regia has been classified as a traditional medium for PGM dissolution and PGM extraction is very high, but the economics of the process is challenging. Platinum extraction from used catalysts by aqua regia solutions has been investigated by several groups:

- Barakat and Mahmoud (2004) evaluated leaching of Pt from a Pt gauze catalyst used during the manufacturing of nitric acid from ammonia. The recovery of Pt using aqua regia was 98% after leaching for 1.5 h at 109°C with a liquid/solid ratio of 10.
- Jafarifar *et al.* (2005) studied the recovery of platinum/rhenium bimetallic spent catalyst containing 0-2% Pt, 0.43% Re and other impurities, by two leaching methods. In the first method, the sample was refluxed with aqua regia yielding 96.5% of Pt at a liquid/solid ratio of 5 for 2.5 h. In the second case, microwave radiation was used and dissolution yield increased to 98.3% at a liquid/solid ratio of 2 for 5 minutes.
- Baghalha *et al.* (2009) studied the kinetics of platinum leaching in aqua regia solutions from mild to severe conditions. At 100°C and liquid/solid ratio of 10, Pt recovery was 99.8%.

2.2.4 Aqueous ozone and dilute chloride media

Viñals *et al.* (2006) thought that aqueous ozone might perhaps be a substitute for the leaching of concentrates and wastes containing precious metals, due to the formation of oxygen as a reaction by-product, and that ozone could be used at very low aqueous concentrations ($\sim 10^{-4}$ M) by injecting O_2/O_3 mixtures at low P_{O_3} (<10kPa) but the disadvantage will be energy consumption. Viñals *et al.* (2006) studied more the leaching of gold and palladium with aqueous ozone in dilute chloride media than with platinum, hence the platinum results were limited. Through surface analysis by SEM, there was no significant attack discovered on Pt in O_3/H_2SO_4 (0.25 M H_2SO_4 , 25°C, 3 h), or in O_3/HCl (0.1-2 M HCl, 25°C, 3 h). Leaching in $O_3/H_2O_2/HCl$ showed significant rates, but only at high HCl concentration (6 M); however, chlorine evolved under these latter conditions. Unfortunately the percentage recovery was not mentioned for Pt, but what was found for Pd and Au was that the recovery was not greater than 40% (Viñals *et al.*, 2006).

2.2.5 Iodine/iodide solutions

According to Baghalha and Zanjani (2009), Pt extraction using iodine/iodide solutions seemed to be more promising than the other halogen systems. As a result, platinum-iodide complexes form more easily (i.e. at lower potentials) and they are more stable in solution than the other platinum-halogen complexes. Hence, they studied the conditions that produced maximum platinum recovery in iodine/iodide solutions and the leach could only reach 76.2% after 3 hours at 75 °C with a solution pH of 1.06.

2.2.6 Summary

- Cyanide does result in good dissolution yields, e.g. 98% Pt and 99% Pd, but requires high temperature and pressure.
- Fluoride seems to be not effective for PGM dissolution, but very effective for substrate dissolution.
- Aqua regia does result in very high and fast PGM extraction, but the economics of the process is challenging due to its unacceptably high reagent use and cost.
- Iodine/iodide solutions seem more promising for the extraction of PGMs because Pt-iodide complexes forms more easily, i.e. at lower potentials and are more stable in solution than the other Pt-halogen complexes.
- Unfortunately, all these methods did not include electrochemical processes in order to understand the kinetic behaviour of platinum in chloride media. Hence electrochemical studies will be conducted to understand the electrochemical behaviour of platinum in chloride/ozone media so as to obtain optimum conditions for leaching studies.

2.3 Thermodynamics

An E_h -pH diagram, also known as Pourbaix diagram, was devised by Marcel Pourbaix. Today it is a well-known tool for the study of thermodynamics where it gives indication of the tendency of electrode reactions to occur, whereas electrochemistry deals with the rates of those reactions. As can be derived from the explanation of Roine and Anttila (2006), an E_h -pH diagram is used to show the thermodynamic stability areas of different species in an aqueous solution. Hence the behaviour of Pt in the presence of an inorganic ligand chloride will be studied by an E_h -pH diagram to better understand the possible stability complexes of Pt chloro-complexes that can be formed. Stability areas are represented as a function of pH and electrochemical potential, and no corrosion kinetics is provided by these diagrams. Dotted lines in the diagrams show the chemical stability area of water. Roine and Anttila (2006) explain that above the upper dotted line, water is decomposed when oxygen is generated on the anode, as represented by the reaction:



They further explain that below the lower dotted line, water is decomposed due to hydrogen formation at the cathode, as represented by the reaction:



2.3.1 Thermodynamics of Pt and chloride ion

The platinum chloro-complexes formation reactions and constants found in literature are reported in Table 4 below.

Table 2.3: Stability constants of Pt with the Cl⁻ ligand (Elding, 1970)

Ligand	Element	Formula	Log β
	Pt		
Cl ⁻	Pt ²⁺	[ML]/[M][L]	5
	Pt ²⁺	[ML ₂]/[M][L] ²	9
	Pt ²⁺	[ML ₃]/[M][L] ³	11.9
	Pt ²⁺	[ML ₄]/[M][L] ⁴	14

Baghalha *et al.*, (2009) studied the thermodynamics in the form of an Eh – pH diagrams to predict Pt-Cl species using HSC software. The major Pt-Cl species identified were PtCl₆²⁻ and PtCl₄²⁻, and these species were found to be stable at pH levels below 6 and potential values of 0.5 to 1.5V. Platinum oxides formed over a wide pH range above 6.

Rojo *et al.*, (2011) studied the thermodynamics of Pt in HCl acidic media and the corresponding chloro-complexes formed were PtCl₆²⁻ and PtCl₄²⁻ at potential values of about 1.0 V and pH values of zero. Similarly Baghalha *et al.*, (2009) observed that platinum oxides form over a wide pH range.

Thermodynamic predictions of the stability of Pt in chloride media were used by Kelsall and Dawson (2007) with a view to possible leaching systems. Their predictions supported those of Rojo *et al.*, (2011) even with respect to the behaviour of platinum oxides.

2.4 Fundamentals of electrochemistry

Most of the information provided here was taken from textbooks in order to provide an overview of the basics of electrochemistry.

2.4.1 Introduction

According to ASM International (1987) aqueous corrosion of metals is an electrochemical process in which the electrode potential E_e and corrosion current i_{corr} are fundamentally important parameters. The corrosion current and the amount of metal corroded are related by Faraday's law:

$$i_{corr}t = \frac{nFw}{M} \quad (2.2)$$

where i_{corr} is the corrosion current in amps, t is the time in seconds, n is the number of... involved, F is the Faraday's constant equal to $96\,500 \text{ Cmol}^{-1}$, M is the molecular mass of the metal in grams, and w is the mass of the corroded metal in grams.

2.4.2 The Nernst equation

For the following oxidation half-cell reaction (CRC Handbook of Chemistry and Physics, (2001-2002):



the electrode potential is given by the famous Nernst equation which can be written as follows:

$$E = E^\circ - \frac{-2.3 RT}{nF} \log \frac{1}{[\text{Cl}^-]^4} \quad (2.3)$$

where E is the cell potential (V), E° is the standard electrode potential (V), T is temperature (K), n is the number of electrons, R is the universal gas constant ($\text{JK}^{-1}\text{mol}^{-1}$) and F is the Faraday constant ($9.648 \times 10^4 \text{ Cmol}^{-1}$).

2.4.3 Butler-Volmer Equation

According to Bard and Faulkner (1980), the expression relating overpotential and current density is the Butler Volmer equation which is expressed by the following reaction:

$$i = \left\{ \exp\left(\beta \frac{nF}{RT} \eta\right) - \exp\left[-(1 - \beta) \frac{nF}{RT} \eta\right] \right\} \quad (2.4)$$

An example of an anodic polarisation is shown in Figure 2.6 below and these curves for the reactions follow the Butler-Volmer equation, where R is the gas constant, T is the absolute temperature, n is the number of charges transferred, F is the Faraday's constant, β is the symmetry coefficient (taken to be close to 0.5), i_0 is the exchange current density.

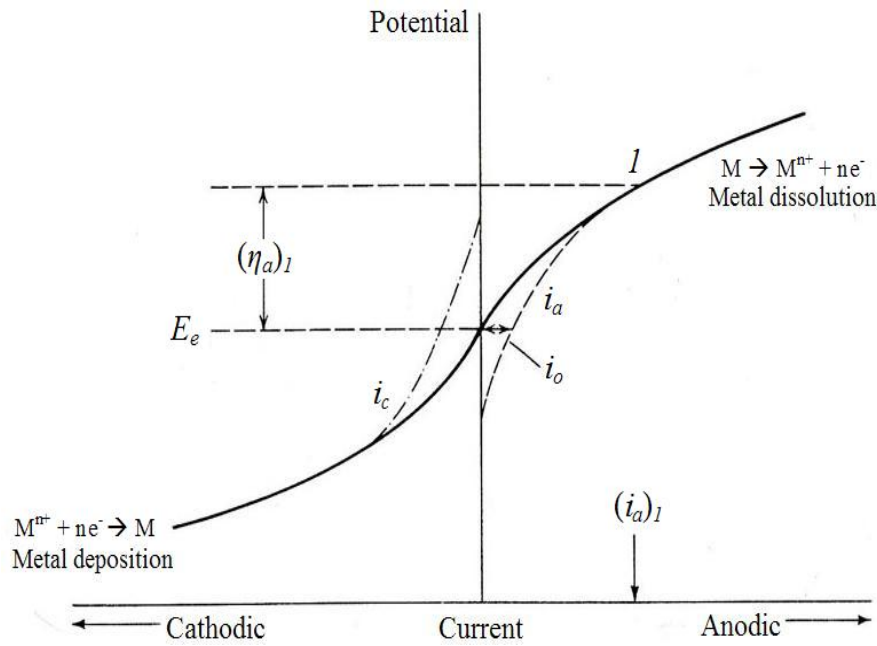


Figure 2.6: Current-potential for a metal dissolution and deposition (ASM International, 1987)

The term η is the overvoltage, defined by:

$$\eta = E - E_{eq} \quad (2.5)$$

and is a measure of how far the reaction is from equilibrium. By dropping the last term in the Butler-Volmer equation, the metal dissolution current is given by:

$$i_a = i_o \exp\left(\beta \frac{nF}{RT} \eta\right) \quad (2.6)$$

Taking logarithms and rearranging yields:

$$\eta_a = b_a \log\left(\frac{i_a}{i_o}\right) \quad (2.7)$$

Where b_a is the Tafel coefficient given by:

$$b_a = \frac{2.303 RT}{\beta nF} \quad (2.8)$$

and can be obtained graphically from the slope of a plot of η_a against $\log i_a$. The intercept of this plot yields a value for i_o . Similarly, at the cathodic overpotentials a Tafel coefficient can be obtained for the metal cation deposition:

$$b_c = - \frac{2.303 RT}{(1-\beta)nF} \quad (2.9)$$

A similar analysis can be performed for the cathodic process and Figure 2.7 (a) shows the two current-potential (polarisation) curves and Figure 2.7 (b) shows an Evans diagram.

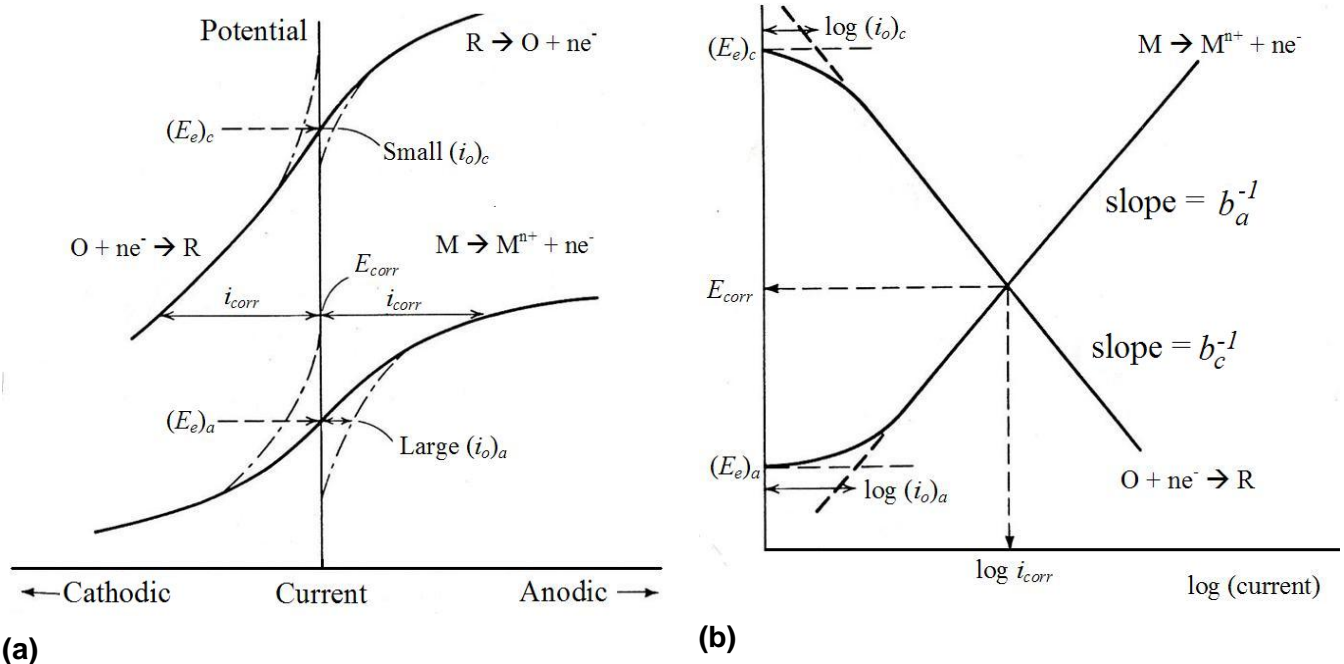


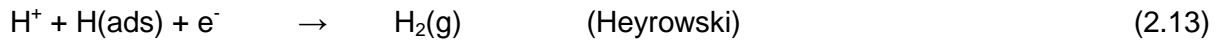
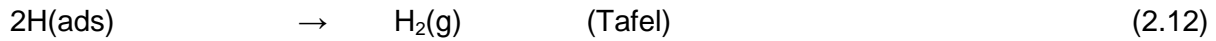
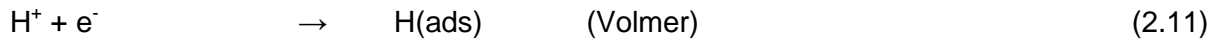
Figure 2.7: (a) Current-potential relationships for the metal/deposition and the accompanied redox reactions (b) Evans diagram (ASM International, 1987)

In the literature diagrams such as Figure 2.7 (b), are often plotted in the form $\log i$ versus E . The algebraic sign of the cathodic current is neglected so that the anodic and cathodic currents can be plotted in the same quadrant. Such diagrams are generally called Evans diagrams. The two linear portions in the $\log i$ versus E curves are the Tafel regions with slopes given by equation 2.8 and 2.9. The exchange currents for the two reactions can be obtained by extrapolating the Tafel lines back to the respective equilibrium potentials.

2.4.4 Passivation

If corrosion is allowed to build up at the surface, supersaturation with regard to solid oxides and hydroxides can occur, leading to film formation (West, 1970). The possibility of this occurring, can be established by inspection of the Pourbaix diagram. It is also known that the two most common processes found in the cathodic region are hydrogen ion reduction to

hydrogen and oxygen gas reduction to hydroxyl (West, 1965). The following steps indicate the hydrogen evolution mechanism as predicted in acidic medium (West, 1965):



The value of i_0 (exchange current density) for hydrogen on platinum metal is reasonably high at values of 10^{-2} A/cm^2 (West, 1965).

2.4.5 Arrhenius equation

According to House (1997), Arrhenius noted that the rate of most reactions varies with temperature and follows the equation below:

$$k = A \cdot e^{-E_a/RT} \quad (2.10)$$

where k is the rate constant, A is the pre-exponential factor, E_a the Arrhenius activation energy in KJ/mol, R is the gas constant and T the absolute temperature in K. Taking logarithms and rearranging, equation 2.10 yields:

$$\ln k = \ln A - \frac{E_a}{RT} \quad (2.11)$$

House (1997) further explains that if the Arrhenius equation is obeyed, a plot of $\ln k$ versus $1/T$ should give a straight line with a slope of $-E_a/2.303R$ and a Y-intercept of $\ln A$, and hence the activation energy E_a of the reaction can be calculated.

2.5 Electrochemistry of platinum

In electrochemistry, platinum is commonly used as an electrode due to the fact that it is highly resistant to corrosion. According to Bao (2007) it is accepted that Pt is covered with an oxide layer known as a passive film in aqueous solutions when a certain potential is exceeded. This process is known as corrosion. According to Shaw and Kelly (2006) corrosion is described as the degradation of a material due to a reaction with its environment. Hence, Ulick R. Evans, known as the “father of corrosion science” recognised Marcel Pourbaix’s work on E_h -pH diagrams as a means of understanding corrosion science better,

though they don't convey any corrosion kinetics. The electrochemical reactions can be divided into two or more partial reactions (oxidation and reduction reactions), and it is accepted to call them corrosion reactions. The following standard reduction potentials and half reactions will be used to understand the electrochemistry better.

2.5.1 Standard reduction potentials

(a) Oxidising agent

As seen in Section 2.1.1 the standard reduction potential of ozone in acidic media is as follows (CRC handbook of Chemistry and Physics, 2001-2002):



(b) Complexing agent

The complexing agent employed in this study is chloride. The standard reduction potential is as follows (CRC handbook of Chemistry and Physics, 2001-2002):

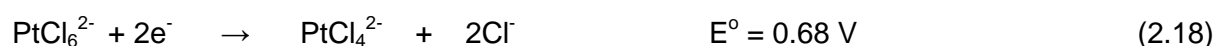


(c) PGM complexes

At standard conditions, the standard reduction potential, the E° , for Pt is as follows (CRC handbook of Chemistry and Physics, 2001-2002):



Hence in aqueous chloride solutions, the standard potentials for the half reactions are (CRC handbook of Chemistry and Physics, 2001-2002):



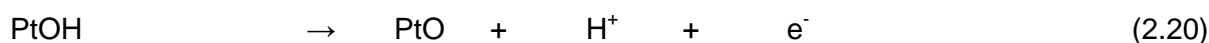
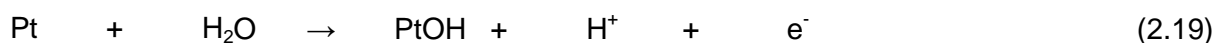
According to Mishra (1993), the standard potential for the formation of Pt chloro-complexes requires an oxidising agent with a reduction potential greater than 0.75V and the most stable chloride complex is PtCl_4^{2-} . Therefore in this study, ozone is a good candidate to act as oxidising agent due to high oxidation potential of 2.076V.

Taking this potential into account, ozone should be able to solubilise Pt metal from catalytic converters providing favourable reaction kinetics. Oxidising agents for which $E^{\circ} > 1.23\text{V}$ will result in the oxidation of water, which will lower the amount of oxidant available for Pt dissolution; hence, more oxidant could be required (Wu, 1993). Oxidation of Pt metal in chloride medium will therefore occur if the potentials of the reduction reactions are high enough. Considering that the standard reduction potentials of all Pt-chloride complexes are lower than that of chloride, ozone will oxidise the metal rather than the chloride ion.

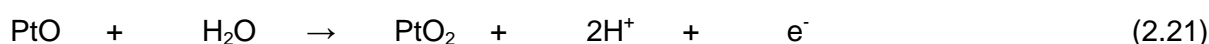
2.5.2 Chemistry of platinum and chloride

Juvekar *et al.*, (2011) studied the oxidation of chloride ions on the Pt electrode, and the dynamics of the electrode passivation and its effect on oxidation. They observed that in the presence of sodium chloride, chloride ions compete with water molecules to occupy the electrode surface. For high positive potentials leading to oxygen evolution, they observed that the concentration of the chloride ions on the surface is expected to be very high because of the high negative charge they possess. On the other hand, it was observed that Pt undergoes passivation, forming an oxide layer which can also be reduced.

The formation of platinum hydroxide and monoxide forms at potentials lower than 1V as seen in the following equations:



Hence, at potentials above 1.2V, platinum oxide at oxidation state +2 oxidizes further to platinum oxide at oxidation state +4 as follows:



Littauer and Shreir (1966) studied anodic polarization of Pt in sodium chloride solutions. They observed that chlorine evolution occurred on a clean Pt surface at a potential of about 1.6 V, but at higher potentials surface oxide formed on the electrode and a rapid potential jump occurred. They also observed the reactions of platinum oxides as reported by Juvekar *et al.*, (2011).

2.5.3 Summary

- The associated conditions of a specific leach solution, i.e. ligand concentration, the PGM complex that can be formed, and therefore, the corresponding standard potentials that can be achieved, will determine whether or not leaching will occur, and the extent thereof.

2.6 Conclusions

- In Chapter 1, Figure 5, it is shown that the recovery of PGMs from autocatalysts has increased tremendously over the past years.
- These tremendous increases indicate that reliable technologies for recovering PGMs are required.
- Different combinations of oxidants can be used in conjunction with the complexants to provide optimum leaching conditions.
- Ozone, being the fourth most powerful oxidising agent known, will be employed in this study as an oxidant in the presence of chloride ions as complexing agents to recover PGMs from virgin automotive catalytic converters.

CHAPTER 3

EXPERIMENTAL

3.1. Thermodynamics

The E_h -pH module of HSC Chemistry allows the construction of diagrams in a highly flexible and fast way, as the user can draw the diagrams exactly at the selected temperature and concentrations (Roine & Anttila, 2006).

3.1.1 Experimental

In order to construct Pourbaix diagrams or E_h -pH diagrams for Pt metal, enthalpy values had to be obtained. Enthalpy values could be obtained for different complexes from which the formation enthalpy could be calculated. A computer package, HSC Chemistry 5, developed by Outokumpu, was employed to construct Pourbaix diagrams for Pt and chloride ion. The IUPAC Database of Stability Constants and NIST Database for Critically Selected Stability Constants were employed to search for the available stability constants for complexes of Pt, with Cl^- , as well as OH^- but there were no stability constants of Pt with OH^- since HSC's database is by no means complete, especially for Pt metal.

From the stability constants obtained in literature, calculations were conducted on that data to obtain the required thermodynamic data. The Gibbs free energy for each complex can be calculated by using the following equation:

$$\Delta G^o = -RT 2.303 \log \beta \quad (3.1)$$

where R is the universal gas constant, T is the temperature and β is the overall formation constant of a specific complex. To calculate the standard Gibb's free energy of formation, equation 3.2 was used.

$$\Delta G_f^o = \sum \Delta G_f^o \text{ products} - \sum \Delta G_f^o \text{ reactants} \quad (3.2)$$

For each of the cations and anions involved in complexation, the standard enthalpy of formation and entropy of formation are listed in Table 6 below. These values were obtained from HSC Chemistry and the CRC Handbook of Chemistry and Physics (70th edition).

Table 3.1: Thermodynamic data for the individual cation and anion

Ion	H _f ^o , kJ/mol	S _f ^o , kJ/(mol.K)
Pt ²⁺	243.55	-9.0000E-02
Cl ⁻	-167.08	5.6735E-02

The database of HSC requires enthalpy (H) and entropy (S) values for each complex. If no entropy data is available a value of zero for the entropy is assumed. This does not result in a crude error of the calculated Gibbs free energy as the entropy values are small and does not contribute substantially to the value of the Gibbs free energy. The subsequent calculated ΔG_f^o value is then used as the enthalpy value. Appendix A contains all the calculated ΔG_f^o values. It has to be noted that much more data is available on the complexation of Pt with chloride than with hydroxide.

3.2 Electrochemistry

A well-known complexing agent in the leaching of gold is chloride. It has many advantages, namely that it is inexpensive and regularly available and suitable for most ore types (Gos & Rubo, 1997). The complexing agent that was employed for this study was supplied by the salt NaCl and the pH was controlled employing HCl. The oxidant employed was ozone.

3.2.1 Materials

3.2.1.1 Hydrochloric acid

Saarchem was the supplier of 32% pure AR HCl with a density of 1.16 kg/dm³. This acid was diluted to 4 M concentration to ease the preparation of sample solutions. Afterwards the 4 M was taken as a stock solution and standardised to determine the concentration.

3.2.1.2 Sodium chloride

Sodium chloride with a purity of 99.5% AR was purchased from ACE (Associated Chemical Enterprises) to supply the complexing agent, i.e. chloride ions.

3.2.1.3 Ozone

Ozone was generated by an electric discharge from medicinal grade oxygen, supplied by Afrox (African Oxygen Limited), employing four ozone generators supplied by Sterizone, in a manifold depicted in Figure 3.1.



Figure 3.1: Ozone generator manifold

Solubility tests and stability tests were conducted using a ultra-violet spectrometer (Analytik Jena Specord S600) to obtain absorbance values, after bubbling ozone through different chloride ion solutions for periods ranging from 5 to 30 minutes.

From Figures 3.2, 3.3 and 3.4 it is clear that the concentration and lifetime of ozone is dependent on pH, temperature and chloride ion concentration.

The concentration of ozone was calculated for each condition by applying the Beer Lambert law

$$A = \epsilon b c \quad (3.1)$$

in the wavelength range of 260 to 400 nm as the wavelength for maximum absorption was not known exactly. A is the absorbance, ϵ the molar absorptivity ($\ell \text{ mol}^{-1} \text{ cm}^{-1}$), b the path length of the sample (cuvette) and c is the concentration of the compound in solution ($\text{mol } \ell^{-1}$). This has to be kept in mind when comparing Figures 3.2 to 3.4.

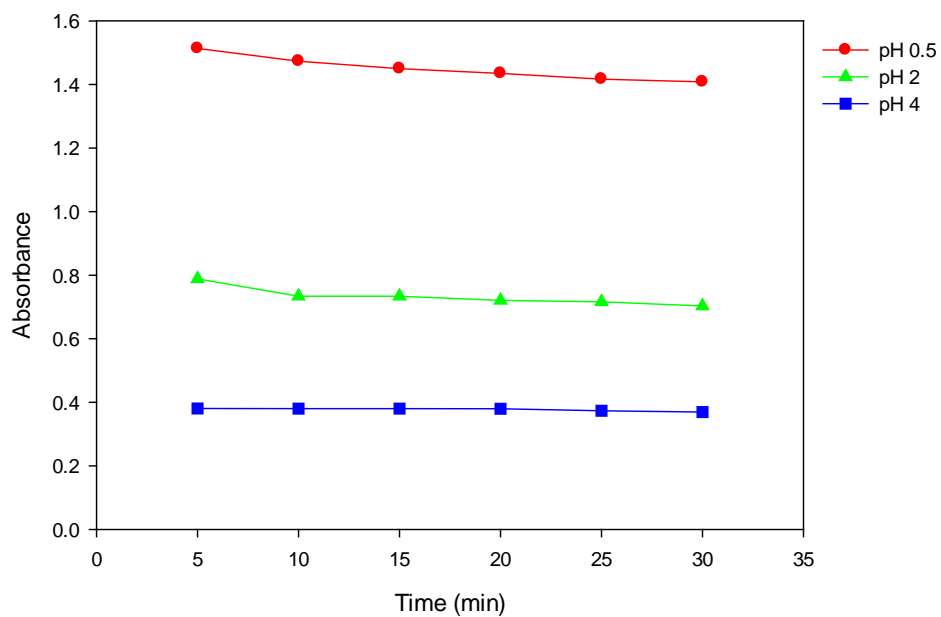


Figure 3.2: Plot of absorbance of ozone for different pH levels at 1M Cl⁻ and 15°C

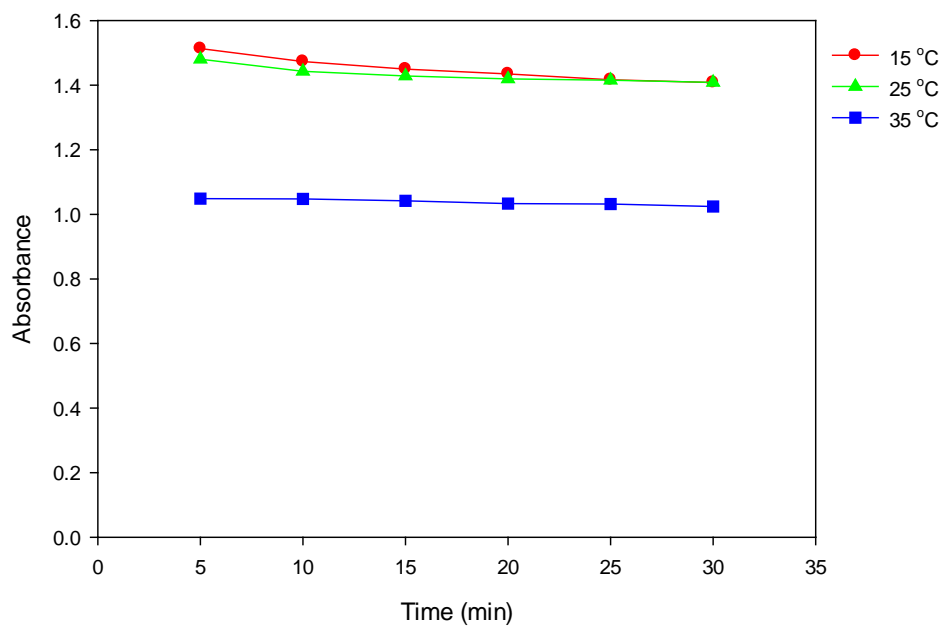


Figure 3.3: Plot of absorbance of ozone for different temperatures at 1M Cl⁻ and pH 0.5

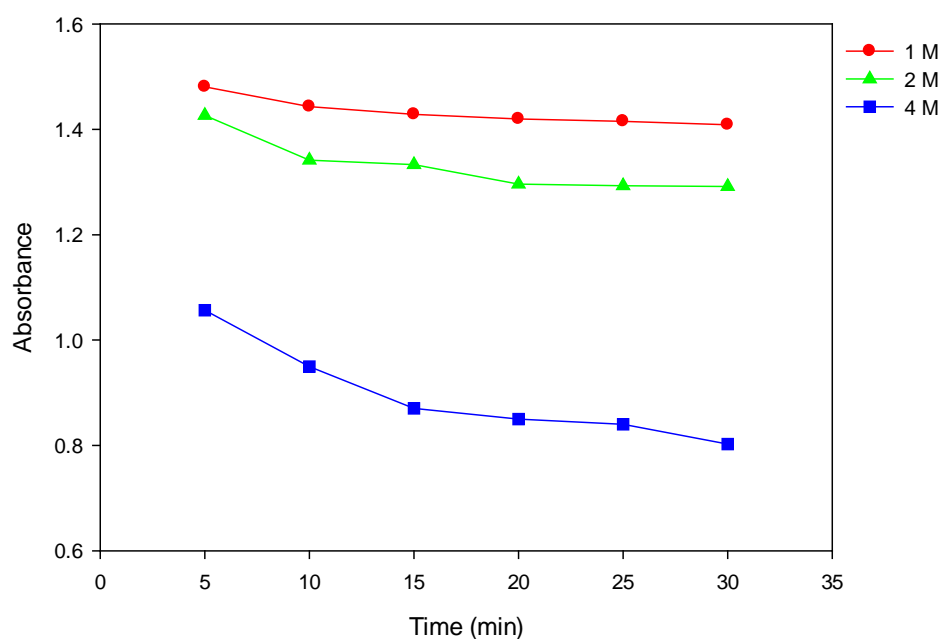


Figure 3.4: Plot of absorbance of ozone for different [Cl⁻] at 15 °C and pH 0.5

Therefore, subsequently, in all electrochemical studies, ozone (which was generated from oxygen at a flow rate of 1.92 l min⁻¹) was bubbled through electrolytes for a fixed period of 5 minutes.

3.2.1.4 The platinum working electrode

A platinum electrode of purity 99.9%, purchased from Pine Instruments, was used as a working electrode. The area of the working electrode was 0.196 cm².

3.2.2 Experimental apparatus

For electrochemical and leaching studies, deionised water from a Millipore Milli-Q system was used for all purposes. A Metrohm Swiss Made pH meter 827 pH lab was used to obtain the necessary pH values by addition of HCl. Twenty-seven solutions of chloride with different concentrations, pH levels and temperatures were prepared as are shown in Table 7 below. Appendix B shows the numbering of the twenty-seven solutions containing chloride.

Table 3.2: Chloride solutions

[Cl ⁻] (mol/dm ³)	Temperature								
	15°C			25°C			35°C		
	pH	NaCl(g)	HCl (ml)	pH	NaCl (g)	HCl (ml)	pH	NaCl(g)	HCl (ml)
1	0.5	19.87	8	0.5	19.87	8	0.5	19.87	8
	2	28.93	0.25	2	28.93	0.25	2	28.93	0.25
	4	29.22	0.003	4	29.22	0.003	4	29.22	0.003
2	0.5	49.09	8	0.5	49.09	8	0.5	49.09	8
	2	58.15	0.25	2	58.15	0.25	2	58.15	0.25
	4	58.44	0.003	4	58.44	0.003	4	58.44	0.003
4	0.5	107.53	8	0.5	107.53	8	0.5	107.53	8
	2	116.59	0.25	2	116.59	0.25	2	116.59	0.25
	4	116.88	0.003	4	116.88	0.003	4	116.88	0.003

3.2.2.1 Experimental methods

Prior to each experiment, the working electrode was wet polished using, first 5.0 µm gamma alumina, followed by 0.05 µm alumina, and rinsed with deionised water. After drying the electrode was placed in the test solution in the electrochemical cell.

3.2.2.2 The electrochemical set-up

A conventional three-electrode electrochemical cell was employed in this study, as shown in Figure 3.5. This consisted of a Pt counter electrode [3], a Ag/AgCl reference electrode [1], and a Pt working electrode [2]. In the electrolyte the current was carried between the working and the counter electrode by ions in solution and external to the cell by means of electron flow, regulated by a potentiostat.

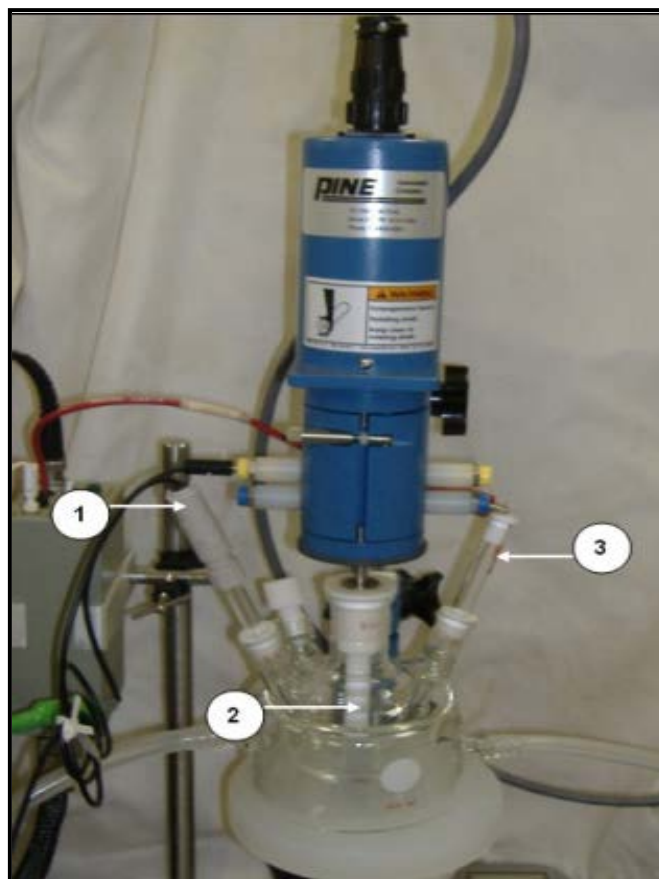


Figure 3.5: Electrochemical cell set-up

A potentiostat is a device used to keep a working electrode WE (2) at a desired potential with respect to a reference electrode RE (1). This is done by a current which is passed from the working electrode to a counter electrode CE (3). A potentiostat, PAR Model 273A, equipped with a rotating disc working electrode and employing PowerSuite Software, was used in this study. The platinum electrode was kept stationary in all instances.

Figure 3.6 displays the complete set-up of electrochemical investigation. A self-regulating water bath [3] was used to control the cell temperature. This water bath was connected to the cell jacket [1] with plastic tubes and the water was circulated to achieve the desired temperature. The electrolyte was purged with pure nitrogen for 15 minutes to remove dissolved gases. Ozone was dispersed through the solution from four ozone generators [4] converting oxygen into ozone.



Figure 3.6: Electrochemical investigation set-up

3.2.2.3 Electrochemical investigation

Appropriate conditions for the formation of stable aqueous ions from thermodynamics (E_h -pH diagrams) were retrieved. The oxidation of Pt (in the form of an electrode) was tested under these conditions.

A polarisation curve is described as an electrochemical measuring technique employed for the determination of kinetics and mechanism of electrode reactions. The potential of the working electrode is controlled with a potentiostat and the current flowing through the electrode is measured. Thus, the amount of current generated during each scan gives an indication of the measure to which oxidation reactions are occurring. Polarisation curves were conducted with and without the presence of ozone. The potential was varied from the equilibrium potential to the anodic direction (+2V) and from equilibrium potential to the cathodic direction (-2V) vs SHE for all the polarisation curves. The potential of Ag/AgCl, KCl (sat.) reference electrode was first converted to SHE scale at each temperature and different chloride ions concentration by using the Nernst equation. Once the equilibrium potential of the reference electrode is known at any temperature and different chloride ion concentrations, the measured potential can be converted to the SHE scale. Then the two curves were combined in order to extrapolate Tafel slopes, E_e and i_0 . For each run, the cell was cleaned and the new solution was added. The Pt electrode was polished prior to each run so as to ensure a smooth and uniform contact surface for the liquid and solid phases. The reference electrode drainage hole, typically at the top of the electrode, was opened

during measurements, allowing electrolyte solution to slowly flow through the porous junction into the external solution.

3.3 Leaching

The dissolution process is facilitated by a complexing agent and an oxidising agent in order to dissolve the metal.

3.3.1 Automotive catalytic converters

The leaching experiments conducted required a Pt-containing sample. Johnson Matthey supplied unused autocatalyst material as the source for the Pt recovery. The autocatalyst comprised a ceramic substrate which was coated with platinum, palladium and rhodium. The exact loadings were supplied by Johnson Matthey and need to remain confidential. The unused automotive converter catalyst was crushed to a particle size range of 1–2 mm in order to enhance the contact surface for the leaching reactions.

3.3.2 Leaching apparatus

The leaching set-up is shown in Figure 3.7. The leaching cell is a round-bottomed container with a five-necked lid [5]. An overhead stirrer [2] facilitates the suspension of the solid particles in solution. The stirrer is inserted through the middle neck of the leaching cell lid. The remaining necks of the cell lid host an ozone disperser, which is linked to the ozone generators [6], a thermostat [3], a thermocouple [4] and a Liebig cooler [1]. The thermocouple, heating mantle and LCD display controller form the electronic temperature controller. Even heat distribution was optimised by inserting a piece of aluminium foil between the cell and the heating mantle. Lastly, the Liebig cooler [1] minimises evaporation and solution loss.

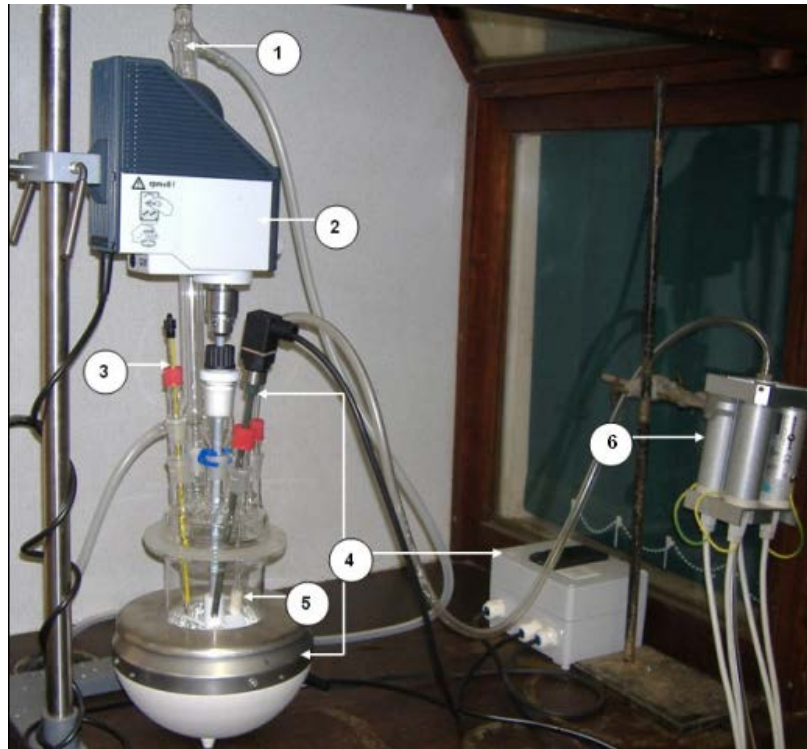


Figure 3.7: Leaching set-up

3.3.3 Physical leaching runs

Once the solution containing the sample material had reached the required temperature, it was stirred at ± 300 rpm for 8 hours but and ozone was dispersed for the duration of each run and for every 2 hours a sample was taken.

3.3.3.1 Treatment of leaching solutions

Upon completion of a leach run, the leach solution was filtered using a Büchner funnel as seen in Figure 3.8, connected to a vacuum pump.

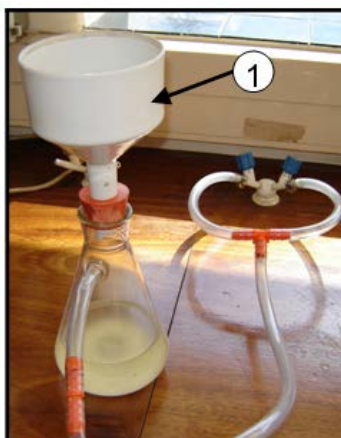


Figure 3.8: Büchner funnel

3.3.3.2 Solution analysis

The leach solutions obtained subsequent to filtration were made up to 2 litres in a standard flask and a final sample of 10 ml was analysed for platinum content using ICP – OES *iCap* 6000 series purchased from Thermo Fischer (Inductively Coupled Plasma – Optical Emission Spectrometer) as illustrated by Figure 3.9.



Figure 3.9: ICP – OES machine

CHAPTER 4

RESULTS AND DISCUSSION

4.1 Introduction

Pourbaix diagrams were used to obtain the different stability regions of the Pt-Cl-H₂O system. All Pourbaix diagrams were constructed using a metal ion concentration of 10⁻³ M, and chloride ion concentrations of 1 M, 2 M and 4 M at temperatures of 15°C, 25°C and 35°C. In the range of temperatures and ion concentrations employed no significant differences were observed between the different Pourbaix diagrams as can be seen in Appendix C. Therefore, only the stability regions of Pourbaix diagrams constructed at 25°C will be discussed in detail.

4.2 Pourbaix diagrams

It can be seen in Figure 4.1 that metallic Pt remains stable over a wide pH and potential range which confirms its property as a noble metal (with high resistance to corrosion and oxidation).

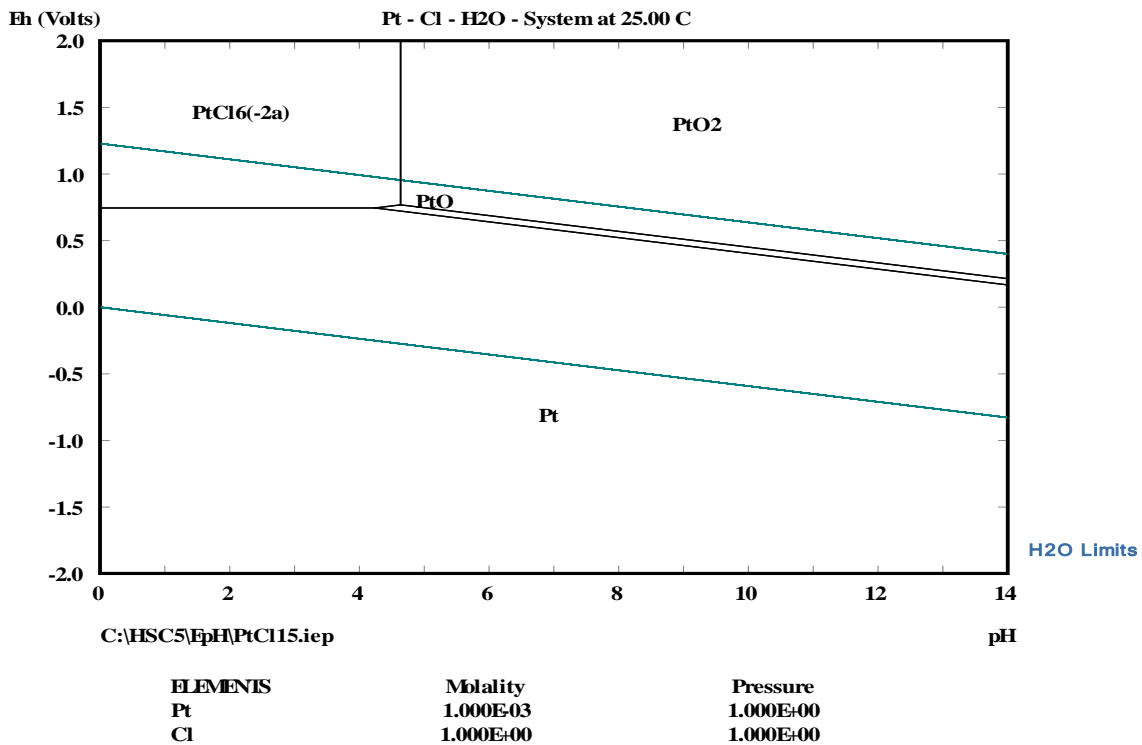


Figure 4.1: E_h-pH diagram of Pt-Cl-H₂O, 10⁻³M Pt⁺, 1M Cl⁻ at 25°C

The Oxides of Pt in the oxidation states II and IV are stable above pH 4; however, with the thermodynamic properties of Pt chloride complexes added to the HSC Chemistry database, it is clear that the aqueous complexes gain stability. With an increase in chloride concentration a small stability area of the PtCl_4^{2-} complex emerges, as can be seen in Figure 4.2. It is clear from the Pourbaix diagrams that platinum chloride complexes can be formed at pH values < 5 and redox potentials above 0.75 V. No formation constants for mixed chloride and hydroxide complexes of platinum are, however, known.

From the Pourbaix diagrams it can be concluded that, at high anodic potentials and pH below 5 Pt may be corroded to form PtCl_4^{2-} or PtCl_6^{4-} complexes, while at higher pH, passivation with the formation of PtO and/or PtO_2 is possible.

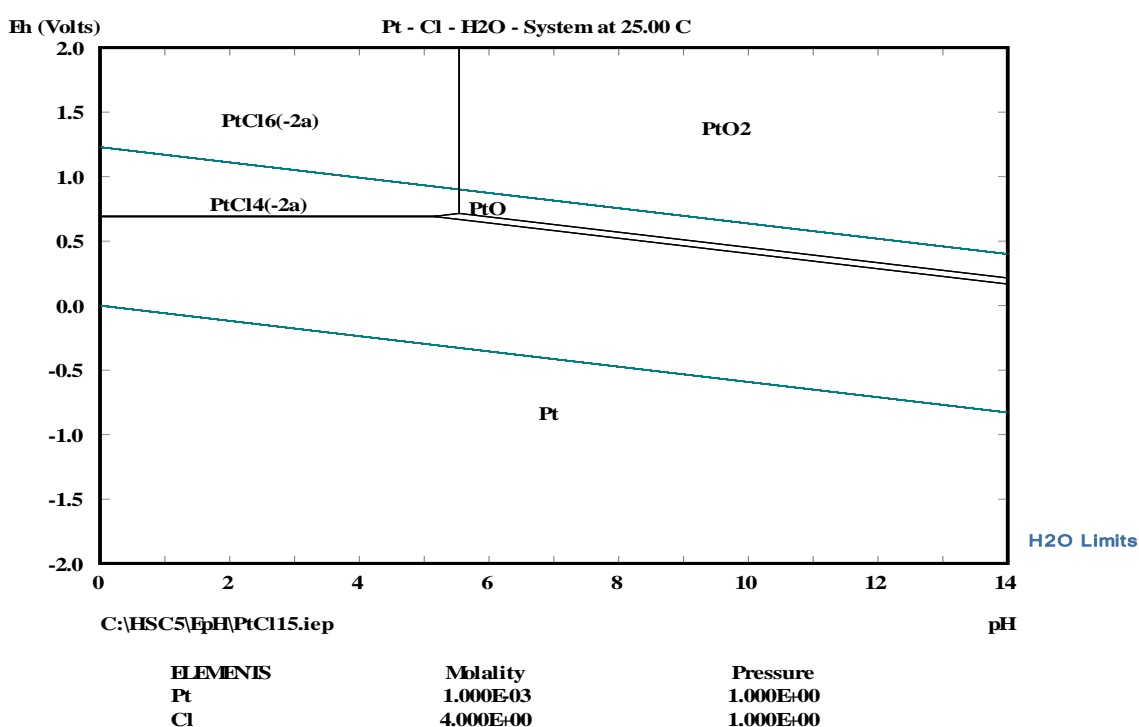


Figure 4.2: E_h -pH diagram of Pt-Cl-H₂O, 10^{-3}M Pt^+ , 4M Cl^- at 25°C

4.3 Potentiodynamic polarisation studies

The second part of this study was concerned with the electrochemistry of platinum. The determination of anodic and cathodic polarisation curves gave rise to the electrochemical data relating to the behaviour of platinum metal in solutions containing chloride ions and ozone.

4.3.1 Potentiostatic polarisation curves (Evans diagrams)

A total of eighty one polarisation curves were obtained under various conditions relating to the composition and the temperature of the supporting electrolyte. As many of these polarisation curves were identical, not all of them will be included in the discussion and are shown in Appendix D. Appendix E will show some of the different influences of temperature, chloride ion concentration and pH levels.

Figures 4.3 to 4.5 shown below are typical examples of the curves obtained and were selected for detailed analysis. In all cases, a constant polarisation rate of $10 \text{ mV}\cdot\text{s}^{-1}$ was employed with a stationary Pt electrode. Various areas of interest were identified in the polarisation curves. These include evidence of passivation, gas evolution and dissolution of passive films occurring at certain potentials.

4.3.2 Influence of temperature

Figures 4.3 (a) and 4.3 (b) illustrate the polarisation curves of platinum at different temperatures, where Figure 4.3 (a) is at 1 M chloride concentration and Figure 4.3 (b) is at 2 M chloride concentration in the presence of ozone.

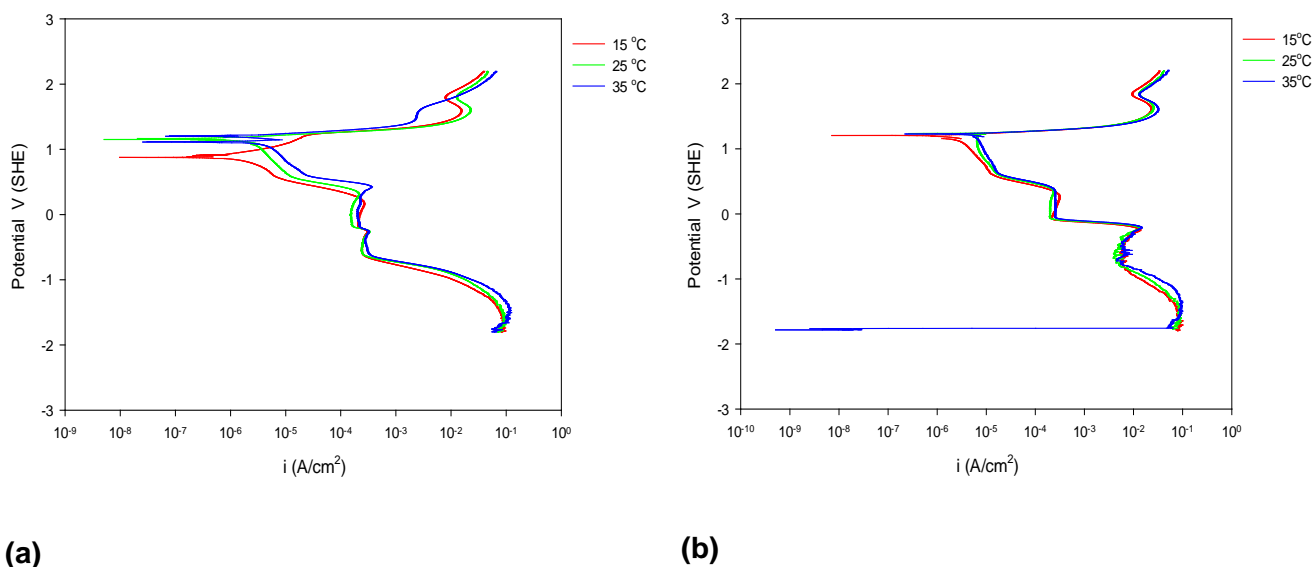
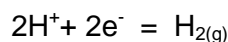


Figure 4.3: (a) Polarisation curve of Pt at different temperatures in 1M $[\text{Cl}^-]$ at pH 0.5 with ozone. (b) Polarisation curve of Pt at different temperatures in 2M $[\text{Cl}^-]$ at pH 0.5 with ozone.

The influence of temperature is not that significant, although a shift of the polarisation curves at higher temperatures can be observed. A striking feature of the cathodic curve in Figure 4.3 (b) is the sudden drop in current at the highest temperature (35°C), which is ascribed to the accumulation of hydrogen bubbles on the platinum electrode surface, indicating the onset of hydrogen evolution, as is expected from the Nernst equation (4.1), for the hydrogen evolution reaction:



$$E_e = E^o + \frac{2.3RT}{nF} \log K^{-1} \quad (4.1)$$

where K is the equilibrium constant.

4.3.3 Influence of chloride concentration

Figures 4.4 (a) and 4.4 (b) illustrate the polarisation curves of platinum at different chloride concentrations. As seen in the below Figures, as the chloride concentration is increased, there is a decrease in potential but increase in current density. Chloride is known to be an aggressive ion towards passive films which explains the shift of the polarisation curves to higher current densities.

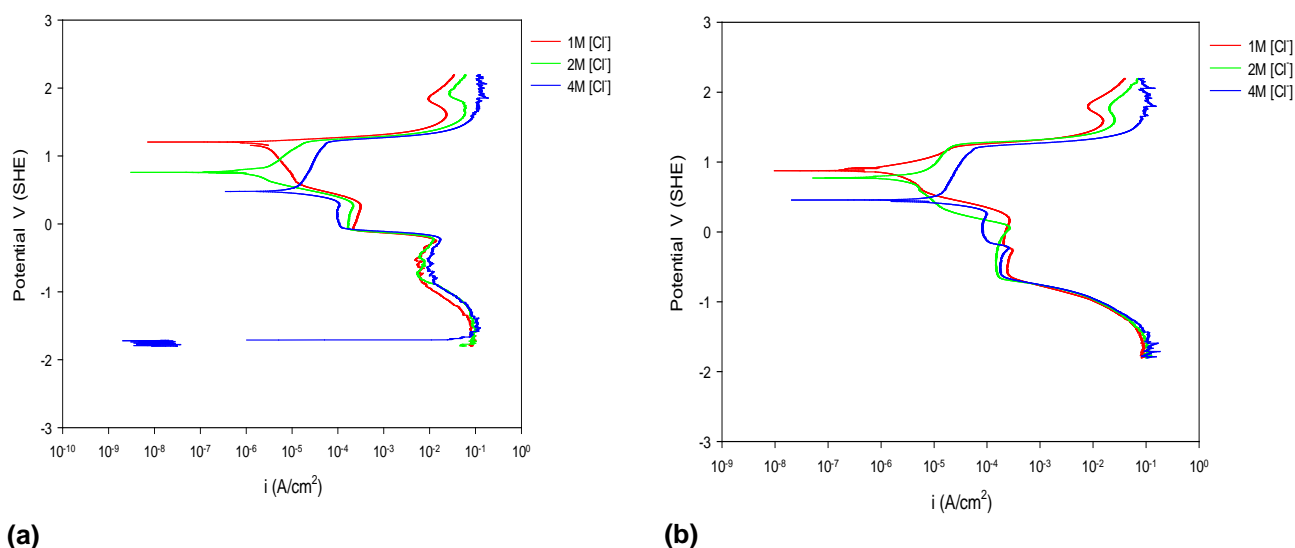


Figure 4.4: (a) Polarisation curve of Pt at different [Cl⁻] at pH 0.5 with ozone at 15°C. (b) Polarisation curve of Pt at different [Cl⁻] at pH 0.5 with ozone at 15°C.

It is also observed that in the cathodic region of Figure 4.4 (a) the current density drops rapidly as a result of the platinum surface being covered by the formation of hydrogen bubbles.

4.3.4 Influence of pH

Figures 4.5 (a) and 4.5 (b) below illustrate polarisation curves of platinum at different pH and temperature levels in 1 M and 4 M chloride ion concentrations in the presence of ozone. It is observed that as the pH increases, there is a decrease in potential but an increase in current density.

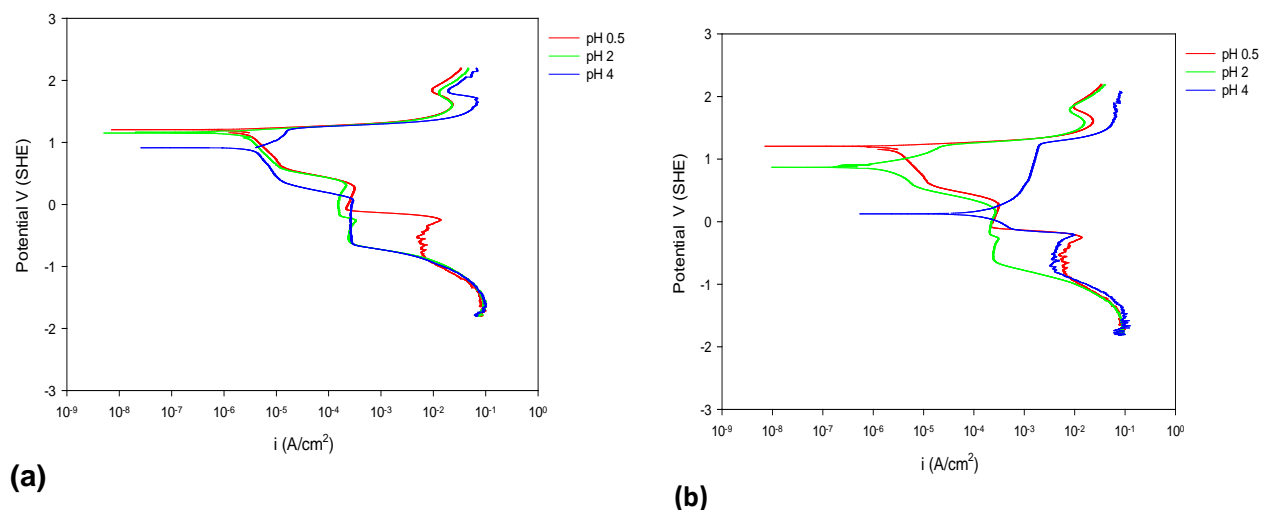


Figure 4.5: (a) Polarisation curve of Pt at different pH levels at 15°C in 1 M [Cl⁻] with ozone. (b) Polarisation curve of Pt at different pH levels at 15°C in 2 M [Cl⁻] with ozone.

The conclusion that can be reached is that the chloride ion concentration, pH and temperature have no overriding influence on the polarisation curves within the ranges studied.

4.3.5 Determination of exchange current density

The anodic and cathodic slopes were determined by constructing the tangent to the Tafel curves at overpotentials of +50 mV and -50 mV and the intersection of the straight lines obtained in order to determine the exchange current density (i_0).

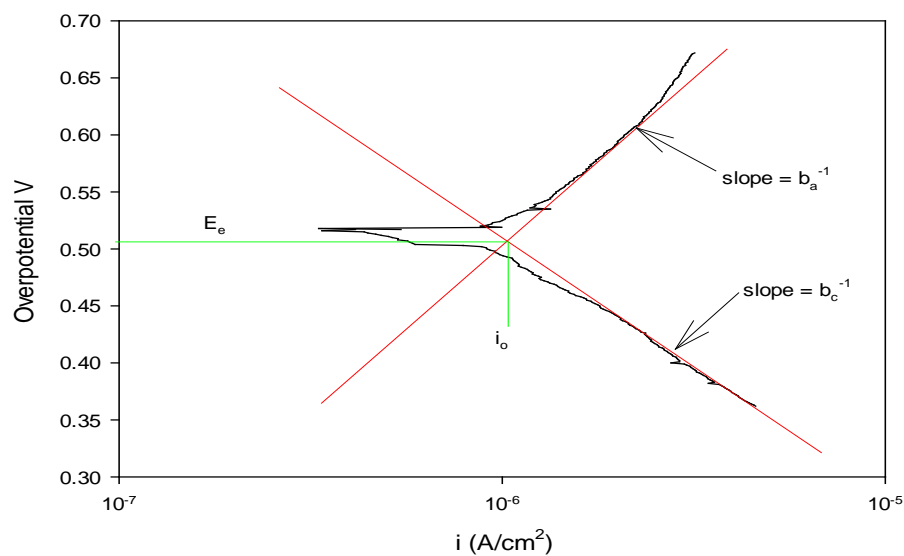


Figure 4.6: Polarisation curve of Pt in 1 M [Cl-] at 15°C, pH level of 0.5 in the absence of ozone

The data in Table 4.1 summaries the results obtained for the Tafel regions in the polarisation diagrams, but in the presence of ozone.

Table 4.1 Tafel parameters determined from experimental polarisation curves

Chloride concentration(mol/dm ³)	pH level	Temperature (°C)	E _e (V)	i _o (A/cm ²)	b _a (V/dec)	b _c (V/dec)
1	0.5	15	1.206	-5.925	0.294	-0.032
1	2	15	0.887	-5.895	0.265	-0.038
1	4	15	0.447	-5.875	0.254	-0.047
2	0.5	15	0.782	-5.860	0.245	-0.048
2	2	15	0.761	-5.761	0.227	-0.050
2	4	15	0.498	-5.683	0.215	-0.055
4	0.5	15	0.485	-5.677	0.136	-0.064
4	2	15	0.457	-5.668	0.132	-0.067
4	4	15	0.291	-5.664	0.113	-0.075
1	0.5	25	1.229	-5.622	0.072	-0.079
1	2	25	1.165	-5.613	0.070	-0.082
1	4	25	0.890	-5.530	0.062	-0.097
2	0.5	25	1.185	-5.435	0.062	-0.107
2	2	25	1.075	-5.407	0.057	-0.114
2	4	25	0.875	-5.396	0.047	-0.114
4	0.5	25	1.205	-5.377	0.043	-0.119
4	2	25	1.148	-5.326	0.041	-0.129
4	4	25	0.699	-5.323	0.036	-0.155
1	0.5	35	1.22	-5.264	0.036	-0.169
1	2	35	1.195	-5.260	0.033	-0.185
1	4	35	0.905	-5.232	0.029	-0.199
2	0.5	35	1.221	-5.186	0.028	-0.256
2	2	35	1.019	-5.179	0.022	-0.272
2	4	35	0.922	-5.159	0.022	-0.284
4	0.5	35	1.211	-5.089	0.019	-0.295
4	2	35	1.105	-5.071	0.016	-0.332
4	4	35	0.934	-5.064	0.016	-0.477

4.3.6 Activation energy of the Tafel region

Figure 4.7 below illustrates how the slopes were obtained from Arrhenius plots to calculate the activation energy. Other graphs can be seen in Appendix F and they followed the same trend.

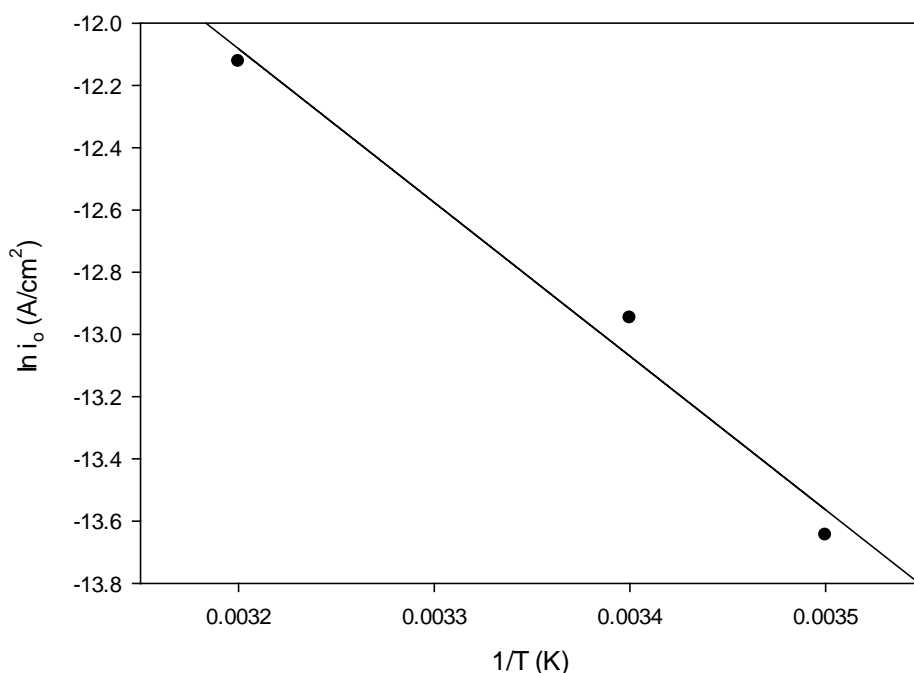


Figure 4.7: Arrhenius plots for determining the activation energy of Tafel processes in 1 M [Cl⁻] of pH 0.5 in the presence of ozone

It can be seen that with increase in temperature, there is an increase in the exchange current density (apparent rate constant). If the Arrhenius equation is obeyed in a plot of $\ln i_0$ vs $1/T$ a straight line should be obtained, unless it can be shown that a change in reaction mechanism is involved. With only three data points this possibility cannot be proven. Nevertheless a linear regression analysis was performed in order to obtain the approximate values of the apparent activation energies. The analyses yielded the activation energies at different chloride concentrations as shown in Table 4.2.

As seen in Table 4.2 the activation energies found range from about 55 to about 81 kJ/mol. These values point to strong interaction between the chloride ions and ozone in the Tafel region. The values are, however too low to indicate definite chemical reactions (the activation energies of which normally lie between 80 and 240 kJ mol⁻¹) and possibly indicate strong chemical adsorption (or weak chemical reaction) on the platinum surface. Physical adsorption is typically expected to have activation energies below about 40 kJ/mol.

Table 4.2: Activation energies of Tafel regions in the presence of ozone

[Cl ⁻](mol/dm ³)	pH level	ln i ₀	1/T(K)	Slope	Activation energy(kJ/mol)
1	0.5	-13.64528	0.0035		
1	0.5	-12.94747	0.0034		
1	0.5	-12.12299	0.0032	-6978.09	58.02
1	2	-13.57619	0.0035		
1	2	-12.92674	0.0034		
1	2	-12.11378	0.0032	-6994.46	58.15
1	4	-13.53013	0.0035		
1	4	-12.73559	0.0034		
1	4	-12.0493	0.0032	-7945.35	66.06
2	0.5	-13.49558	0.0035		
2	0.5	-12.51681	0.0034		
2	0.5	-11.94336	0.0032	-9787.75	81.38
2	2	-13.26758	0.0035		
2	2	-12.45232	0.0034		
2	2	-11.92724	0.0032	-8152.62	67.78
2	4	-13.08795	0.0035		
2	4	-12.42699	0.0034		
2	4	-11.88118	0.0032	-6609.61	54.95
4	0.5	-13.07413	0.0035		
4	0.5	-12.38323	0.0034		
4	0.5	-11.71997	0.0032	-6909	57.44
4	2	-13.0534	0.0035		
4	2	-12.26578	0.0034		
4	2	-11.67851	0.0032	-7876.26	65.48
4	4	-13.04419	0.0035		
4	4	-12.25887	0.0034		
4	4	-11.66239	0.0032	-7853.23	65.29

As seen in Table 4.3, in the absence of ozone, the activation energies are very low compared with the values in Table 4.2. From the results it appears that increasing the pH in different chloride ion concentration, is generally associated with a decrease in the activation energy, although it has to be pointed out that the pH was not constant in these data sets. The activation energies found suggest physical adsorption in the Tafel region.

The conclusion is that if ozone is present in the solution, the chemical adsorption of chloride ions seems to be promoted.

Table 4.3: Activation energies of Tafel regions in the absence of ozone

[Cl ⁻](mol/dm ³)	pH level	ln i ₀	1/T(K)	Slopes	Activation energy(KJ/mol)
1	0.5	-14.69544	0.0035		
1	0.5	-14.56417	0.0034		
1	0.5	-14.41908	0.0032	-1312.7	10.91
1	2	-14.25096	0.0035		
1	2	-14.13812	0.0034		
1	2	-14.07363	0.0032	-1128.47	9.38
1	4	-13.83182	0.0035		
1	4	-13.82721	0.0034		
1	4	-13.80649	0.0032	-103.635	0.86
2	0.5	-13.67521	0.0035		
2	0.5	-13.67061	0.0034		
2	0.5	-13.49558	0.0032	-875.14	7.28
2	2	-13.39195	0.0035		
2	2	-13.32516	0.0034		
2	2	-13.17546	0.0032	-748.475	6.22
2	4	-13.16625	0.0035		
2	4	-13.14322	0.0034		
2	4	-12.9728	0.0032	-852.11	7.08
4	0.5	-12.85074	0.0035		
4	0.5	-12.84383	0.0034		
4	0.5	-12.78165	0.0032	-310.905	2.58
4	2	-12.67111	0.0035		
4	2	-12.57208	0.0034		
4	2	-12.41317	0.0032	-990.29	8.23
4	4	-12.24505	0.0035		
4	4	-12.19208	0.0034		
4	4	-10.58689	0.0032	-529.69	4.4

4.3.7 Discussion of potentiodynamic results

4.3.7.1 Absence of ozone

In the absence of ozone, as illustrated by Figure 4.8, possible anodic and cathodic reactions can be identified and are marked with letters A, B, C, etc. All the polarisation curves behaved similarly.

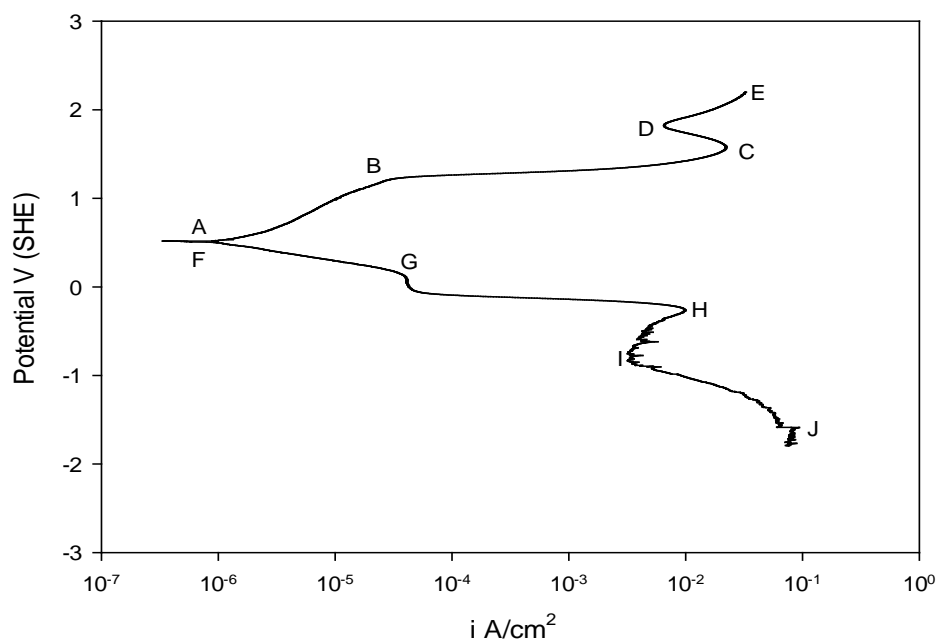


Figure 4.8: Polarisation curve of Pt in 1M [Cl⁻], pH of 0.5 at 15°C without ozone

Point A on the anodic side represents the equilibrium potential. Region AB represents the possibility of metal oxidation, probably to an oxide or a hydroxide. All the electrode potentials quoted were obtained from CRC Handbook of Chemistry and Physics, (2001-2002).



The possibility of the formation of platinum chloro-complexes can, however, not be ruled out, for example the reactions:



Region BC can be ascribed to water oxidation by the following reaction:



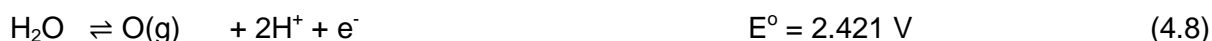
Point C can be ascribed to chlorine evolution as represented by the following reaction:



There is also a possibility of platinum oxide in oxidation state +4 being oxidized further to oxidation state +6 as shown by the following reaction:



The current minimum between D and E can probably be ascribed to the formation of a surface film of unknown composition; the potential at which it forms is not found in the available potential tables. Point E can be ascribed to oxygen evolution by the following reaction:



On the cathodic side there are also several possible reactions that can take place, where Point F is the equilibrium potential. Region FG (Tafel region) can be ascribed to the desorption of chemisorbed gases on the platinum surface. At a potential of about -1 V the stepwise reduction of platinum oxides is feasible (refer reactions below):

Point G also coincides with regular hydrogen evolution, i.e. $2\text{H}^+ + 2\text{e}^- = \text{H}_2$ at 0 V.



Region HI is ascribed to the reduction of platinum hydroxide according to the following reaction:



Region J indicates the onset of hydrogen evolution.

4.3.7.2 In the presence of nitrogen

In the presence of nitrogen shown by Figure 4.9 below, Region AB on the anodic side represents the equilibrium potential. Region BC represents the possibility of metal oxidation,

probably to an oxide or a hydroxide as shown by reactions 4.2 to 4.4. Region CD can be ascribed to water oxidation by the equation 4.5. Point D can be ascribed to chlorine evolution, as shown in reaction 4.6. There is also a possibility of platinum oxide in oxidation state +4 being oxidized further to oxidation state +6 as shown by reaction 4.7. Same as in Figure 4.5 the current minimum between D and E probably can be ascribed to a surface film of unknown composition; the potential at which it forms is not found in the available potential tables. Region EF can be ascribed to oxygen evolution by reaction 4.8.

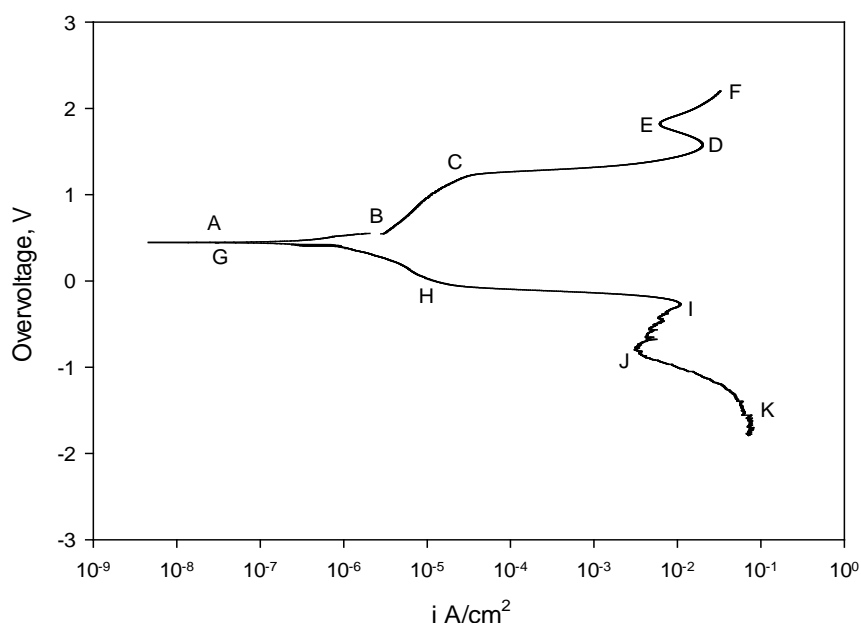


Figure 4.9: Polarisation curve of Pt in 1M [Cl⁻] pH of 0.5 at 15°C with N₂

On the cathodic side Point G is classified as the equilibrium potential. Region GH can be ascribed to the desorption of chemisorbed gases on the platinum surface. At a potential of about -1 V the stepwise reduction of platinum oxides is feasible according to reaction 4.9 and 4.10. Region IJ is ascribed to the reduction of platinum hydroxide according to reaction 4.11. Region JK indicates the onset of hydrogen evolution.

4.3.7.3 In the presence of ozone

In the presence of ozone, as illustrated by Figure 4.10, possible reactions on the anodic side are described by Point A which is at the equilibrium potential. As the potential proceeds Region AB can also present water oxidation, formation of an oxide on platinum and a hydroxide as described by reactions 4.2 to 4.5. Region B represents chlorine evolution which

is represented by reaction 4.6. Furthermore, an oxide can oxidise further according to reaction 4.7. Region CD indicates oxygen evolution which is described by reaction 4.8.

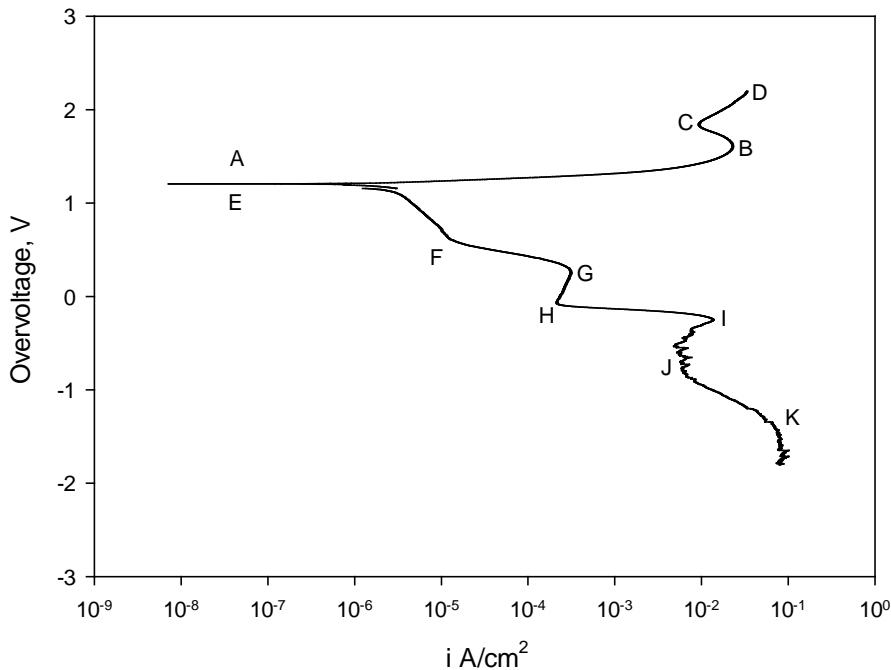
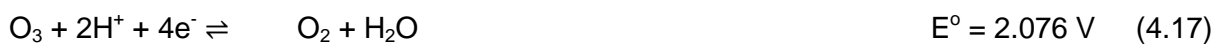


Figure 4.10: Polarisation curve of Pt in 1M [Cl⁻] pH of 0.5 at 15°C in the presence of ozone

On the cathodic side, region E indicates the equilibrium potential and region EF represents ozone being reduced to oxygen because it has a high redox potential of 2.07 V according to the following reaction:



Hence it reduces first. Region FG and GH can be ascribed to the desorption of chemisorbed gases on the platinum surface. Region IJ can be ascribed to the reduction of platinum hydroxide according to reaction 4.11 and Region JK indicates the onset of hydrogen evolution. Figure 4.11 represents an overview of polarisation curves in the presence and absence of ozone and nitrogen. It can be seen that ozone does have a significant influence on the electrode potential but has a less prominent influence on the current densities.

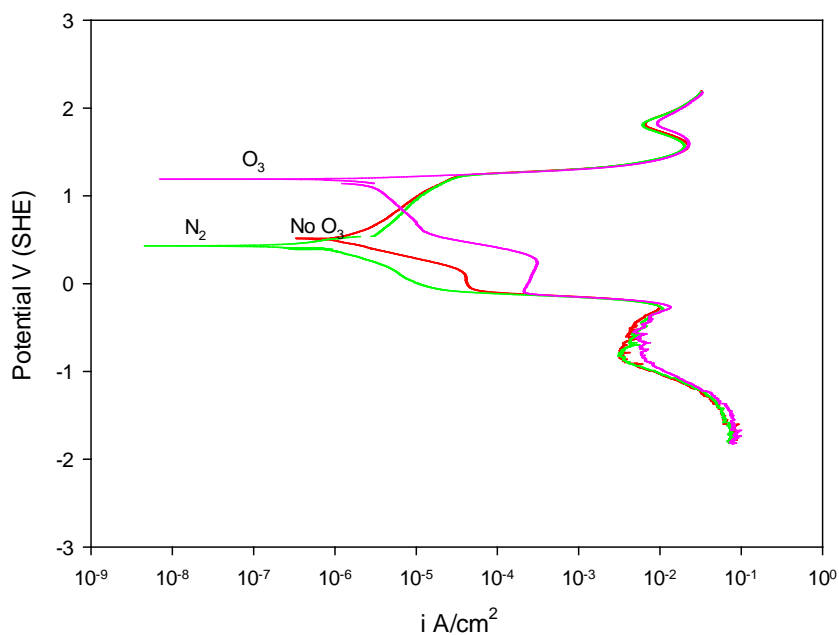


Figure 4.11: Polarisation curves of Pt in 1M [Cl⁻] pH of 0.5 at 15°C without ozone, with N₂ and in the presence of ozone

4.4 Leaching

Based on the outcome of the thermodynamic and electrochemical studies, leaching was conducted on several, but not all, solutions of different chloride ion concentrations, different temperatures and different pH levels in the presence of ozone. From polarisation curves discussed in section 4.3.2 to 4.3.3 it can be concluded for this study that optimum conditions for dissolution of platinum occur only at low pH values, low temperatures and low chloride concentrations.

4.4.1 Recovery of Pt in chloride/ozone media

Figure 4.12 illustrates the percentage extraction of platinum in 1 M [Cl⁻] at 15 °C of different pH levels. It is observed that percentage extraction increases with increase in time but as the pH increases, there is a decrease in percentage extraction. After 8 hours, only about 37 to 40 % could be extracted, poor extractions clearly prove that Pt is highly resistant to oxidation.

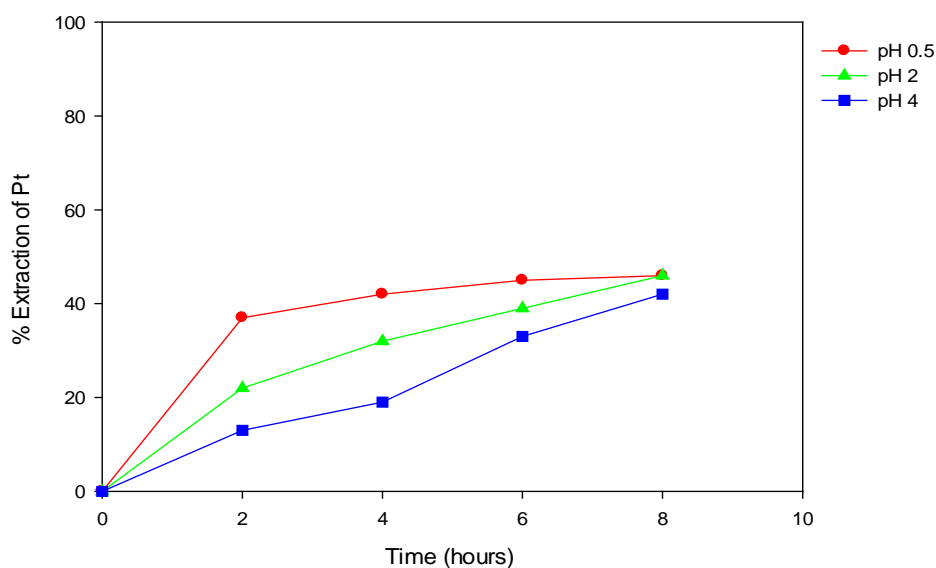


Figure 4.12: Percentage recovery of Pt in 1 M [Cl⁻] at 15°C at different pH levels

From Figure 4.13 it is clear that there is a tendency for the percentage extraction of Pt to reach a constant value after 4h of extraction. This points to the availability of a constant amount of ozone to drive the reactions. From Figure 2.2 (Section 2.1.2) it is furthermore clear that the solubility of ozone is lowered substantially with an increase in temperature, which is also reflected in the extraction rates obtained in Figure 4.13.

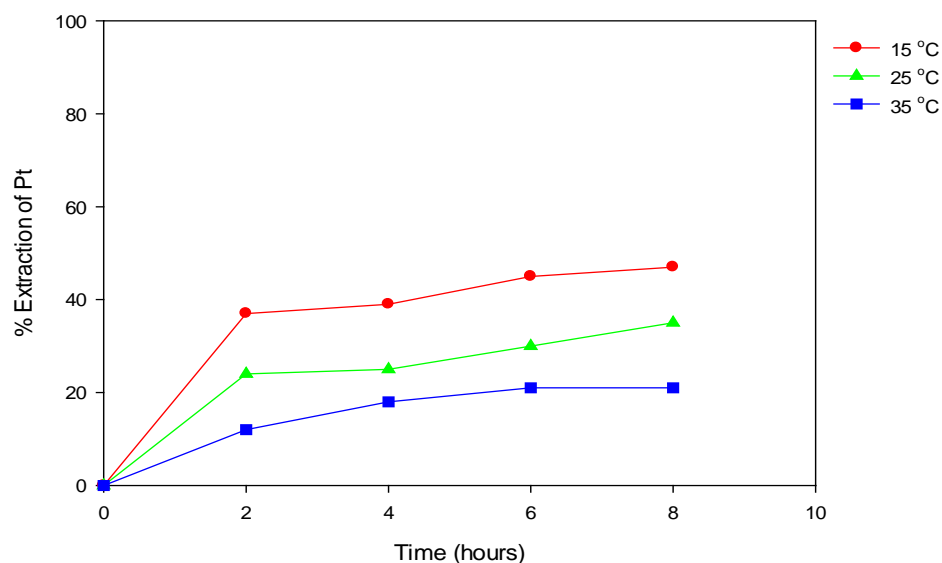


Figure 4.13: Percentage recovery of Pt in 2 M [Cl⁻] of pH 2 at different temperatures

Figure 4.14 illustrates the percentage extraction of platinum in different chloride concentrations and it is observed that as the concentration and time are increased, there is a decrease in percentage extraction. It is observed that at low chloride concentration, percentage extraction is at least 62 %.

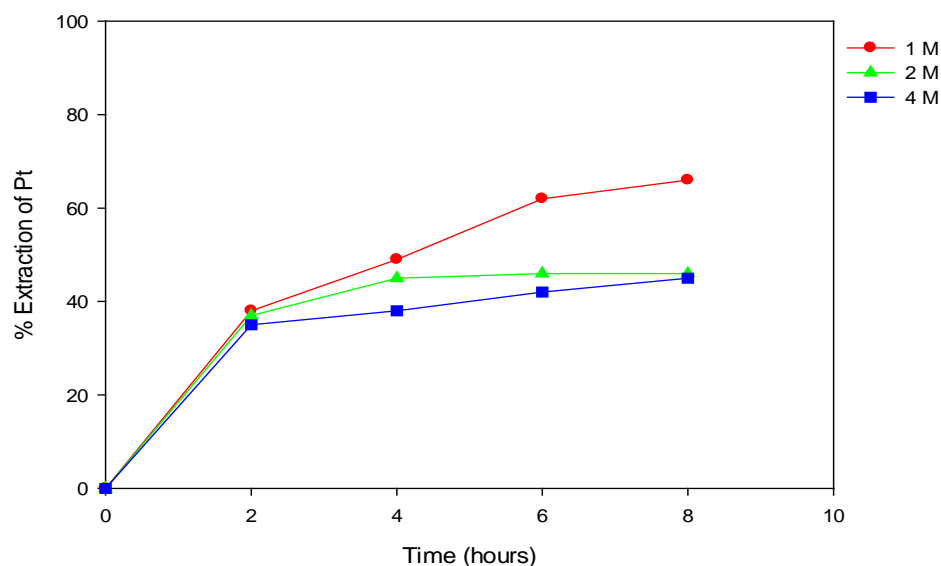


Figure 4.14: Percentage recovery of Pt in different Cl⁻ concentrations of pH 0.5 at 25 °C

Table 4.4 represents only the highest percentage extraction after 8 hours in a 2 litres standard flask in different conditions. Other percentage extraction can be seen in Appendix G.

Table 4.4: Total percentage extraction of Platinum after 8 hours

Total % extraction of Pt	Time (hours)	Conditions
66	8	1 M [Cl ⁻], pH 0.5, 15 °C
46	8	2 M [Cl ⁻], pH 2, 15 °C
33	8	4 M [Cl ⁻], pH 4, 15 °C

4.4.2 Summary

- These percentage recoveries were not as high as the percentage recoveries of aqua regia and cyanide; perhaps ozone was being affected by factors such as pH, temperature, and ionic strength.

- Viñals *et al.* (2006) also conducted a study for the PGM recovery but they did not reach over 50 %. The activation energies obtained in electrochemistry were also too low to indicate definite chemical reactions.

- It is also noteworthy that the leaching runs conducted in this study were done on a virgin catalytic converter samples. The comparison between used autocatalyst samples on the leaching efficiency must also not be ignored.

CHAPTER 5

CONCLUSIONS AND RECOMMENDATIONS

5.1 Conclusions

The demand for Pt is on the rise because of stringent environmental regulations and the development of fuel cells. Although it is gaining considerable importance, it is difficult to increase its production volume because not only is it rare, but also requires vast amounts of energy and other resources for its extraction from mineral resources. The hydrometallurgical processing of secondary Pt sources requires further investigation and optimization.

The thermodynamic investigation regarding the construction of Pourbaix diagrams of Pt with chloride confirmed the possibility of the formation of stable aqueous complexes. A lot more data is required on the complexation of Pt with hydroxide and chloride in order to portray a more realistic picture of the different stability regions.

From the electrochemical polarisation curves, the influence of ozone, halide ion concentrations, pH levels and temperature on the kinetics of Pt, it was concluded that increase in halide ion concentration has a positive effect on the kinetics. Different pH levels also influenced the kinetics of Pt in different halide ions. Increases in temperature did not have much significance.

From the electrochemical results it can be concluded that ozone could be used as an oxidising agent, but in the leaching results obtained it can only be used provided that optimum conditions of the life-time of ozone is thoroughly studied or known.

5.2 Recommendations

Further investigations regarding the leaching processes and variables concerning the process are thus recommended. The following are suggested investigations:

- The influence of rotation speed on the electrochemical and leaching studies.

- The influence of aqueous ozone concentration on the electrochemical and leaching studies.
- The influence of leaching time to recover Pt.
- Further electrochemical studies need to be conducted in order to attain Tafel slopes and activation energies that can be used for Pt in chloride/ozone media.

References

USEPA (2002). Indicators of the Environmental Impacts of Transportation, Center for Transportation and the Environment (www.itre.ncsu.edu/cte); ORNL, Transportation Energy Data Book. ORNL (www.ornl.gov) Cited by: Victoria Transport Institute. (2012). Transportation Cost and Benefit Analysis II – Air Pollution Costs (www.vtppi.org) (Assesed 20 August 2012).

ASM International. (1987). Metal Handbook, Volume 13 (Corrosion). Metals Park, Ohio.

Baghalha M., Homa K.G., Hamid R.M. (2009), Kinetics of platinum from spent reforming catalysts in aqua-regia solutions, *Hydrometallurgy*, 95, p. 247-253.

Bao J.E., Macdonald D.D. (2007). Oxidation of hydrogen on oxidized platinum Part 1: The tunneling current, *Journal of Electroanalytical Chemistry* 600, p. 205-216.

Barakat M.A., Mahmoud M.H.H. (2004), Recovery of platinum from spent catalyst, *Hydrometallurgy*, 72, p. 179-184.

Bard A.J., Faulkner L.R. (1980). *Electrochemical Methods, Fundamentals and Applications*, Wiley, New York.

Barefoot R.R. (1997). Determination of Platinum at Trace levels in Environmental and Biological Materials, *Environmental Science and Technology*, Vol.31, No. 2, p. 309-314.

Chen J., Huang K. (2006), A new technique for extraction of platinum group metals by pressure cyanidation, *Hydrometallurgy*, 82, p.164-171.

Cotton F.A., Wilkinson G. (1980), *Advance Inorganic Chemistry*, John Wiley & Sons, New York.

CRC Hanbook of Chemistry and Physics (70th Edition), (1989-1990), CRC Press.

CRC Handbook of Chemistry and Physics (82 nd edition). (2001-2002). CRC Press.

Davies A., Tran T., Young D. (1993), Solution chemistry of iodide dissolution of gold, *Hydrometallurgy*, 32, p. 143-159.

Dawson R.J., Kelsall G.H. (2007), *Journal of Applied Electrochemistry*, 37, p. 3-14.

De Sá Pinheiro A.A., de Lima T.S., Campos P.C., Afonso J.C. (2004). Recovery of platinum from spent catalysts in a fluoride-containing medium, *Hydrometallurgy*, 74, p. 77-84.

Donah J., Masschelein W.J. (1987). The photochemical generation of ozone: Prenet state-of-the-art. *Ozone: Science and Engineering* 9:315-334. cited by: Summerfelt S.T. (1997) *Review of Ozone Processes and Application As an Oxidizing Agent in Aquaculture*. American Fisheries Society.

Duyvesteyn W.D.C., San J., Houyuan L., Duyvesteyn S.S. (1994). Dissolution of platinum group metals from materials containing said metals, United States Patent, 5, 304, 359.

Elding L. (1970). *Acta Chem. Scand.*, 24, 1331; 1527.

Fornalczyk A., Saturnus M. (2009). Removal of platinum group metals from the used auto catalytic converter, *Metalurgija* (48) 2, p. 133-136.

Giandomenico C.M. (2000). Johnson Matthey Public Limited Company, *Platinum-Group Metals, Compounds*, Kirk-Othmer Encyclopedia of Chemical Technology.

Goldschmidt V.M. (1954). *Geochemistry*, Oxford University Press, Oxford.

Goldschmidt V.M. (1954). *Geochemistry*, Oxford University Press.

Gos S., Rubo A. (1997). *Randol Gold Forum '97*. Monterey, p161-166.

Hahn J. (1997). 'n Kineties-meganistiese studie van reaksies van atmosferiese stikstof-enswawelverbindinge deur osoon, p. 55-62.

Hahn J., Lachmann G., Pienaar J.J. (2000). *South African Journal of Chemistry*, 53, p. 132-138.

Hartley Frank R. (1991). *Studies of inorganic chemistry II, chemistry of the platinum group metals, Recent developments*, Elsevier. Cited by: Giandomenico C.M. (2000). Johnson Matthey Public Limited Company, *Platinum-Group Metals, Compounds*, Kirk-Othmer Encyclopedia of Chemical Technology.

Heck R.M., Farrauto R.J. (2001). Automobile exhaust catalysts, *Applied Catalysis A: General* 221, p. 443-457.

Hennion F.J. (1983). Availability of precious metals from spent catalysts, *Platinum group metals-an in-depth view of the industry, 1983, IPMI Seminar, Williamsburg, VA*, p. 61-81.

Hoffmann J.E. (1988). Recovering platinum-group metals from autocatalysts, *Journal of Metals*, 40 (6), p. 40-44.

House J.E. (1997). Principles of chemical kinetics, Wm. C. Brown Publishers, Illinois State University.

HSC Chemistry 5, (2002). Outokumpu Research Anttin Roine.

Iglesias S.C. (2002). Degradation and Biodegradability Enhancement of Nitrobenzene and 2,4-Dichlorophenol by Means of Advance oxidation Processes Based on Ozone, PhD Thesis, University of Barcelona.

Jafarifar D., Daryanavard M.R., Sheibani S. (2005). Ultra-fast microwave-assisted leaching for recovery of platinum from spent catalyst, Hydrometallurgy, 78, p. 166-171.

Juvekar V.A., Patil R.S., Naik V.M. (2011). Oxidation of chloride ion on platinum electrode: Dynamics of electrode passivation and its effect on oxidation kinetics, Industrial and Engineering Chemistry Research, American Chemical Society, p. 12946-12947.

Langlais B., Reckhow D.A., Brink D.R. (1991). Ozone in Water Treatment: Application and Engineering, Lewis Publishers, Chelsea, Michigan, USA.

Langlais B., Reckhow D.A., Brink D.R. (1991). Ozone in Water Treatment: Application and Engineering, Lewis Publishers, Chelsea, Michigan, USA. Cited by: Nawrocki J., Ziolek M., Hordern B.K. (2003). Catalytic ozonation and methods of enhancing molecular ozone reactions in water treatment, Applied Catalysis B: Environmental 46, p. 639-669.

Littauer E.L., Shreir L.L. (1966). Anodic Polarisation of Platinum in Sodium Chloride Solutions, Electrochimica Acta, Vol. 11, p. 527-536.

Masschelein W.J. (1992). Unit Processes in Drinking Water Treatment, Marcel Dekker, New York. Cited by: Nawrocki J., Ziolek M., Hordern B.K. (2003). Catalytic ozonation and methods of enhancing molecular ozone reactions in water treatment, Applied Catalysis B: Environmental 46, p. 639-669.

Mishra R.K. (1993). A review of platinum group metals recovery from automobile catalytic converters, Precious Metals, p. 449-475.

Nawrocki J., Ziolek M., Hordern B.K. (2003). Catalytic ozonation and methods of enhancing molecular ozone reactions in water treatment, Applied Catalysis B: Environmental 46, p. 639-669.

Platinum Interim Review. (2011). Johnson Matthey Public Limited Company.

Rakovsky S., Anachkov M., Zaikov G. (2009). Fields of ozone applications, Chemistry and Chemical Technology, Vol. 3, No. 2, p. 139-140

Rice R.G. (1989) Recent Advances in Ozone Treatment of Drinking Water, Proceedings of the Seventh International Conference on Chemistry for the Protection of the Environment, Lublin, Poland. Cited by: Wu B.Y. (1996). Effects of Ozonation on Fouling of Heat Exchangers, PhD Thesis, The University of Wisconsin-Milwaukee.

Robson G.G. (1985). Johnson Matthey.

Roine A.A., Antilla K. (2006). HSC Chemistry 6.0 Outotec.

Rojo T., de Aberasturi D.J., Pinedo R., de Larramendi I.R., de Larramendi J.L.R. (2011) Recovery by hydrometallurgical extraction of the platinum-group metals from car catalytic converters, Minerals Engineering, doi: 10.1016/j.mineng.2010.12.009, p. 3-4.

Ryder J.M., Dymock K. (1990). Recycling of Metalliferous Materials, IMM, London, p. 255.

Shaw B.A., Kelly R.G. (2006). What is Corrosion? The Electrochemical Society Interface, Spring, p. 24-26.

Sotelo J.L., Beltran F.J., Benitez F.J., Beltran-Heredia J. (1987). Industrial & Engineering Chemistry Research, 26, p. 39-43.

Ullmann's Encyclopedia of Industrial Chemistry, Vol A 18, p. 349. Cited by: Iglesias S.C. (2002). Degradation and Biodegradability Enhancement of Nitrobenzene and 2,4-Dichlorophenol by Means of Advance oxidation Processes Based on Ozone, PhD Thesis, University of Barcelona.

Viñals J., Juan E., Ruiz M., Ferrando E., Cruells M., Roca A., Casado J. (2006). Leaching of Gold and Palladium with Aqueous Ozone in Dilute Chloride Media, Hydrometallurgy, 81, p. 142-151.

West J.M. (1965). Electrodeposition and Corrosion Processes, Van Nostrand.

West J.M. (1970). Electrodeposition and Corrosion Processes, 2nd ed., Van Nostrand.

Woo S.I., Jeon S.H., Kim C.H.K. (2000). Recovery of Platinum-Group Metals from Recycled Automotive Catalytic Converters by Carbochlorination, Ind. Eng. Chem. Res, 39, p-1185-1192.

Wu B.Y. (1996). Effects of Ozonation on Fouling of Heat Exchangers, PhD Thesis, The University of Wisconsin-Milwaukee.

Wu K.Y.A. (1993). Recovery of Precious Metals from Automotive Catalytic Converters, PhD Chem Eng Dissertation, University of Tulsa.

Zanjani A., Baghalha M. (2009). Factors affecting platinum extraction from used reforming catalysts in iodide solutions at temperatures up to 95 °C, Hydrometallurgy, 97, p. 119-125.

Zysk E.D. (1986). Platinum Group Metals Seminar 1985, Washington D.C. p. 49.

Appendix A: Calculated Standard Gibb's free energy of formation

R	T	Constant
8.314	298.15	2.303

Ion	H_f^o, KJ/mol	S_f^o, KJ/(mol.K)
Pt ²⁺	243.55	-9.0000E-02
Cl ⁻	-167.08	5.6735E-02

Ligand	Element		Log β	ΔG_o(KJ/mol)	ΔG_f^o(KJ/mol)
	Pt	Formula			
Cl ⁻	Pt ²⁺	[ML]/[M][L]	5	-28.54	57.85
	Pt ²⁺	[ML ₂]/[M][L] ²	9	-51.39	-148.99
	Pt ²⁺	[ML ₃]/[M][L] ³	11.8	-67.36	-348.96
	Pt ²⁺	[ML ₄]/[M][L] ⁴	14	-79.92	-545.52

Appendix B: Solution numbering

Solution number	Cl ⁻ concentration (mol/dm ³)	pH level	Temperature (°C)
1	1	0.5	15
2	1	2	15
3	1	4	15
4	2	0.5	15
5	2	2	15
6	2	4	15
7	4	0.5	15
8	4	2	15
9	4	4	15
10	1	0.5	25
11	1	2	25
12	1	4	25
13	2	0.5	25
14	2	2	25
15	2	4	25
16	4	0.5	25
17	4	2	25
18	4	4	25
19	1	0.5	35
20	1	2	35
21	1	4	35
22	2	0.5	35
23	2	2	35
24	2	4	35
25	4	0.5	35
26	4	2	35
27	4	4	35

Appendix C: Pourbaix diagrams of Pt with chloride.

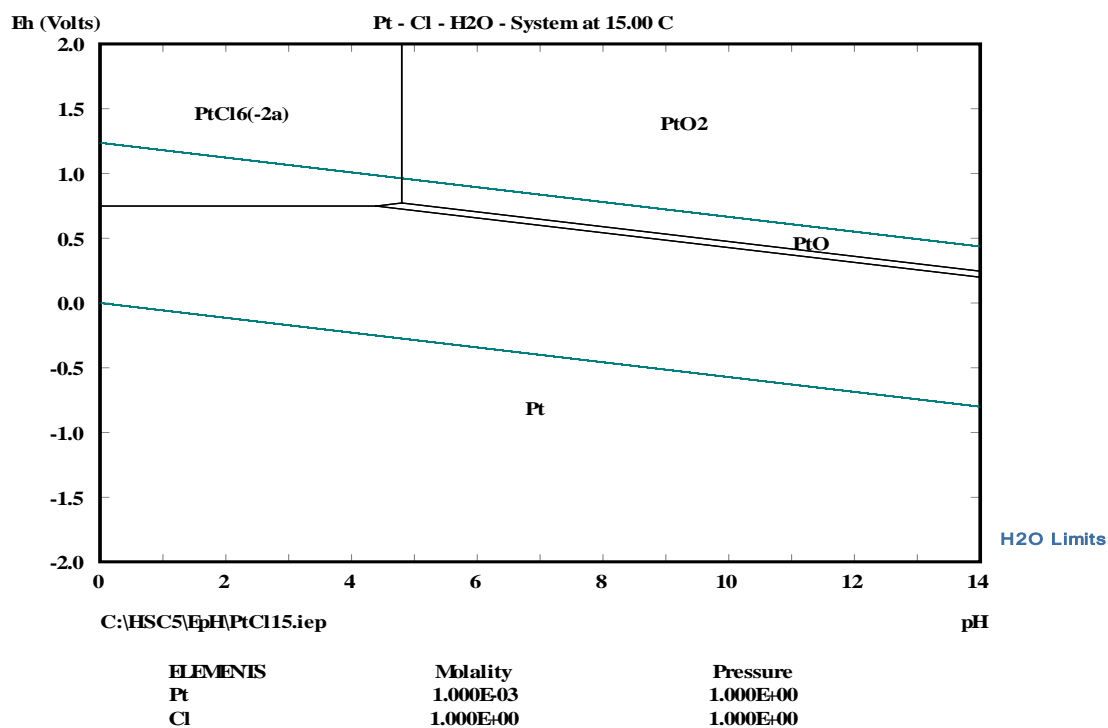


Figure C1: E_h-pH diagram of Pt-Cl-H₂O, metal concentration 10⁻³M, [Cl⁻] of 1 M at 15°C

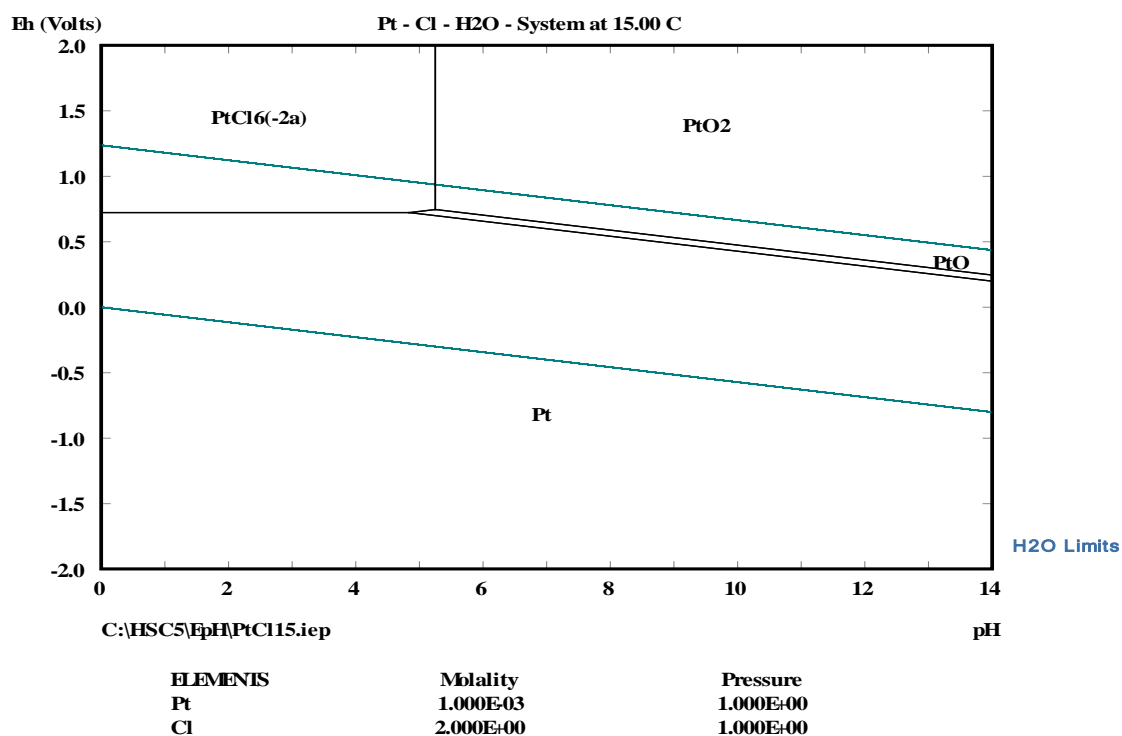


Figure C2: E_h-pH diagram of Pt-Cl-H₂O, metal concentration 10⁻³M, [Cl⁻] of 2 M at 15°C

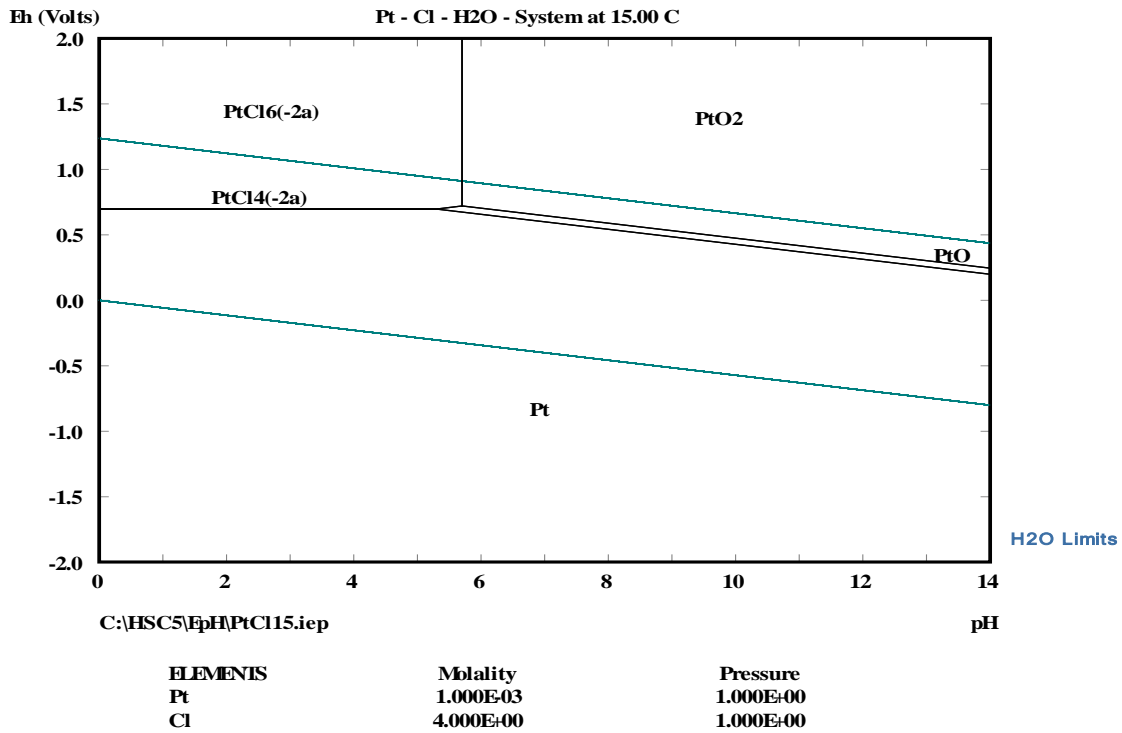


Figure C3: E_h-pH diagram of Pt-Cl-H₂O, metal concentration 10⁻³M, [Cl⁻] of 4 M at 15°C

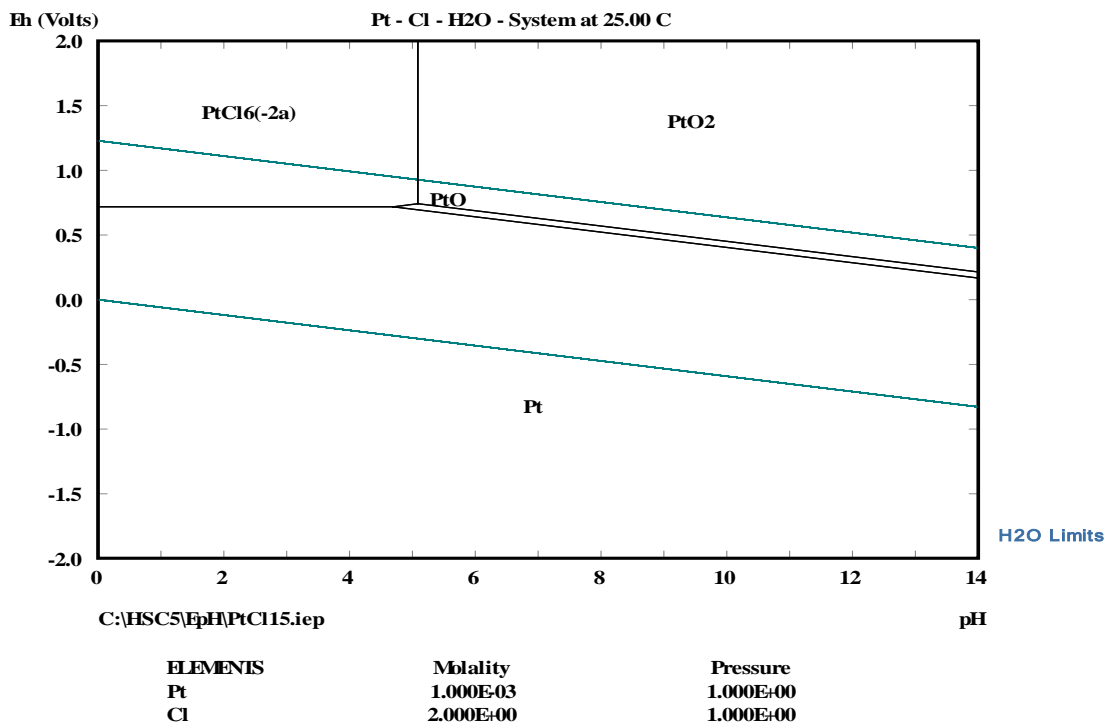


Figure C4: E_h-pH diagram of Pt-Cl-H₂O, metal concentration 10⁻³M, [Cl⁻] of 2 M at 25°C

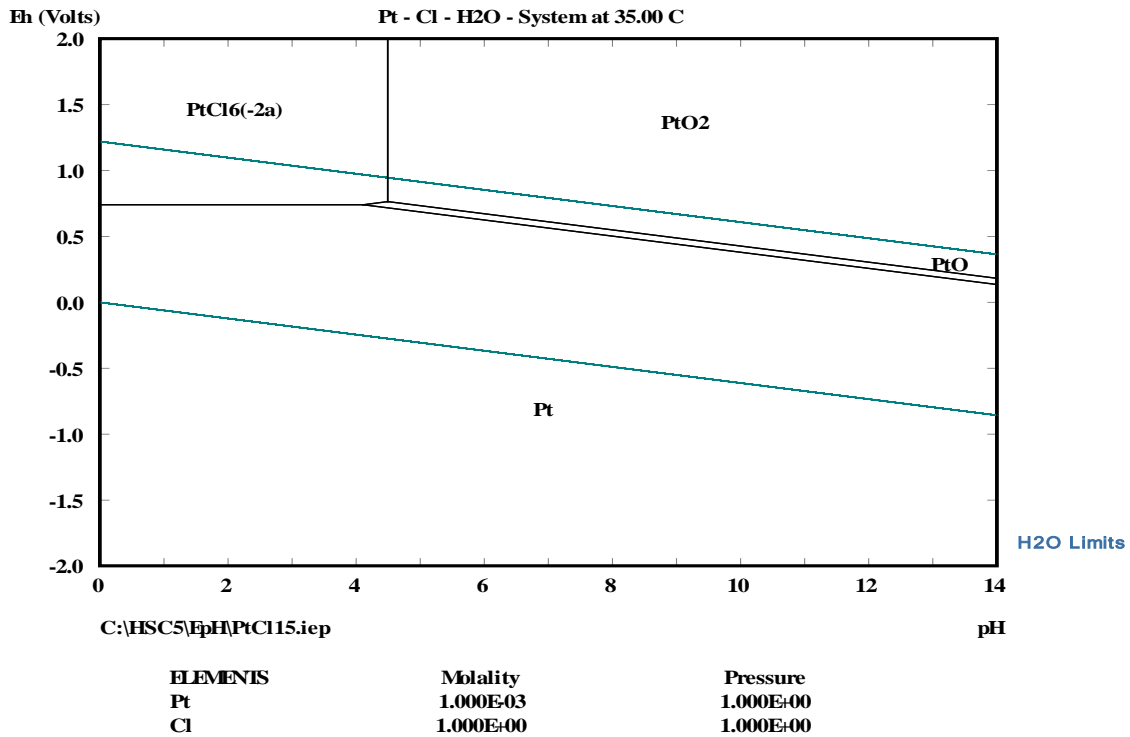


Figure C5: E_h-pH diagram of Pt-Cl-H₂O, metal concentration 10⁻³M, [Cl⁻] of 1 M at 35°C

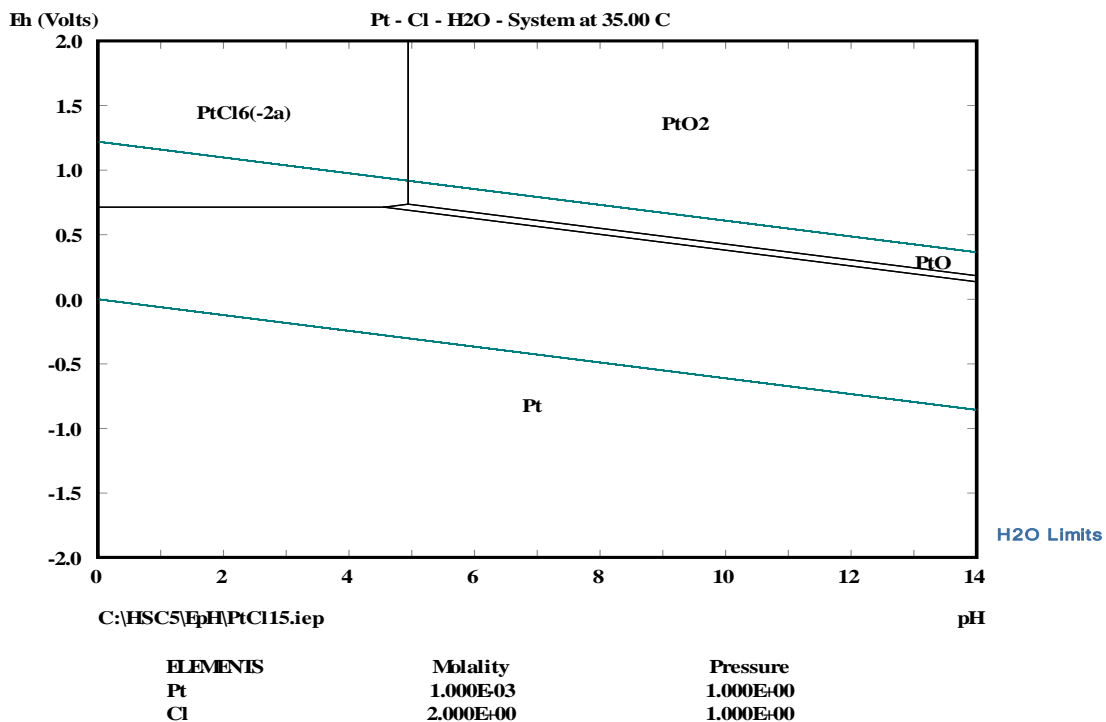


Figure C6: E_h-pH diagram of Pt-Cl-H₂O, metal concentration 10⁻³M, [Cl⁻] of 2 M at 35°C

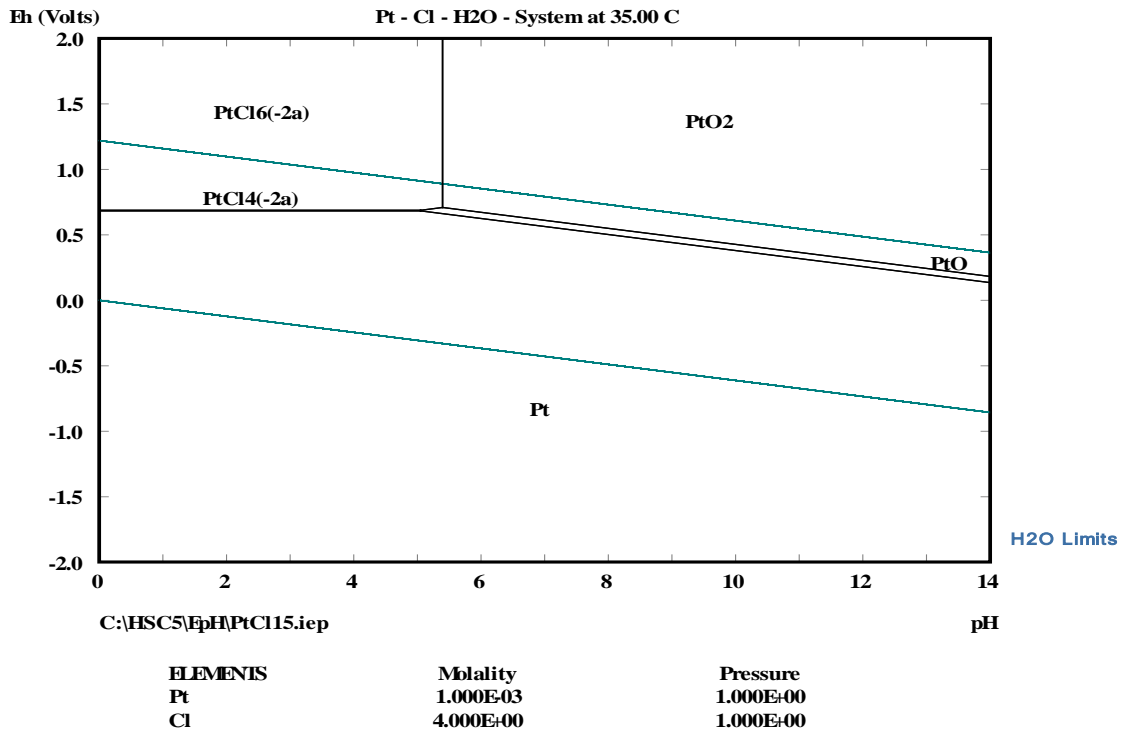


Figure C7: E_h-pH diagram of Pt-Cl-H₂O, metal concentration 10⁻³M, [Cl] of 4 M at 35°C

Appendix D: Polarisation curves

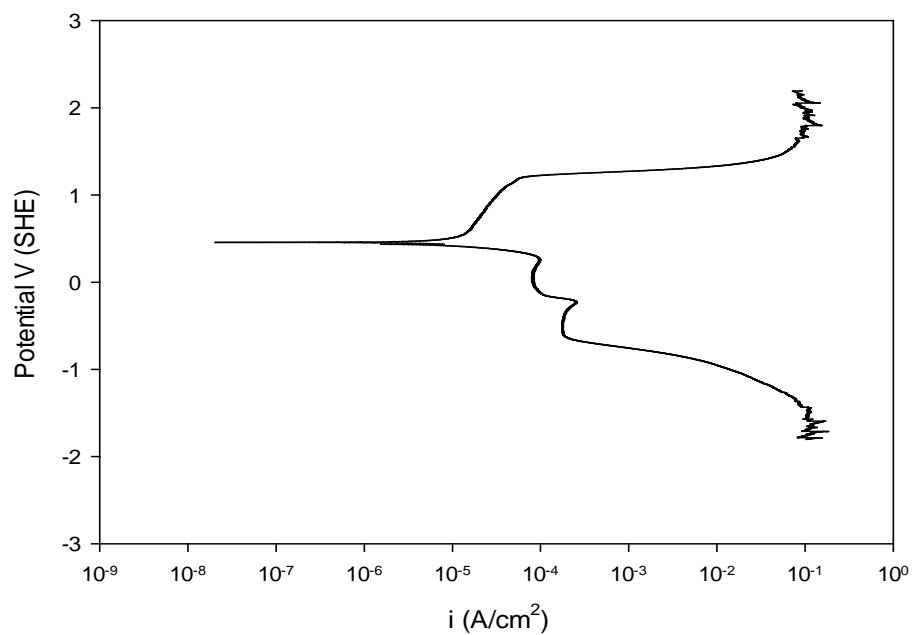


Figure D1: Polarisation curve of Pt in 4 M $[Cl^-]$ pH of 2 at $15^\circ C$ in the presence of ozone

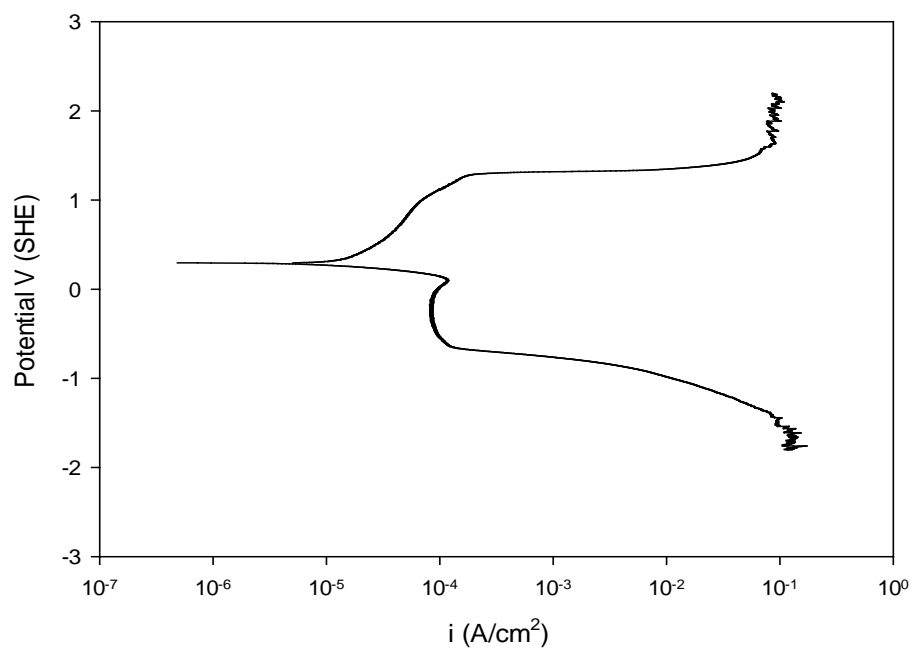


Figure D2: Polarisation curve of Pt in 4 M $[Cl^-]$ pH of 4 at $15^\circ C$ in the presence of ozone

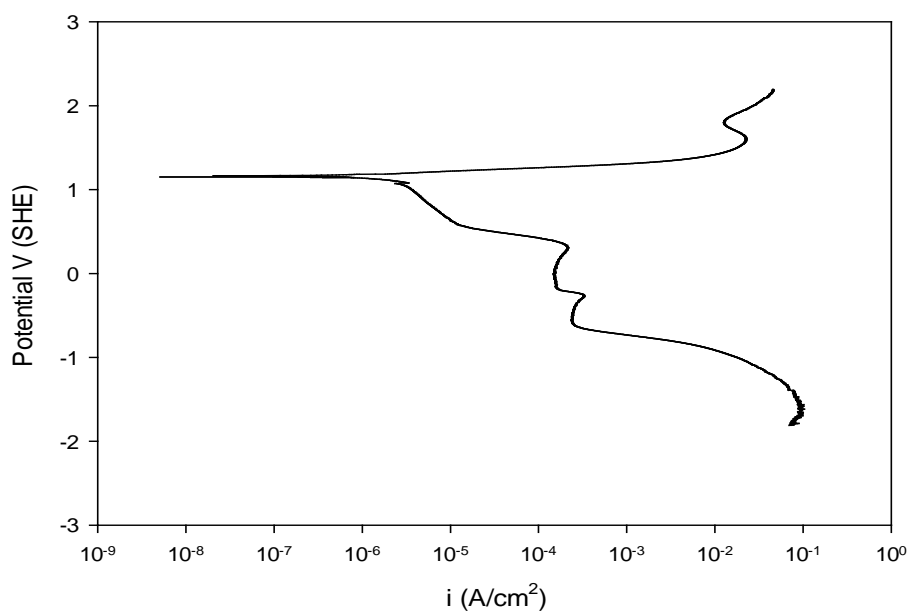


Figure D3: Polarisation curve of Pt in 1 M [Cl⁻] pH of 2 at 25°C in the presence of ozone

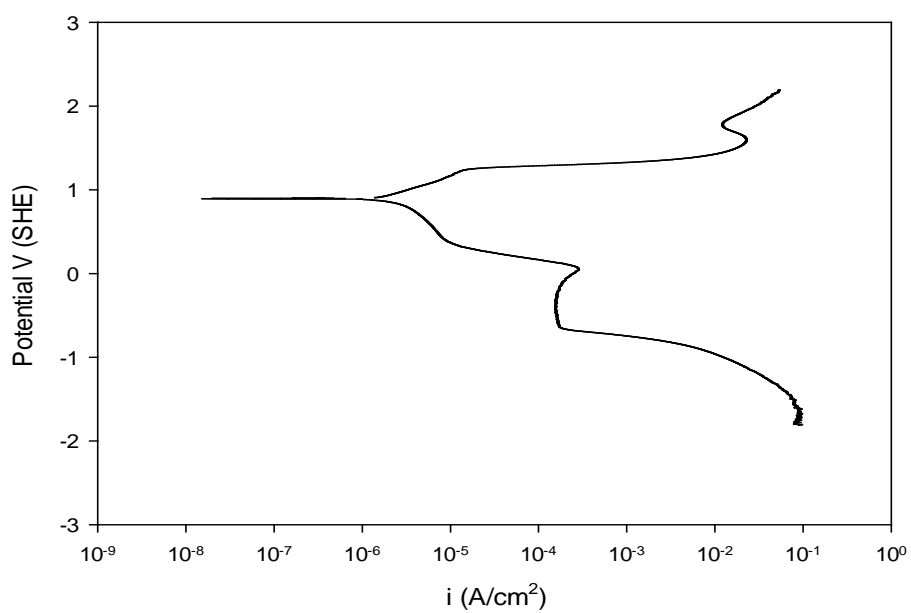


Figure D4: Polarisation curve of Pt in 1 M [Cl⁻] pH of 4 at 25°C in the presence of ozone

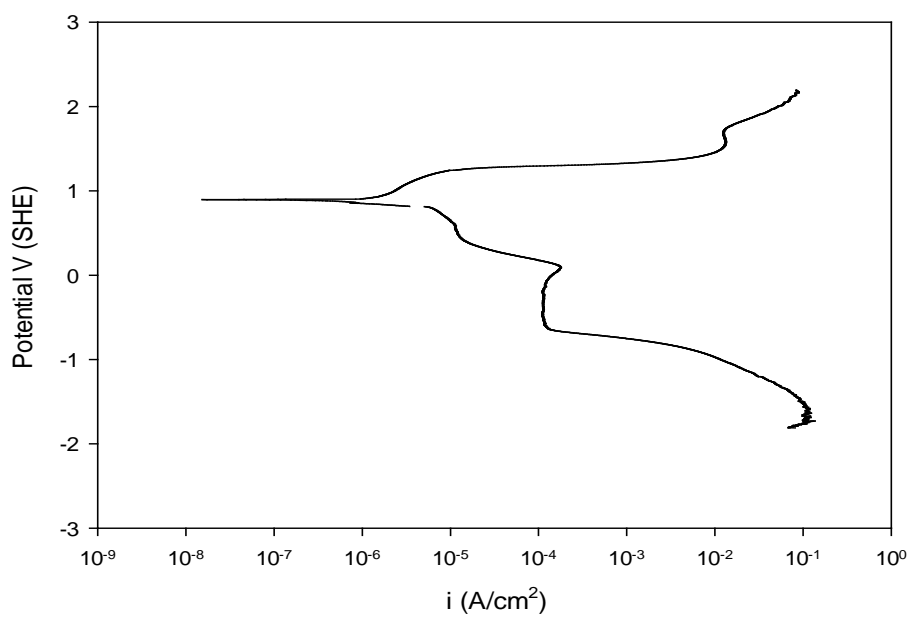


Figure D5: Polarisation curve of Pt in 2 M [Cl⁻] pH of 2 at 25°C in the presence of ozone

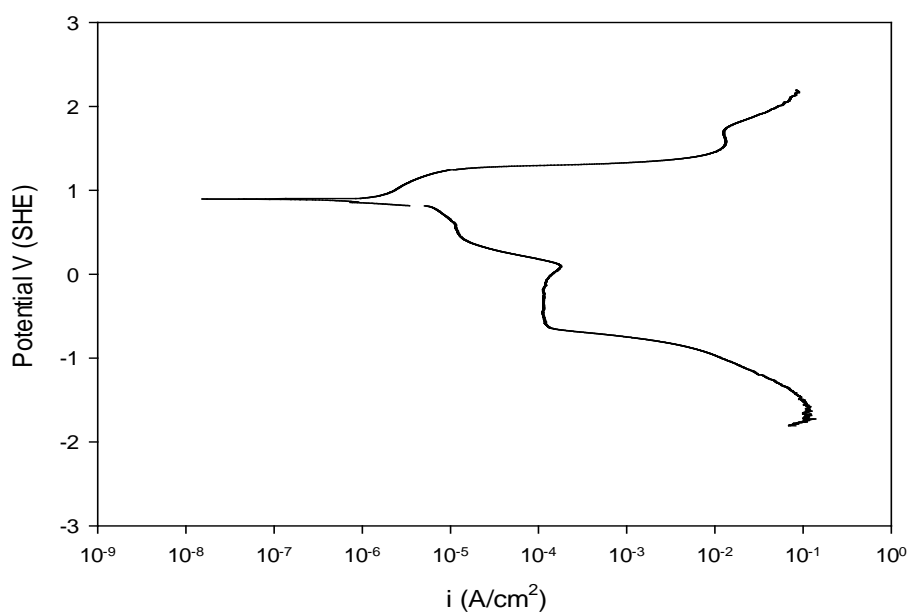


Figure D6: Polarisation curve of Pt in 2 M [Cl⁻] pH of 4 at 25°C in the presence of ozone

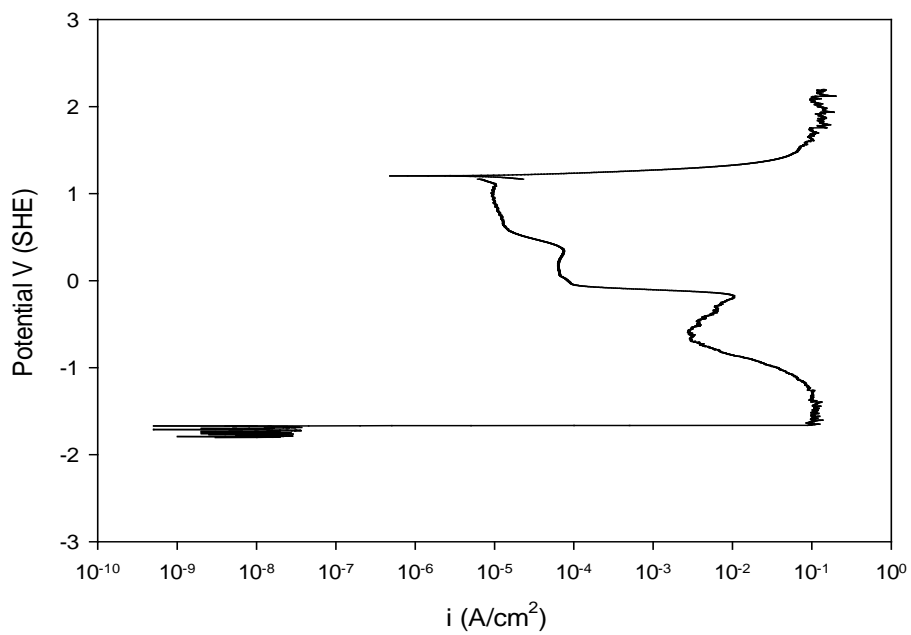


Figure D7: Polarisation curve of Pt in 4 M [Cl⁻] pH of 0.5 at 25°C in the presence of ozone

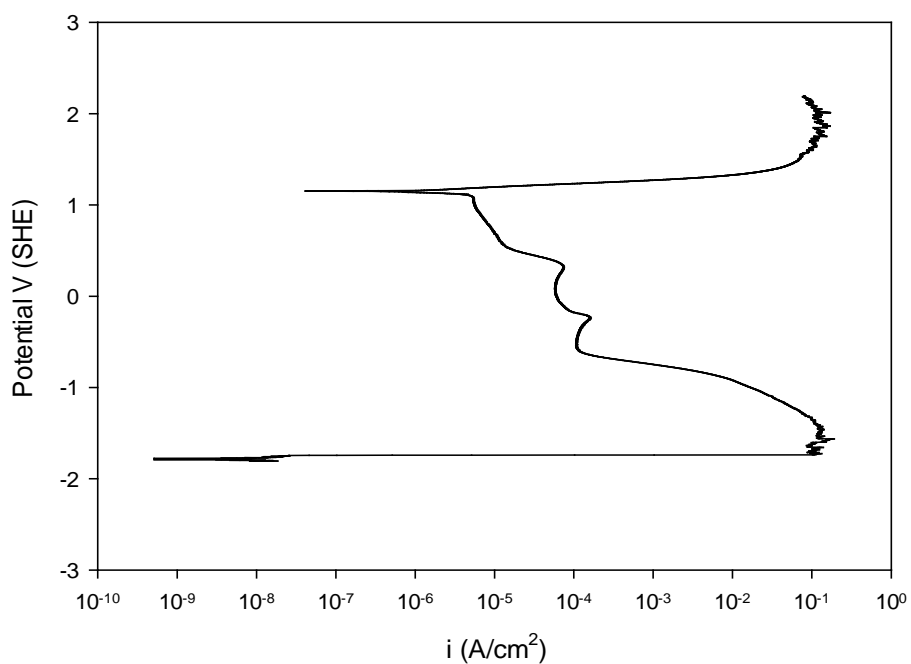


Figure D8: Polarisation curve of Pt in 4 M [Cl⁻] pH of 2 at 25°C in the presence of ozone

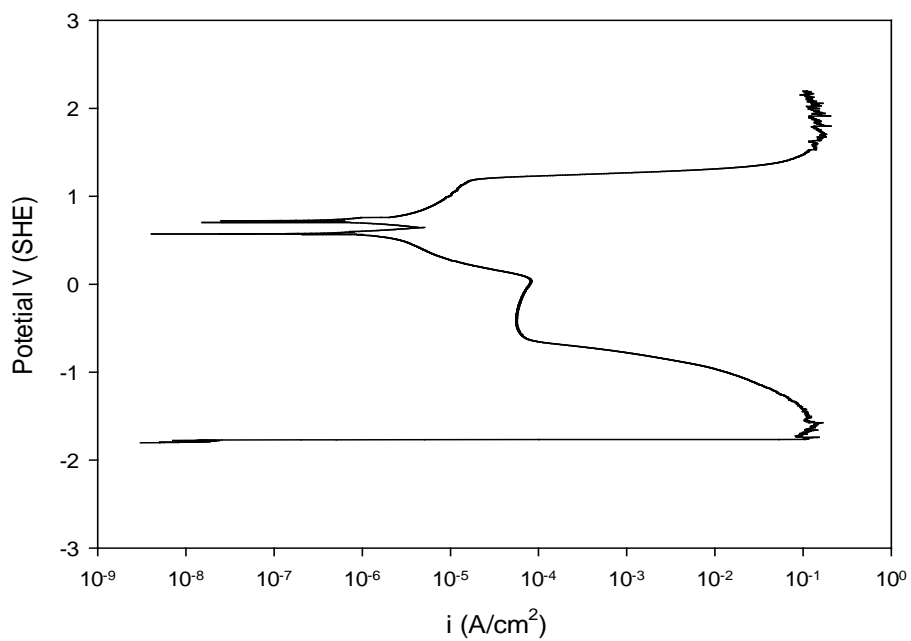


Figure D9: Polarisation curve of Pt in 4 M [Cl⁻] pH of 4 at 25°C in the presence of ozone

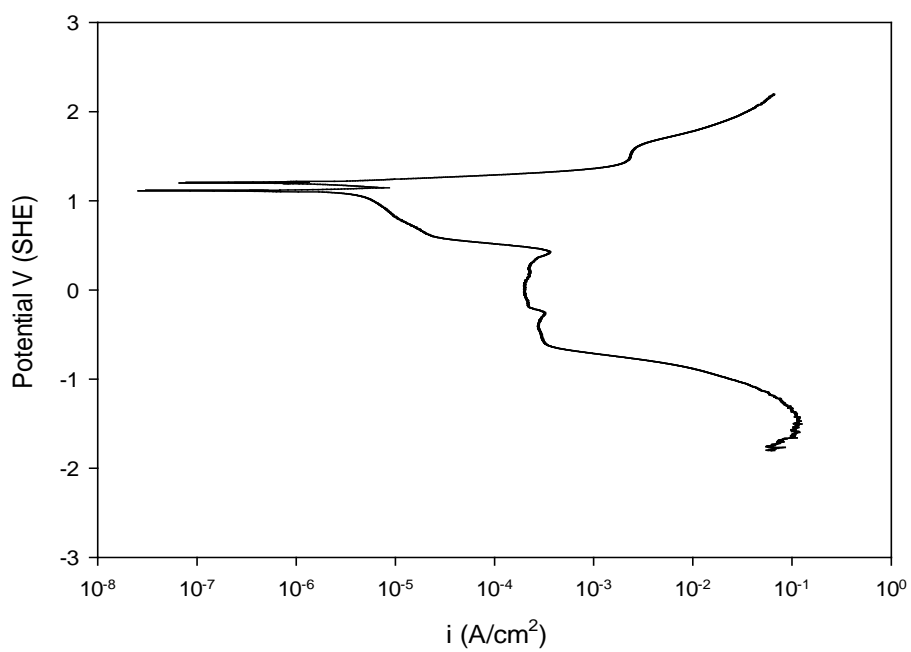


Figure D10: Polarisation curve of Pt in 1 M [Cl⁻] pH of 2 at 35°C in the presence of ozone

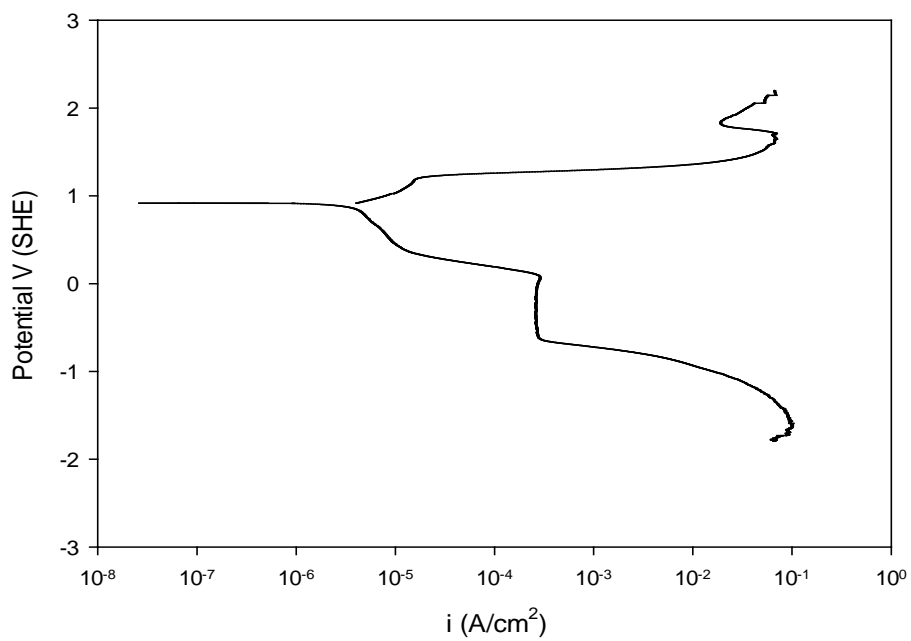


Figure D11: Polarisation curve of Pt in 1 M [Cl⁻] pH of 4 at 35°C in the presence of ozone

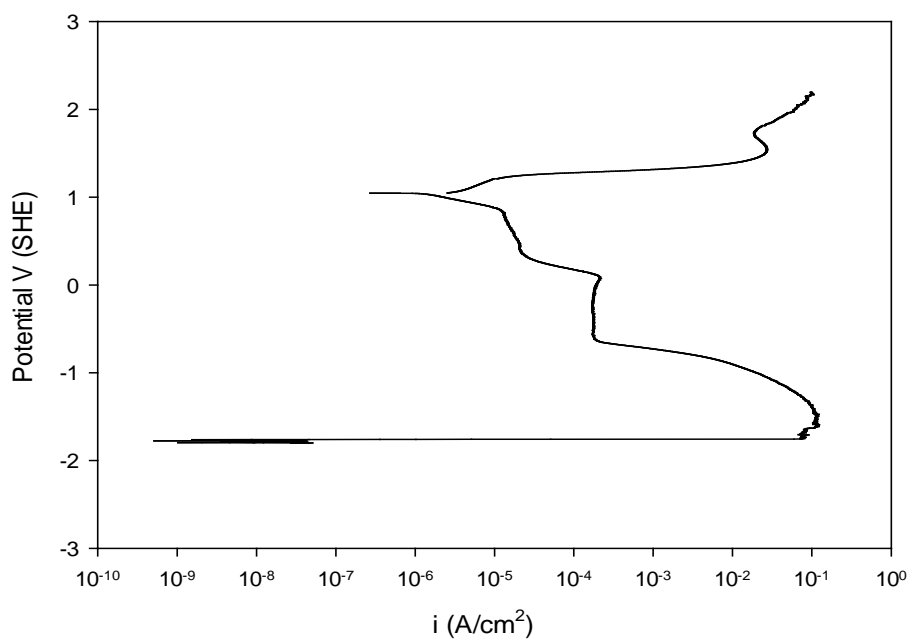


Figure D12: Polarisation curve of Pt in 2 M [Cl⁻] pH of 2 at 35°C in the presence of ozone

Appendix E: Influence of temperature, Chloride ion concentration and pH

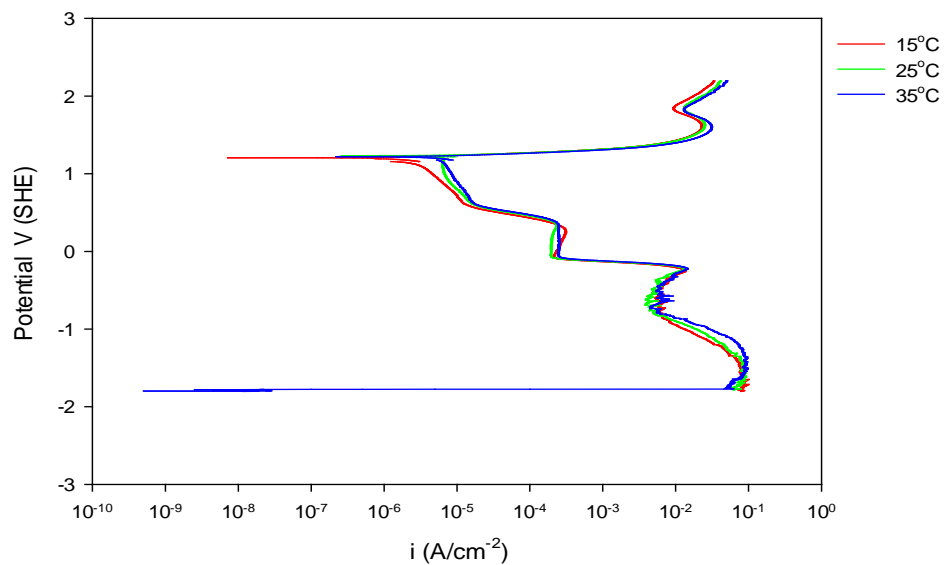


Figure E1: (a) Polarisation curve of Pt at different temperatures in 1 M [Cl⁻] at pH 0.5 with ozone

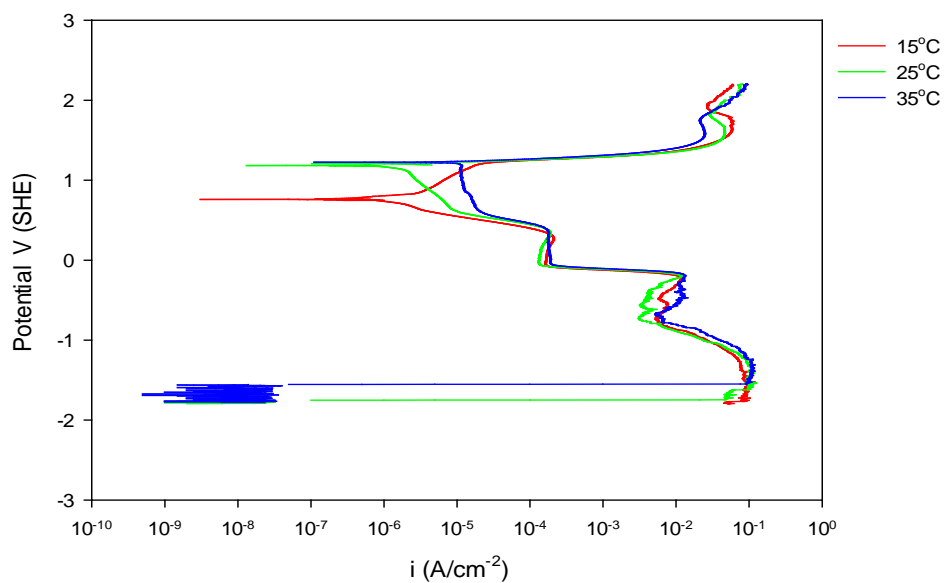


Figure E2: (a) Polarisation curve of Pt at different temperatures in 2 M [Cl⁻] at pH 0.5 with ozone

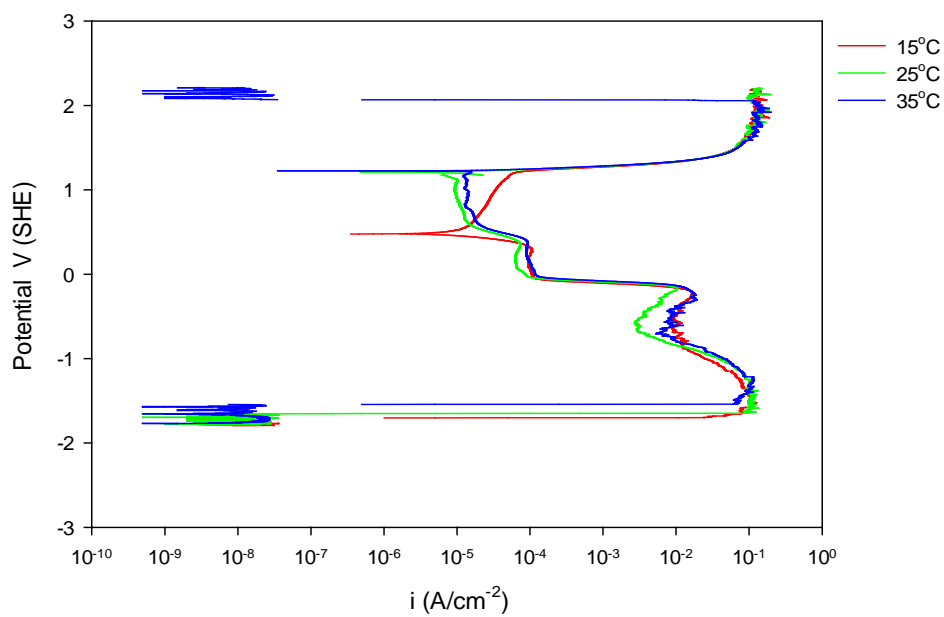


Figure E3: (a) Polarisation curve of Pt at different temperatures in 4 M [Cl⁻] at pH 0.5 with ozone

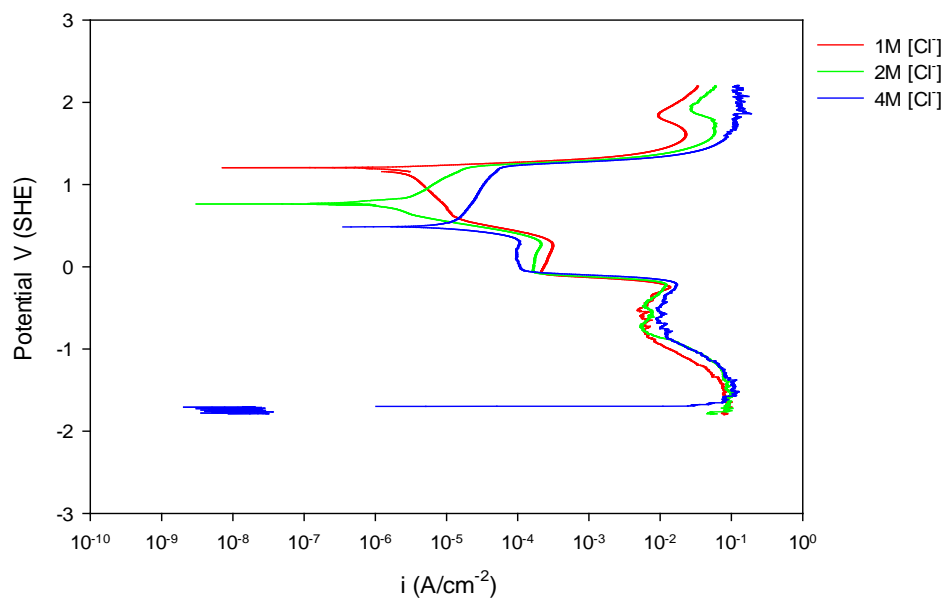


Figure E4: (a) Polarisation curve of Pt in different chloride concentrations at pH 2 with ozone

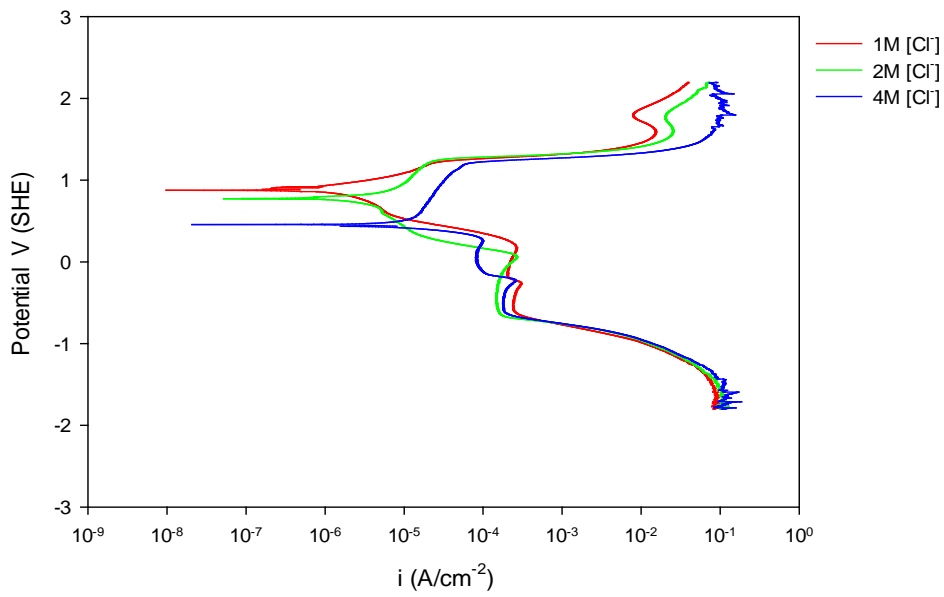


Figure E5: (a) Polarisation curve of Pt in different chloride concentrations at pH 2 with ozone

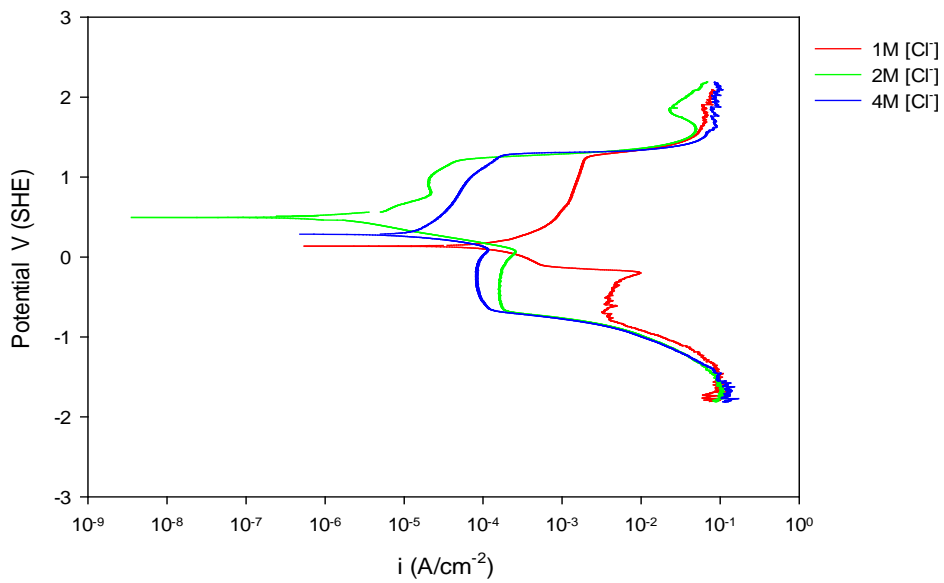


Figure E6: (a) Polarisation curve of Pt in different chloride concentrations at pH 2 with ozone

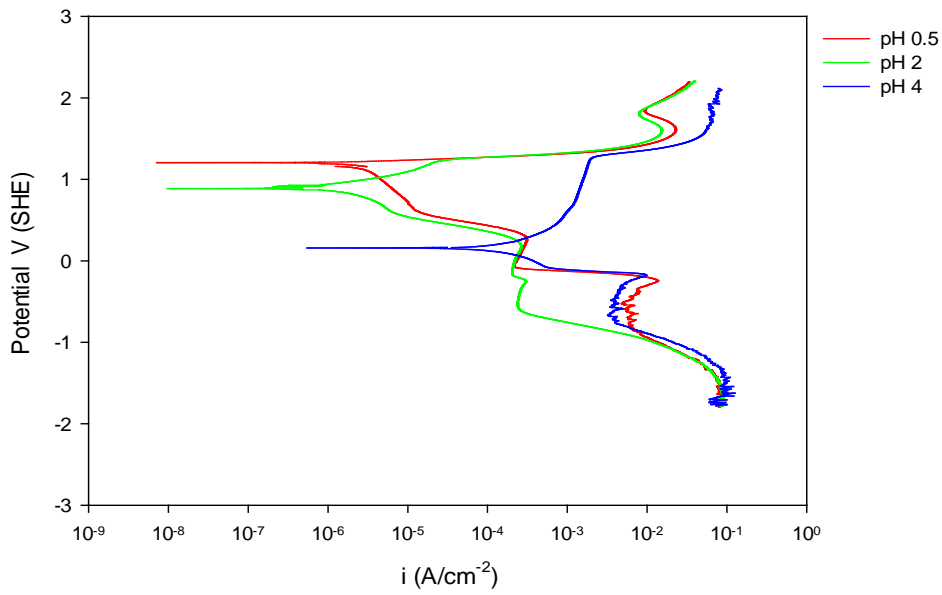


Figure E7: (a) Polarisation curve of Pt at different pH levels in 1 M [Cl⁻] at pH 0.5 with ozone at 25°C

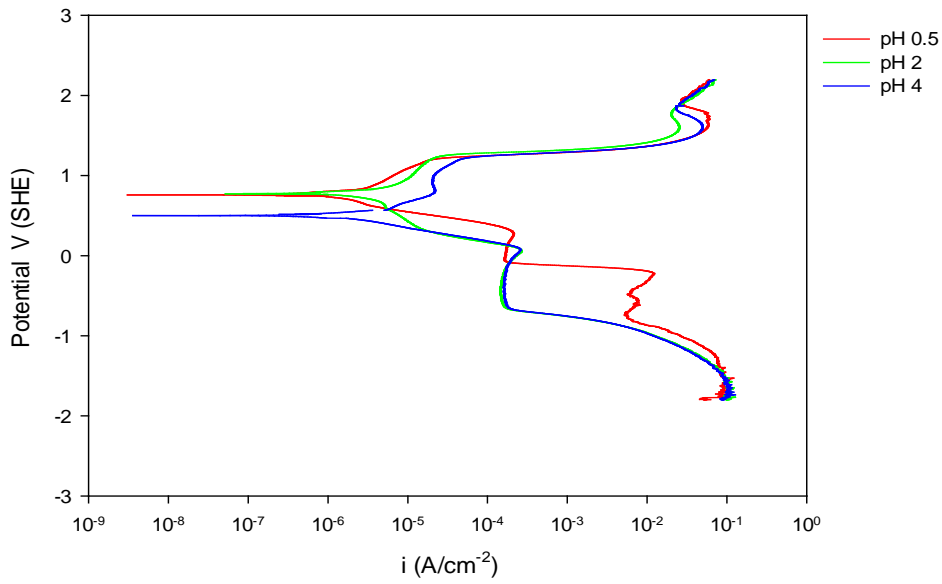


Figure E9: (a) Polarisation curve of Pt at different pH levels in 2 M [Cl⁻] at pH 0.5 with ozone at 25°C

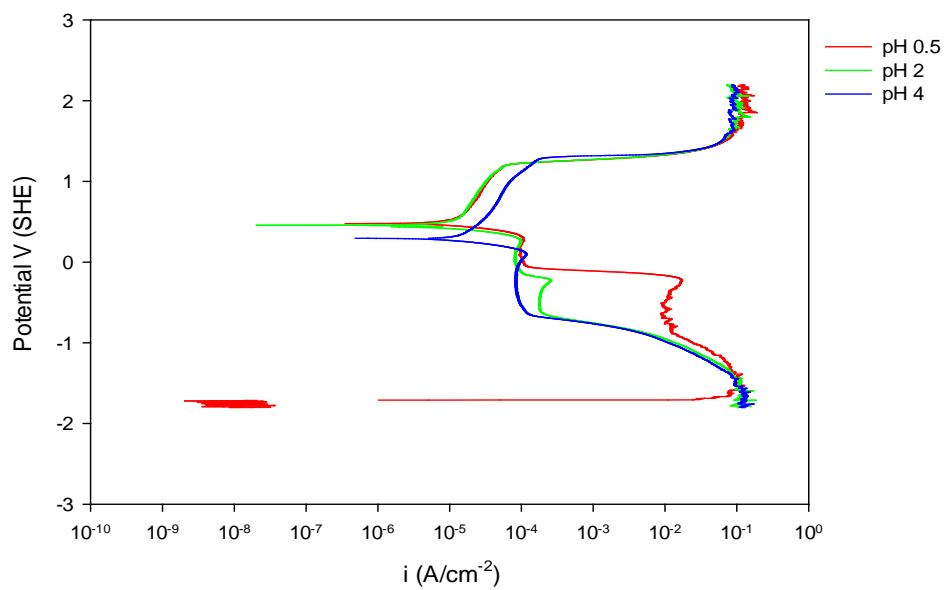


Figure E9: (a) Polarisation curve of Pt at different pH levels in 4 M [Cl⁻] at pH 0.5 with ozone at 25°C

Appendix F: Arrhenius plots for determining the activation energy of Tafel processes

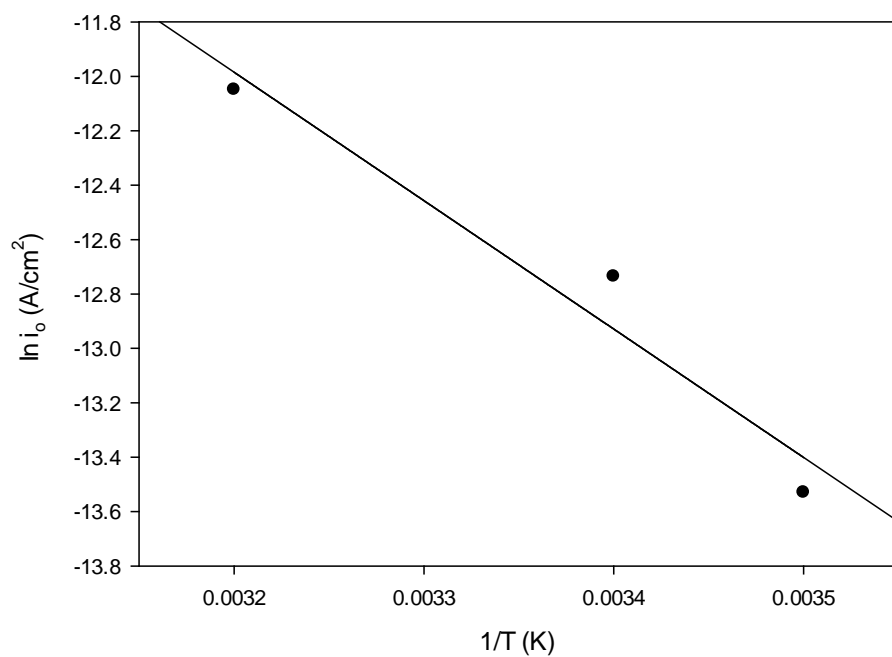


Figure F1: Arrhenius plots for determining the activation energy of Tafel processes in 1 M [Cl⁻] of pH 2 in the presence of ozone

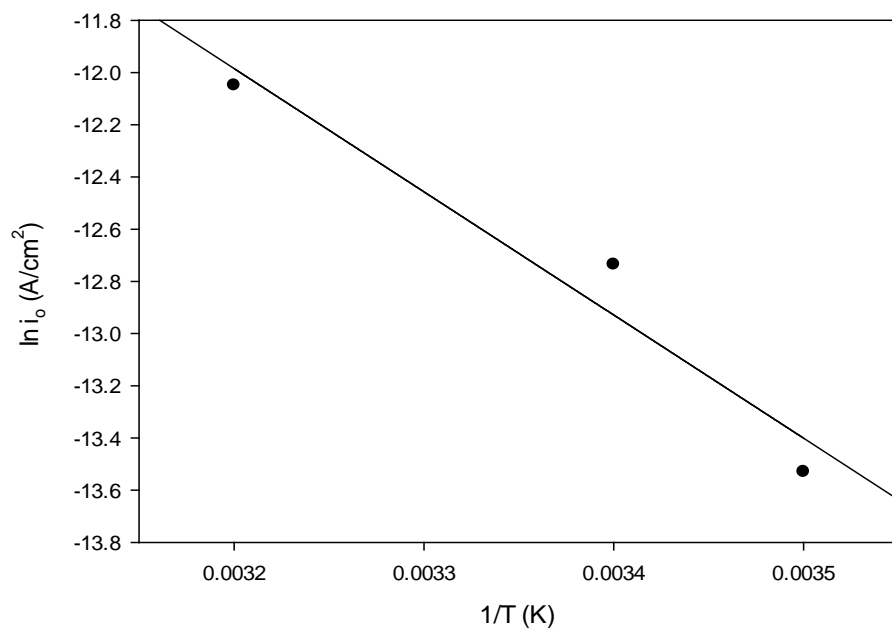


Figure F2: Arrhenius plots for determining the activation energy of Tafel processes in 1 M [Cl⁻] of pH 4 in the presence of ozone

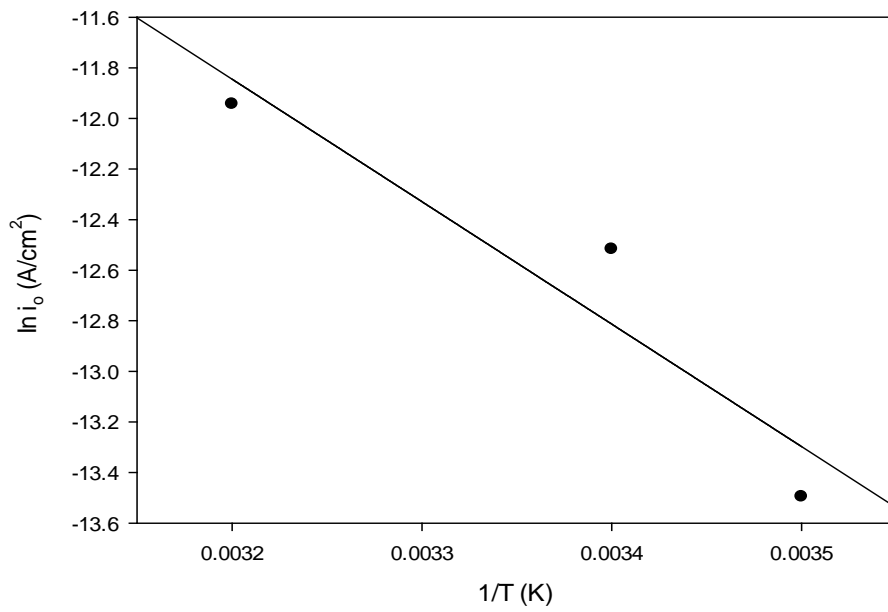


Figure F3: Arrhenius plots for determining the activation energy of Tafel processes in 2 M [Cl⁻] of pH 0.5 in the presence of ozone

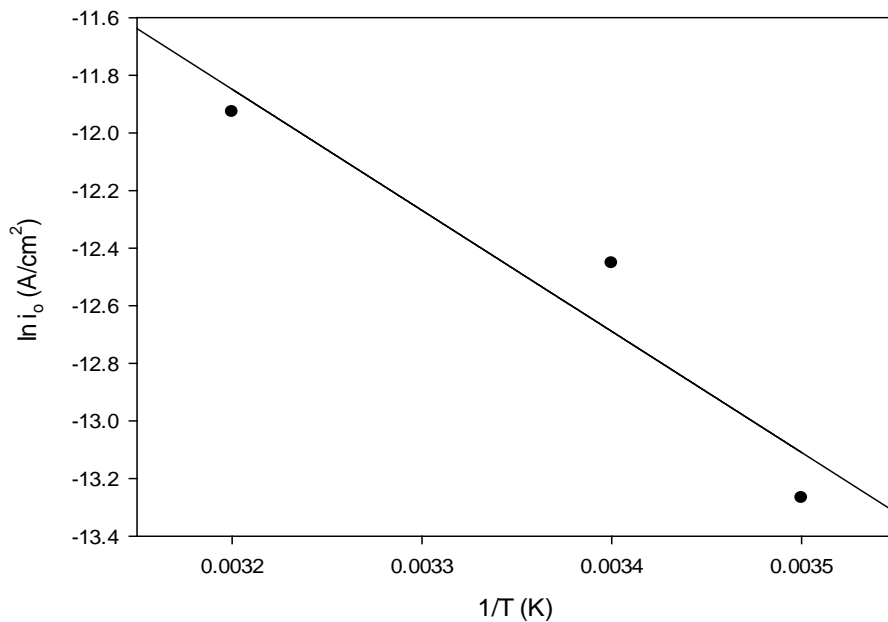


Figure F4: Arrhenius plots for determining the activation energy of Tafel processes in 2 M [Cl⁻] of pH 2 in the presence of ozone

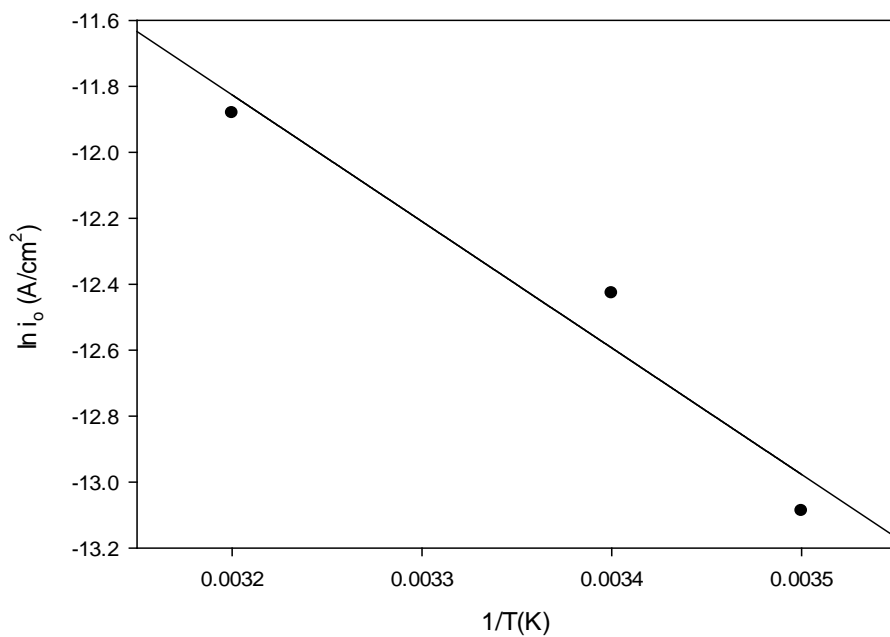


Figure F5: Arrhenius plots for determining the activation energy of Tafel processes in 2 M [Cl⁻] of pH 4 in the presence of ozone

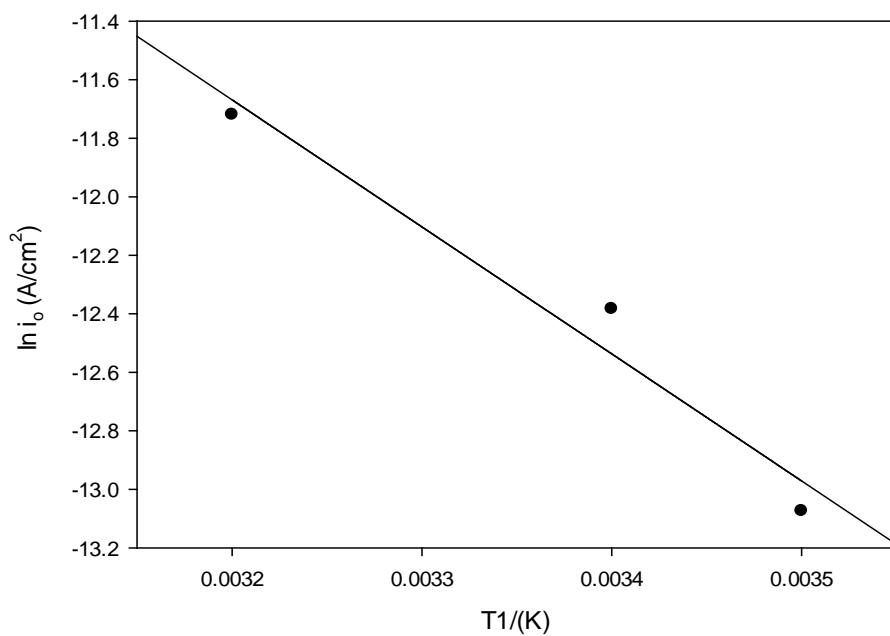


Figure F6: Arrhenius plots for determining the activation energy of Tafel processes in 4 M [Cl⁻] of pH 0.5 in the presence of ozone

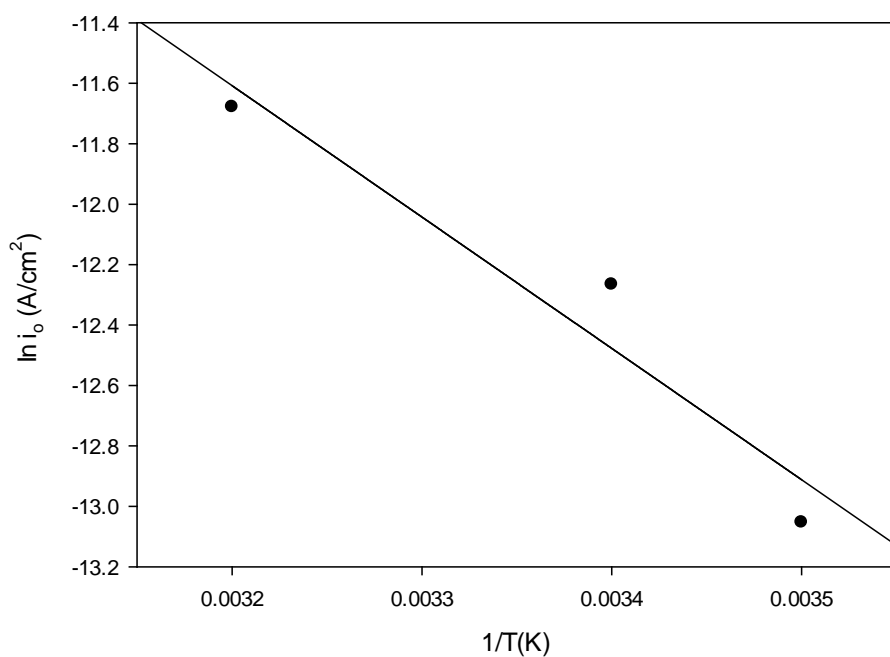


Figure F7: Arrhenius plots for determining the activation energy of Tafel processes in 4 M [Cl⁻] of pH 2 in the presence of ozone

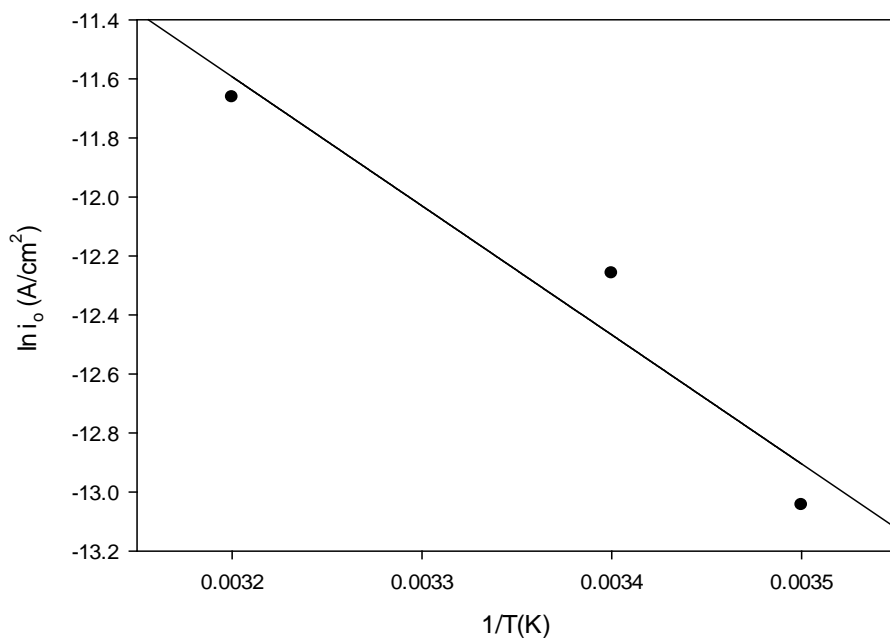


Figure F8: Arrhenius plots for determining the activation energy of Tafel processes in 4 M [Cl⁻] of pH 4 in the presence of ozone

Appendix G: Percentage recovery of platinum

Total % extraction of Pt	Time (hours)	Conditions
45	8	4 M [Cl ⁻], pH 0.5, 35 °C
21	8	4 M [Cl ⁻], pH 2, 35 °C
12	8	4 M [Cl ⁻], pH 4, 35 °C

Total % extraction of Pt	Time (hours)	Conditions
46	8	1 M [Cl ⁻], pH 4, 15 °C
39	8	1 M [Cl ⁻], pH 2, 25 °C
32	8	1 M [Cl ⁻], pH 4, 35 °C

Total % extraction of Pt	Time (hours)	Conditions
45	8	2 M [Cl ⁻], pH 2, 25 °C
37	8	2 M [Cl ⁻], pH 0.5, 35 °C
29	8	2 M [Cl ⁻], pH 4, 35 °C